Interactions in stomatal function

Pedro José Aphalo
Ing. Agr. (Buenos Aires), M. Sc. (Buenos Aires)

A thesis submitted in fulfilment of the requirements
for the degree of Doctor of Philosophy
to the
University of Edinburgh
1991

Abstract

The modelling of stomatal responses is hindered by gaps in our knowledge of the inter-
actions between the effects of different environmental variables, and of the mechanistic
basis for correlations between physiological variables. The objective of this thesis was
to fill some of these gaps by studying short term stomatal responses to the environ-
ment, and by contrasting some current models against this new information. Four
questions were addressed through simulation and gas-exchange experiments on *Hedera
helix* subsp. *canariensis* (Willd.) Coutinho.

(1) *What is the relationship between stomatal responses and the rate of photosynthesis?*
The CO_2 flux density and stomatal conductance are closely correlated, but there is
not a simple causal link between them. This relationship is complex, and depends
on both parallel but independent responses to light of stomata and photosynthesis,
and indirect response of stomata mediated by photosynthesis. This indirect response
occurs through CO_2 depletion in the air spaces of the mesophyll and stomatal response
to CO_2. No evidence was found in favour of the proposed effect of photosynthesis on
stomata through an unknown messenger.

(2) *What is the nature of the interaction between stomatal responses to humidity and
temperature?* The hypothesis that these responses are brought about by a single re-
sponse to relative humidity at the leaf surface was tested, and shown to be incompatible
with the responses of *Hedera helix*. It is suggested that the most appropriate variable
for expressing humidity is, in this context, the water vapour deficit at the leaf surface.

(3) *What is the role of the boundary layer in the control of stomatal opening?* Real
world and simulation experiments were used to show that responses to bulk air water
vapour and CO_2 mol fractions are both dependent on stomatal responses to CO_2 and
humidity. It is also shown that a feedforward response to humidity requires feedback
through another variable for stability under natural conditions. Response to wind speed
is due to changes in humidity and CO_2 mol fraction at the leaf surface.

(4) *Are our current knowledge, and the resulting models, good enough for predicting*

short-term stomatal responses to changes in the environment? The need for a careful analysis of simulation models is stressed. Ball's empirical model of stomatal conductance was analysed. The original interpretation was found to be flawed, and a new one was proposed. The new interpretation views the model as a description of the relationship between CO_2 flux rate and stomatal conductance, rather than of stomatal conductance alone. It is shown that this model is useful for describing the behaviour of the intercellular CO_2 concentration. The model was tested against data from the experiments. It was found that the responses to temperature and humidity are not treated in a satisfactory way. The response of the model to other variables is realistic. A modification to the model is described and tested. It is concluded that the model is a good starting point for the development of simulation models to be used as submodels in canopy and regional models.

Declaration

This thesis has been composed by myself and it has not been submitted in any previous application for a degree. The work reported within was executed by myself, unless otherwise stated.

June 1991

Preface

The aim of ecophysiological research in a changing global environment

In the past, ecophysiological research has disregarded changes in the global environment, except when considering long term processes such as species evolution. In the last few decades the rate of change has markedly increased as a result of the impact on the environment of mankind through technology. This has made the prediction of both (1) the future change in the global physical environment, and (2) the consequences of this change for living organisms, become urgent matters. Surface properties and gas exchange of vegetation may affect the global environment through modification of the energy balance, the carbon cycle and the hydrological cycle. The recognition that vegetational change (a transition from one surface type to another) has an effect on the physical behaviour of the environment at a global scale is novel within ecophysiology, and is important as a justification for the development of this discipline. Changes in the biosphere that feed back into changes in the physical environment are very important, but they are not the only important ones. A knowledge of the effects of environmental change on the ecosystem and all its components —either functional, structural, population, or genetic— is also needed to predict changes in the biosphere, and ultimately their consequences for the future of mankind. The ultimate objective should be to predict both the physical and biological environment that future generations will encounter, and to assess the risks of following contrasting strategies in the use of resources.

Predicting the future change of world vegetation, and its effect on global climate and environment is a taxing task. It makes necessary the integration of events over a wide expanse of time and space. This complexity requires the use of adequate conceptual tools such as general systems theory and hierarchy theory. The physiological response of individual plants and animals propagate throughout the system in several different ways. There is evidence that the effect of an increased CO_2 concentration in the

atmosphere can be different in different ecosystems, and on different plant species (e.g. Morison, 1990). A physiological response does not need to affect the short term spatial integral of a response to have an effect on future worldwide changes. In the long-run, effects on competition and species survival, or population biology can be as important as more direct effects.

The crucial question is: Given a long enough expanse of time, can physiological responses of organisms significantly affect the global system? The answer is clearly "yes" when these responses are being driven by changes in the global environment and as a consequence of this they occur simultaneously on different parts of the earth's surface. The situation is different when responses are driven by local disturbances happening at random, in which case they would tend to cancel out upon integration in a larger spatial scale. The most dangerous situation would be for the whole system to enter into a loop with positive feed-back, in which changes in the climate and in the vegetation would go in the same direction and reinforce each other. This would happen if an increase in CO_2 in the atmosphere, or a change in temperature, were to lead to a decrease in the flow of CO_2 towards sinks (e.g. forests biomass and oceans). At the present time, there are indications of negative feedback, but it is possible that in the foreseeable future the speed of change may accelerate over a threshold above which instability will ensue.

It is true that in the past much ecophysiological research has been done at the organ or single plant level and that whole canopy and global effects have usually been neglected. However, we must not now make the opposite mistake by blindly swinging towards a whole canopy-centered approach. To obtain an understanding of the whole system, we must establish relationships between the behaviour of the system at different spatial and temporal scales, taking into account both physical and biotic components, and using alternative viewpoints —i.e. ecophysiology, ecosystem analysis, population biology.

Why study stomatal responses?

The effect of changes in stomatal conductance on the flow rates of water vapour and CO_2 depends on the spatial scale considered. At larger scales the stomatal control of the fluxes decreases, and the magnitude of this decrease depends on the value of other conductances, mainly the boundary layer conductance between the leaf and the reference level in the atmosphere were molar fractions remain unchanged. Although stomatal conductance does not have a great effect on whole canopy or regional water exchange in many situations (Jarvis & McNaughton, 1986), it is a necessary variable

for the understanding of how plants interact with their environment (Cowan, 1988). That stomatal responses have a smaller effect on flow rates through entities at larger spatial scales than individual leaves, does not mean that the stability and evolution of the whole system are independent of these responses.

The consideration of a simple example can help. Even in a situation where a change in the integrated stomatal conductance of all the leaves of the plants in the canopy has no effect on the total water flux per unit of ground area, a change in stomatal conductance of one genotype or species will have an effect on the partitioning of water resources between individuals of the same, or different, species. In many situations this can be of the greatest importance: for example it can alter the amount of water used by a crop competing with weeds; it can drive evolution through natural selection; it can even determine the survival of the vegetation cover.

So, even though in many situations we would not expect that changes in stomatal responses resulting from changes in the environment would lead in the short term to big changes in global CO_2 and water fluxes, such changes could have, for example, important effects on the species composition of vegetation by altering competitive relationships, and on the economic productivity of forest and agricultural systems.

Independently of changes in the global environment, an understanding of stomatal behaviour is important to applied fields such as forestry, agriculture, horticulture, and irrigation. Hence, in most situations where water supply to crops is limited, yield depends on the efficient use of this supply. Water use efficiency depends on stomatal behaviour through its effects on the rates of transpiration and photosynthesis.

Scope of this project

To predict the effect of long term changes in climate on the short term responses of stomata, it is first necessary to have an adequate knowledge of these responses in plants grown under normal conditions. To have a model of short-term stomatal responses based on a simplified but realistic representation of the mechanism involved, the first unavoidable step is to study this mechanism. For this, it is *not* necessary to grow plants under future environmental conditions, and it is easier not to do so. Longer term effects, such as changes in stomatal dimensions and frequency, cannot affect the nature of the *mechanism* of short term responses. Once a satisfactory model is available it can be reparameterized for plants grown under different conditions with less exhaustive experimentation.

Although research on stomata started long ago and has been intense (Meidner,

1987), the complexity of their responses are still a challenge to our understanding. Interactions between responses to different stimuli, and the dynamics of the responses need further study. It is also important to assess whether current knowledge is good enough for the prediction of steady-state stomatal responses, as is required in mechanistic models of CO_2 and water fluxes at larger spatial scales, for example forest canopies. Climatic variables that are expected to change significantly in the near future are CO_2 molar fraction of the air, temperature, rainfall and humidity. Stomatal responses to light and CO_2 are closely linked. These are the variables on which the emphasis has been placed.

Objective

The modelling of stomatal responses to the environment is hindered by gaps in our knowledge of the interactions between the effects of different environmental variables, and of the mechanistic basis for correlations between physiological variables. The general objective of this project was to fill some of these gaps by studying short term stomatal responses to the environment, and by contrasting some current models against this new information. Specific objectives are defined in detail by the following questions:

1. What is the relationship between stomatal action and the rate of photosynthesis?

2. What is the nature of the interaction between stomatal responses to humidity and temperature?

3. What is the role of the boundary layer in the control of stomatal opening?

4. Is our current knowledge, and are the resulting models, good enough for predicting short-term responses of stomata to changes in the environment?

The responses of *Hedera helix* plants were studied under controlled conditions in the laboratory. A computer controlled gas-exchange system was used to measure the flows of water vapour and CO_2 between a leaf and the air in an enclosing chamber. From these measurements conductances and molar fractions were computed. The effect of the boundary layer was both measured and modelled. A recently developed model of g_s^w and some of its derivatives was contrasted with the observed response, and as a result, changes to this model were proposed.

Dedication

A Tarja y el osito Pú

Acknowledgements

I wish to thank:

- Prof. Paul G. Jarvis for supervising my work at Edinburgh, for encouraging me to finish this PhD whenever problems looked unsurmountable, and for commenting on the draft thoroughly, leading to a much improved thesis.

- Dr. John Grace and Dr. Helen Lee for their many useful comments and suggestions.

- Dr. Chris Jeffree for helping with the interpretation of SEM images.

- Prof. Rodolfo A. Sánchez for teaching me how to do research and for encouraging me to look farther than our laboratory in Argentina.

- Susie Jackson and Diana Guthrie for making this thesis possible by helping me cope with the problems caused by being far from my home country.

- Tarja for her patience, understanding and support.

- My parents for their support.

- All the new friends that made my life in Edinburgh enjoyable.

- Consejo Nacional de Investigaciones Científicas y Técnicas (República Argentina), British Council (United Kingdom) and the Overseas Research Student awards scheme (United Kingdom) for providing the funding.

Contents

List of Tables

List of Figures

List of symbols

Basic symbols

In equations only S.I. units without scale factors are used, and are not indicated. For displaying data, scale factors are frequently used with these same basic units, and are given along with the data. The units given here apply to the equations.

Symbol	Definition
A	Molar flux density of CO_2 at the leaf surface (mol m^{-2} s^{-1}).
b	Thickness of the boundary layer (m).
D	Air water vapour deficit at position indicated (mol mol^{-1}).
D	Diffusivity in air (mol m^{-3} s^{-1}).
E	Molar flux density of water vapour at the leaf surface (mol m^{-2} s^{-1}).
$\mathcal{E}$	Molar flux density of water vapour per unit land area (mol m^{-2} s^{-1}).
g	Conductance per unit leaf area (mol m^{-2} s^{-1}).
$\mathcal{G}$	Conductance per unit land area (mol m^{-2} s^{-1}).
h	Relative humidity (fraction).
I	Quantum flux density (mol m^{-2} s^{-1}).
J	Molar flow rate (mol s^{-1}).
l	Length or dimension of a leaf in the wind direction (m).
ℓ	Proportional length of short section of a split IRGA cell (fraction).
P_{atm}	Atmospheric pressure (Pa).
PAR	Radiation within the wavelength range 400–700 nm.
s	Signal from instrument (V).
S	Leaf area (m^2).
T	Temperature (°C).
u	Wind speed (m s^{-1}).
β	Sensitivity of IRGA (V mol^{-1}).
λ	Wavelength of light (nm).
χ	Molar fraction of gas indicated by superscript in air (mol mol^{-1}).

Subscripts

Subscripts denote location in the leaf or gas system.

Symbol	Definition
a	Air outside the boundary layer of the leaf.
b	Boundary layer.
cyl	Compressed air cylinder, used as reference.
hum	Humidifier inlet.
i	Air in the intercellular space of the leaf.
in	Leaf chamber inlet.
in,IRGA	IRGA reference cell.
l	Leaf.
out	Leaf chamber outlet.
s	Leaf surface, or air at the leaf surface.
std	Standard concentration.
t	Total (for conductances).
tot	Mixing tray outlet.
trap	Water trap outlet.

Superscripts

Superscripts denote the substance, entity, or property to which the base symbol refers.

Symbol	Definition
air	Air.
c	CO_2.
dew	Dew point.
dry	Dry, CO_2-free air.
w	Water vapour.
w*	Saturating water vapour.

Accents

SYMBOL   Definition

~   Standardized to $\chi^c_{in,IRGA} = 350\,\mu mol\ mol^{-1}$.

ˇ   Measured with the IRGA.

Chapter 1

Introduction

This chapter is a brief review of current ideas about stomatal responses, as observed from different viewpoints and at various scales. Both real world experimentation and simulation modelling are reviewed. The purpose of the chapter is to create the context for a detailed discussion of the responses at the leaf scale later in this thesis. The next two chapters describe the gas-exchange apparatus, and plant material used in the experiments. The four chapters that follow address individual objectives, and discuss the relevance of the results obtained in view of current knowledge. The last chapter is a summary discussion.

1.1 Stomatal responses in the real world

1.1.1 What variables do stomata sense? And where?

Stomata are sensitive to light, CO_2, humidity, and temperature. They are also sensitive to chemical signals, and through them to other environment variables such as soil water content, photoassimilate demand and stress events such as drought. CO_2 is thought to be sensed on the inner side of the guard cells (Meidner & Mansfield, 1968, page 76), and so the concentration seen by them is χ_i^c (Mott, 1988). It has been proposed that air water vapour content is sensed at or near the outer surface of the leaf through localized transpiration from guard cells (Lange *et al.*, 1971; Mansfield, 1986) or through sensing of relative humidity by the guard cells (Ball, 1988). However, it has also been suggested that cuticular transpiration from the outer leaf surface is negligible and that the response to humidity depends on a restriction of water supply to guard cells through subsidiary cells (Nonami *et al.*, 1990). In a whole leaf, the response of g_s^w to light depends on both the response to light of the guard cells, and an indirect effect of mesophyll photosynthesis through χ_i^c, and it has been suggested that it also acts

through another unknown messenger. Stomata respond indirectly to the soil water content. A chemical signal, most probably abscisic acid, synthesized in the roots and carried to the shoots by the xylem sap flow decreases stomatal aperture when soil dries, even if the shoot water status is not affected (Jones, 1990; Davies *et al.*, 1990; Zhang & Davies, 1991).

1.1.2 The basis of stomatal movements

The stomatal pore opens and closes as a consequence of change in shape of the guard cells. The driving forces for shape changes are the absolute turgor pressure of the guard cells and the difference in turgor pressure between them and the epidermal cells that surround them (Cowan, 1977). The change in shape is dependent on the elasticity of the cell walls in different directions, which is a consequence of the orientation of microfibrils (Weyers & Meidner, 1990), and on wall thickness in different parts of the cell. There have been reports of walls stiffening as stomata open (Weyers & Meidner, 1990), and suggestions of an effect of abscisic acid on the elastic modulus of guard cell walls (Kondo, 1989). However, the active movement of stomata depends on the build up and release of osmotic potential in the guard cells by transport and synthesis of solutes. Fujino (1967) and Fischer (1968) discovered the central role of K^+ in stomatal movements. The balancing anion can be organic (e.g. malate) or inorganic (e.g. Cl^-). Sugars can also be osmotically significant (Zeiger, 1990).

Zeiger *et al.* (1977) have proposed a chemiosmotic hypothesis for solute transport leading to stomatal opening in which the primary motive force for solute accumulation is an H^+ gradient (Zeiger, 1983; Zeiger, 1986, give an account of this model). Different opening stimuli contribute to an H^+ gradient by H^+ extrusion, and this gradient drives the uptake of K^+. More recent evidence of the dynamics of solute fluxes during opening and closing points to a more complex mechanism. Both a proton pump and membrane potential-sensitive K^+ channels play a role in solute accumulation and release (MacRobbie, 1988; Raschke *et al.*, 1988). Blue light effects on stomata could be mediated by a plasma membrane redox system distinct from the proton translocating ATPase (Raghavendra, 1990), however there is not enough data available to establish whether this is the case or not (Zeiger, 1990). Starch hydrolysis and CO_2 fixation are additional sources of osmotica (Zeiger, 1990). Stomatal closure is not just brought about by stopping the opening mechanism, but rather by a closing mechanism —a transient increase in solute efflux (MacRobbie, 1988). Closure is affected by respiratory inhibitors and hypoxia (Weyers *et al.*, 1982; Pemadasa, 1981). The effect of CN^- and DCMU on stomatal opening is different under blue and red light, indicating

that the response to light is dependent on more than one source of energy and that different mechanisms are involved depending on the wavelength of light (Schwartz & Zeiger, 1984; Shimazaki, 1989). Respiration is not always the source of energy: under red light photophosphorylation can play this role. However, there is uncertainty on the importance of guard cell chloroplasts as a source of energy for stomatal opening under white light illumination (Zeiger, 1990; Dahse et al., 1990).

Stomata respond to light both directly and indirectly. *Direct* responses are those in which light is sensed in the guard cells, *indirect* ones are those in which light is sensed in other cells of the leaf.   There are three photosystems involved in direct responses to light: guard cell photosynthesis and a blue light absorbing system are the primary systems (e.g. Sharkey & Ogawa, 1987; Zeiger, 1990), and phytochrome has a regulatory role (Holmes & Klein, 1985). The role of phytochrome is considered by Zeiger (1990) to be limited to its effect on circadian rhythms. According to Holmes (1989) phytochrome plays a more important role by regulating the speed with which stomata open and close.

The mechanism of response to CO_2 is not known (Mott, 1990), and most hypotheses are as undetailed as stating that it "...acts at some point in the ion accumulation mechanism" (Morison, 1987), or "...the main action of CO_2 is upon ion transport processes in the cell membranes" (Mansfield, 1983). Edwards & Bowling (1985) explained their experimental results by postulating an electrogenic proton pump in the plasmalemma which is inhibited by CO_2.   Mansfield et al. (1990) have recently reviewed the literature on the action of CO_2 on guard cells. These authors suggest that there are two opposing actions of CO_2 on stomata: (1) stomatal aperture through enhanced malate synthesis, and the usually prevailing action, (2) stomatal closure through one or more of the following mechanisms: modulation of photophosphorylation, modulation of oxidative phosphorylation, a direct action on the plasma membrane, and/or an unknown mechanism.

Responses to water vapour pressure are not a simple passive effect on guard cell and epidermal water relations. When subjected to step changes in air humidity stomata display a response that has two phases (Grantz, 1990). Initially there is a passive phase during which the response is opposite to that in the succeeding active phase. During the passive phase there is no movement of solutes. In the later phase closure is concurrent with the decrease of solute content of the guard cells (Grantz, 1990). It was not known until recently which way of expressing air humidity (e.g. h vs. χ_a^w) was most appropriate because the sensing mechanism is unknown. However the experiments reported in Chapter 5 and information from experiments comparing stomatal behaviour in a helium-oxygen mix with that in air (Mott & Parkhurst, 1991) show that D_s^w drives

this response through transpiration (either the total flow or a component of it).

No temperature sensor has been postulated in guard cells and the effect of temperature is most probably the result of a balance between its effects on the different metabolic pathways of the cells, but this is still an open question (Zeiger, 1983). In whole leaves some of these effects could be indirect through χ_i^c because temperature affects A through its effects on the rates of respiration and photosynthesis. Stomatal aperture usually has an optimum temperature not far from the growth temperature. Temperature not only affects steady-state stomatal aperture but also the rate of aperture change. Meidner & Heath (1959) observed a Q_{10} of 2.2 for rate of opening in response to a dark to light transition in onion.

There are two main methods in use to study the responses of isolated guard cells: protoplasts, which are cells devoid of walls, and "isolated" stomata. Guard cell protoplasts are produced from peeled epidermis, by enzymatic digestion, and separation from epidermal cell protoplasts (Zeiger, 1983; Weyers & Meidner, 1990). "Isolated" stomata are used *in situ* in peeled epidermis, in which epidermal cells have been selectively killed, usually by low pH (Squire & Mansfield, 1972; Weyers & Meidner, 1990). Although the physical characteristics of these cells and their normal environment is lost, they allow study of certain aspects of their functioning without the difficulties of interpretation brought about by the presence nearby of several dissimilar kinds of cells, as in a whole leaf. Guard cell protoplasts respond to light by swelling and by changing the pH of the medium in which they are suspended (Zeiger & Hepler, 1977). There is a concurrent flow of solutes and changes in membrane potential (Zeiger, 1990).

Before the availability of the techniques described in the previous paragraph, most metabolic studies were done on epidermal peels. Information on the effect of having K^+ salts of different anions in the medium, or substances that generate artificial ion channels in membranes, and their interactions with responses to light and CO_2 was obtained in this way (e.g. Wardle & Short, 1981). Epidermal peels with living epidermal cells have also been used in many experiments on responses of stomatal aperture to hormones. Stomata normally close in response to abscisic acid, and open in response to cytokinins and indol-3-ylacetic acid (e.g. Mansfield, 1983). Interactions between hormones are complex, and affect the sensitivity to CO_2 (Snaith & Mansfield, 1982).

The role of the subsidiary cells is both mechanical and as a source and sink of solutes. In grasses K^+ and Cl^- shuttle between guard cells and subsidiary cells concurrently with stomatal movements (Pallaghy, 1971; Raschke & Fellows, 1971). In dicotyledoneae the role of the adjacent epidermal cells is not so clear. Not all species have morphologically distinct subsidiary cells. Penny & Bowling (1974) have suggested from data for *Commelina communis* that K^+ moves between guard cells and epidermal

cells *through* the subsidiary cells, and that active transport is involved. In the same species, Penny *et al.* (1976) observed a similar pattern of change in Cl^- concentrations across the stomatal complex. In both dicotyledoneae and monocotyledoneae there are no plasmodesmata connecting mature guard cells with neighbouring cells, so solutes transported between them must go through the apoplast (Weyers & Meidner, 1990).

Although in the last few years our knowledge of the mechanism of solute transport in guard cells has advanced quickly, there is still no clear picture of its regulation in any plant species. As discussed above, stomatal responses to environmental stimuli are mainly transduced into a solute potential and its concomitant turgor potential. Any hypothesis about the intermediate steps leading from the presence of a stimulus to the accumulation of solutes is, at this time, very dependent on our preconceptions. It has to be based on what is known to happen, or assumed to happen in other organisms and on the kind of system within these organisms that we take as a model for stomata. We can boldly divide the possible mechanisms by which stimuli interact into three groups as follows.

1. Mechanisms based on what is known about energy transduction and solute transport. In this case environmental signals would be transduced into a proton gradient. This gradient being the common step unifying the different responses, this is the model originally proposed by Zeiger (1983). Although there is experimental evidence showing the important role of proton extrusion in stomatal opening, there is no evidence that the generation of this proton gradient is the step at which the interactions occur —i.e. the stage where transduction paths for different stimuli converge.

2. Mechanisms based on what is known about action of hormones, transmission of nerve impulses, and other regulatory systems in animals in which Ca^{2+} plays a very important role as a messenger. This model was recently suggested by MacRobbie (1988) but the evidence is scanty. It is known that there are Ca^{2+} channels in the plasma membrane and tonoplast of plants, and most probably also Ca^{2+} ATPase in the plasma membrane (Sussman & Surowy, 1987; Marmè, 1988). A few Ca^{2+}, calmodulin regulated enzymes have also been found in plants (Marmè, 1988). Ca-dependent protein kinase activity has been detected in guard cell protoplasts, and calmodulin is also present in these cells (Mansfield *et al.*, 1990). Cytosolic calcium regulates ion channels in the plasma membrane of *Vicia faba* (Schroeder & Hagiwara, 1989). In *Commelina communis* abscisic acid induces an increase in cytosolic free Ca^{2+} that precedes stomatal closure (McAinsh *et al.*, 1990). Abscisic acid, darkness, and cytokinins might employ

Ca^{2+} as second messenger (Mansfield *et al.*, 1990).

3. Mechanisms based on what is known about other sensory systems like chemiotaxis in *Escherichia coli* or vision in humans. These systems sense changes in time of the level of the stimuli. In *Escherichia coli* this sensory adaptation (range adjustment) is effected by methylation of the receptor protein, and this allows the bacterium to sense the change in concentration by comparing the concentration to which it was exposed during the last second to that which it was exposed during the last three seconds (Stryer, 1988). The phosphorylation —and activation— status of several plant enzymes has been shown to be altered by light (Budde & Randall, 1990). Chlorophyll, phytochrome and a blue light photoreceptor seem to be involved with different enzymes (Budde & Randall, 1990). There is no evidence of which I am aware that shows cross-adaptation of a receptor protein in plant cells —i.e. change in the sensitivity to one stimulus caused by a different one. However, there is evidence of adaptation of light sensors allowing them to function over several orders of magnitude of I (Galland, 1989). The overshoot many times observed in stomatal responses to step increases in the quantum flux density of blue light could be caused by partial adaptation.

Thus interactions between responses to different environmental stimuli could happen by transduction into a proton gradient, a pool of osmotica, the release of a common messenger like Ca^{2+}, or by cross-adaptation of the sensitivity of receptors. A direct effect on the proton gradient could be either through proton pumps or through ion channels or ports (e.g. in the human eye light closes Na^+ channels causing the hyperpolarization of the membrane, but this response depends on the basal light level).

From a systems viewpoint, the sensory mechanism of guard cells can follow one of two contrasting hypothetical models. I am going to call them the *balance* model and the *set-point* model. In the balance model the effects of different stimuli contribute to an intermediate pool of a chemical species or to a potential gradient. In contrast, in the set-point model stimuli affect the 'setting' of a control system. There is evidence in favour of the idea that stomatal sensing of environmental variables is carried out by a system that follows the set-point model. There seems to be a mechanism for building up osmotic potential that can use different osmotica according to their availability. In particular, anions can be substituted one for another (Mansfield, 1983).

Based on control engineering common sense, one might think that a system that follows the set-point model would be more reliable because it would be able to sense one variable independently of changes in other state or environmental variables. However, there is little evidence available that could allow us to distinguish between these two

hypotheses.

1.1.3 Conductance of leaves to water vapour and CO_2

The total conductance of a leaf is the result of the stomatal, cuticular, and boundary layer conductances. For a given set of conditions g_t^w depends not only on the density and size of stomatal pores, but also on the shape and size of the leaf. The conductance of a leaf surface and its boundary layer is not based on a totally diffusive process. It depends on wind speed and the aerodynamic characteristics of the leaf. This is mainly due to their effects on the thickness of the boundary layer. However, it has also been proposed that there can be mass flow of air through the leaf due to differences in pressure at different points of its surface (Vogel, 1978). These local pressure differences depend on the local wind speed (e.g. the wind profile near the edges of a leaf is different to that at its center).

Leaf surface conductances are measured as spatial averages. g_s^w is the result of the conductance of individual stomata, and their distribution. g_b^w is the average conductance of a boundary layer that is of non-uniform thickness (e.g. Grace & Wilson, 1976). g_c^w is a property of the cuticle, and depends on its integrity, but it has been also proposed that it could depend on χ_s^w (Grace, 1977). They are related as follows:

$$g_t^w = \frac{1}{1/g_l^w + 1/g_b^w},$$ (1.1)

where

$$g_l^w = g_s^w + g_c^w.$$ (1.2)

The boundary layer affects responses of g_t^w to bulk air concentrations of CO_2 and water vapour by altering these concentrations at the place where they are sensed by stomata, and also by being a component of g_t^w (see Equation 1.1 above). Although g_s^w is a property of the leaf, it is brought about by the responses of individual stomata. Most environmental variables are sensed directly by the guard cells, and this has to be taken into account in any analysis of the responses of g_s^w, g_l^w, or g_t^w. Driving variables must be defined at the leaf surface to be meaningful. The value of these variables at the leaf surface (e.g. χ_s^w and χ_s^c) depends, for a given value of the corresponding variables in the bulk air (e.g. χ_a^w and χ_a^c), on the thickness of the boundary layer. The boundary layer affects both the total conductance, the effective conductance controlling flow rates of water, CO_2, and sensible heat, and the concentrations at the leaf surface where they affect stomata. In natural conditions the boundary layer conductance also affects the energy balance of the leaf, and so its temperature which then affects stomata. (See

also Chapter 6.)

As pointed out above, g_b^w and g_s^w are spatial averages. The thickness of the boundary layer depends on the local wind speed, which changes across the leaf surface as a function of the distance to the leaf edge and wind direction (e.g. Nobel, 1983). Aperture of stomata varies both randomly (Laisk *et al.*, 1980; van Gardingen *et al.*, 1989), and systematically through the leaf surface (Smith *et al.*, 1989): the aperture of individual stomata varies around a local mean value, this mean value being usually higher at the center of a leaf than at the edges.

Leaf conductance and CO_2 assimilation rate are usually correlated under naturally occurring conditions. This correlation is not mechanistic as it can be readily broken (Jarvis & Morison, 1981). For example, light is sensed both directly by guard cells and indirectly through mesophyll photosynthesis. (See also Chapter 4.) However some authors do not accept the practical validity of this view and interpret the operational link that is frequently observed between g_s^w and A in mechanistic terms (e.g. Wong *et al.*, 1979).

1.1.4 Conductance of canopies

If we move our reference level from the air immediately outside the leaf boundary layer, to some plane in the turbulent layer of air above the canopy where the driving variables are once again independent of the fluxes, we add new sources of resistance to the flow of water vapour and CO_2 between the leaf mesophyll and this more distant reference level. This additional resistance is represented as an aerodynamic conductance across the canopy boundary layer to the base of the mixed layer above. It is very important to realize that by changing the reference level we are also changing what we assume to remain unchanged. When our reference is just outside the leaf boundary layer we assume all the conditions in the rest of the canopy, including g_s^w of other leaves, to remain constant.

Heterogeneity of surface properties also occurs at the canopy scale (Grace, 1991), and it depends on the type of vegetation —e.g. crops are usually homogeneous, but natural vegetation such as savannas and open woodlands can be patchy.

Stomatal control of canopy transpiration compared to leaf transpiration has been analysed in recent reviews (Jarvis & McNaughton, 1986; Finnigan & Raupach, 1987; McNaughton & Jarvis, 1991). The effect of a change in stomatal conductance is larger on the transpiration of an individual leaf than on the transpiration of a canopy because of the shorter path length. This shorter path has a higher conductance of which g_s^w is a more important component. When analysing a canopy, conductances and flow

densities are expressed per unit land area, and they represent the spatial integral of the conductances and flow densities at the leaf surfaces that make up the canopy.

McNaughton & Jarvis (1991) use the concept of feedback loops in control systems to describe the effect of stomatal conductance and other variables on leaf and canopy transpiration. They drew block diagrams of the control systems that operate at the leaf and canopy scales, and from these diagrams derived control equations. Starting with a very small area of a leaf they build by stages a description of transpiration of a canopy by nesting control structures that describe the different sources of feedback at each level. The control of transpiration by stomatal conductance decreases as new sources of feedback are included by scaling up. The previously proposed concept of decoupling between leaf transpiration and the environment (Jarvis & McNaughton, 1986) is represented by the feedback caused by boundary layer conductance ($\mathcal{G}_b^w$) through its effects on temperature and humidity (McNaughton & Jarvis, 1991).

Depending on the gain of the different feedback loops, brought about mainly by differences in $\mathcal{G}_b^w$, the dependence of $\mathcal{E}$ on $\mathcal{G}_s^w$ varies. If $\mathcal{G}_b^w$ is high as in some tree canopies, then $\mathcal{E}$ depends strongly on $\mathcal{G}_s^w$. In contrast, in short vegetation canopies, $\mathcal{G}_b^w$ is small and $\mathcal{E}$ is controlled mainly by radiation.

1.2 Models of stomatal response

1.2.1 Classification of models

Simulation models can be either mechanistic or empirical. Empirical models are also called descriptive because they simply describe the relationship between two or more variables while mechanistic models include indications of causality (Hall & Day, 1977). Other criteria can be used for a classification of models: (1) spatial scale, (2) time scale, (3) whether they are goal oriented or not, (4) whether they are static or dynamic.

1. Spatial scale differentiates models by the size of the object whose behaviour is modelled —e.g. a single stoma, a leaf, a plant, a canopy, or a region.

2. The time scale is related to the time lapse during which the behaviour happens —e.g. from minutes, days, and growth season to centuries or millennia.

3. I will call those models that are based on the idea that the system modelled —the plant, or one of its processes— tends to towards a goal, *goal oriented*. They can be seen as based on teleological ideas —e.g. stomata respond to light so as to keep χ_i^c constant. Both mechanistic and empirical models can be goal oriented.

In the first case the goal arises from assumptions about a mechanism, or causal chain of events, in the second case the apparent goal comes from observation.

4. Static models are used to simulate steady-state responses. Dynamic models simulate the changes in time of a state variable in response to changes in the value of driving variables.

Which kind of model is to be preferred? It depends on the objective, but in general mechanistic models are better than empirical models when used for extrapolation. Another advantage of mechanistic models is that they summarize the knowledge about a system in a testable way, thus helping our understanding of the system. This is balanced by the need for a much better understanding of the functioning of a system to be able to build a mechanistic model. Whether to construct dynamic or static models depends entirely on their intended use —e.g. In the case of stomata, if we are interested in responses to sunflecks, we need a dynamic model. Empirical goal oriented models provide insights about the results of a process, but not about the causal mechanism involved.

In the next two sections I shall consider only models at the scale of a single leaf. As the mechanism of stomatal response is not well known, few attempts have been done to build mechanistic models. Empirical models are much more common.

1.2.2 Empirical models

Several authors have developed static empirical models of g_s^w responses (e.g. Jarvis, 1976; Thorpe *et al.*, 1980; Lösch & Tenhunen, 1981; Avissar *et al.*, 1985). Thorpe *et al.* (1980) developed a simple model of stomatal conductance of an apple leaf that includes only the effects of light and water vapour deficit. Jarvis (1976) proposed a more comprehensive model that takes into account responses to temperature, CO_2 and leaf water potential, as well as light and water vapour deficit. The model was fitted to field data for *Picea sitchensis* and *Pseudotsuga menziesii*, and also to measurements done in the laboratory. Avissar *et al.* (1985) developed a model for a tobacco leaf that includes the same variables except that soil water potential replaces leaf water potential. These three models include only multiplicative factors for the effects of the different variables. The functions used to empirically describe the individual responses are not the same in all the models. Lösch & Tenhunen (1981) designed a model to describe the responses of *Polypodium vulgare*. They used data measured in epidermal strips as a basis, to generate an intermediate result of the degree of aperture of a single stoma which was used to compute g_s^w, so although it is an empirical model of stomatal responses, it could be considered a semi-mechanistic model of leaf responses.

This model includes interactions between the effects of temperature and D_a^w, and water potential and D_a^w. Aphalo (1988) used a dynamic empirical model of g_s^w as a submodel in a model of water vapour, CO_2, and energy flux densities between a leaf and the atmosphere. Kirschbaum *et al.* (1988) developed a dynamic model that simulates stomatal responses to lightflecks.

Some static empirical models use the correlation between g_s^w and another plant response (A) to achieve a simpler mathematical description, but they do not include any causal relationship, so they are in no way mechanistic (e.g. Ball *et al.*, 1987). Ball's model uses one variable as a surrogate for others, it is in other words an indirect description. It could be called "operational" in the sense that it makes use of a relationship that seems to be an operational goal of the plant mechanism. This apparent goal comes from empirical observation, not from a causal mechanism. (See Chapter 7 for a detailed discussion of Ball's model and some of its derivatives).

1.2.3 Mechanistic models

A dynamic mechanistic model of stomatal action was developed by Penning de Vries (1972). This model includes, as part of the mechanism, the water relations of the guard cells. Stomatal aperture is calculated from pressure potentials which depend on the effect of environmental variables on the water potential and its components. The author made many assumptions about the mechanism because not enough data was available. This model was used to describe the stomatal behaviour of turnip.

Optimization models search for an explanation in a much longer time scale. The question is why has certain behaviour been selected during evolution and not how it is *implemented* by the physiology of the plant. They are goal oriented, but this goal has a mechanistic basis in natural selection. The most popular of these models was proposed by Cowan & Farquhar (1977), and it applies to a leaf in an individual plant (Cowan, 1988). It treats transpiration as a cost and photosynthesis as a benefit and assumes that the plant behaves so that the daily integral of A is maximum for a given daily integral of E. Solving the model under this assumption leads to constant marginal cost relative to marginal benefit with respect to changes in g_s^w throughout the day, i.e.

$$\frac{\frac{\partial E}{\partial g_s^w}}{\frac{\partial A}{\partial g_s^w}} = \frac{\partial E}{\partial A} = \lambda. \tag{1.3}$$

This hypothesis has been tested by measuring λ to see whether it does remain constant throughout a day under natural or controlled conditions. There are data bearing out this model (e.g. Farquhar *et al.*, 1980), but also data opposing it (Fites &

Teskey, 1988). The assumption of constant λ is readily broken in controlled conditions —by changing environmental variables in ways not usually occurring in nature. In the field λ has been shown not to be constant but at the same time A and E were close to the values expected had λ been constant (Williams, 1983). The departure of λ and g_s^w from their modelled optima was largest in the early morning and late afternoon. The assumed objective of using water resources with maximum efficiency is probably not always valid. Then, it is not surprising that the model fails to describe the behaviour of some species.

Chapter 2

Gas exchange system

A gas exchange system previously developed by A. P. Sandford and P. G. Jarvis was used in the experiments. The hardware has undergone only minor changes, but the software has been completely rewritten. Because of this, the emphasis in the discussion that follows will be on the program and algorithms used to control the system. However, a description of the system hardware is given because it is required for understanding the algorithms. Some data on its performance is also provided.

The system is designed to be capable of controlling the molar fractions of CO_2 and water vapour in the bulk air in the chamber. By doing all the calculations in real-time, it can also control both molar fractions at the leaf surface and the CO_2 molar fraction in the intercellular spaces. Leaf or air temperature is controlled. Values of CO_2 flux density, transpiration and conductance are computed and displayed in real-time.

2.1   Hardware

The gas-exchange system is configured as an open differential system. Its air circuit diagram can be divided into three main blocks: air-conditioning gear, leaf-chamber, and measuring instruments (Fig. 2.1). In the following sections each of these blocks, as well as ancillary equipment, are described.
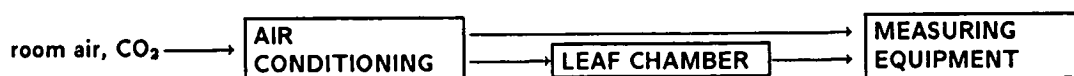
Figure 2.1. Simple block diagram of the air circuit of the gas-exchange system.
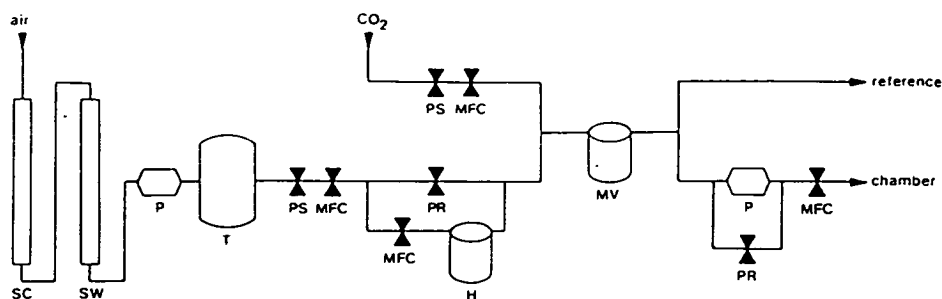
Figure 2.2. Air circuit diagram of air-conditioning block. SC: CO_2 scrubbing column; SW: water vapour scrubbing column; P: diaphragm pump; T: steel tank; H: humidifier; MFC: mass-flow controller; PS: pressure regulator; PR: pressure relief valve; MV: mixing vessel. Detailed diagrams are given by Sandford (1987).

2.1.1 Conditioning of ingoing air

The molar fractions of CO_2, and water vapour of the air going into the chamber can be adjusted by means of mass-flow controllers driven by electrical signals. The flow rate of air at the chamber inlet can also be controlled. A diagram of this 'air-conditioning' part of the system is given in Fig. 2.2.

Room air is pumped through columns of 'soda-lime' (to remove CO_2), and silica-gel and 'drierite' (to remove water vapour). Part of this flow of dry, CO_2-free air bubbles through water kept at 35.0 °C. By mixing these two flows of air, moist CO_2-free air is obtained. This moist air is then mixed with pure CO_2 coming from a cylinder. The molar fractions of CO_2 and water vapour depend on the electrically controlled throughputs of the mass-flow controllers (FC 261, and FC 260; Tylan (UK) Ltd., Swindon, U.K.). A diaphragm pump (B100SE, Charles-Austen Pumps Ltd, Byfleet, Surrey, U.K.) is then used to push the air at a slight over-pressure through another mass-flow controller (Tylan FC 260) and the leaf chamber.

2.1.2 Leaf chamber

The chamber used has a volume of 1250 cm^3. It has a double glazed glass window at the top and is made of nickel-plated brass. The details of its construction and dimensions can be seen in the diagram in Fig. 2.3. The temperature of the leaf chamber is controlled by means of a Peltier unit (14 V, 8 A; 'Cambion' Part No. 803-1008-01, Cambridge Thermionic Corp., Cambridge, Mass., U.S.A.) on which it sits. This unit is driven by a temperature controller (type 070, Eurotherm Ltd., Durrington, West Sussex, U.K.) that
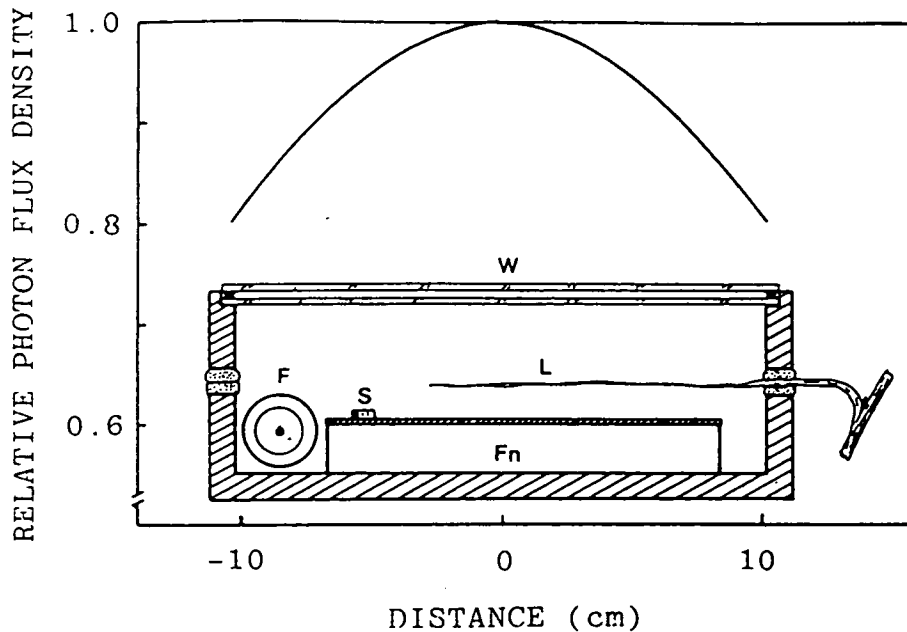
Figure 2.3. Spatial distribution of photon flux density on a horizontal plane situated 50 cm below a vertically positioned metal-halide reflector lamp (Wotan 'power-star'; HQI-R 250 W/NDL; Wotan Lamps Ltd., London). Measured with a Li-Cor cosine corrected PAR sensor (type Li-190SB, Li-Cor Ltd., Lincoln, Nebraska). A diagram of a lengthwise cross-section of the leaf chamber is overlaid. L: leaf, S: light sensor, W: window, F: fan, Fn: fins for heat exchange. Drawn to scale, width of the chamber: 12.4 cm.

uses a thermojunction as sensor. Depending on whether this thermojunction is attached to the enclosed leaf, or left free inside the chamber, either leaf or air temperature is kept constant at a preset value. Ventilation inside the chamber is achieved by means of an axial fan located at the same end as the air inlet and outlet. The speed of the fan is controlled by a variable voltage source.

A silicon photo-diode (type BPW21, R.S. Components Ltd., Corby, Northants, U.K.) is used as a light sensor. This diode is sensitive to 'visible' light but its spectral response is not flat for photon flux density of PAR. It was calibrated for different light sources against a recently calibrated PAR quantum sensor (type Li-190SB, Li-Cor Ltd., Lincoln, Nebraska).

Leaf and air temperatures are measured with small thermojunctions made from 0.1 mm diameter copper and constantan wires. The thermojunctions were kept in contact with the shaded surface of the leaf. An ice-point reference unit (Zeref, Hanovia Ltd., Slough, Berkshire, U.K.) is used for the reference junctions.

2.1.3 Light source

A metal-halide reflector lamp was used as a light source (Wotan 'power-star' HQI-R 250 W/NDL; driven by a choke for 400 W HQI lamps, type IZL; Wotan Lamps Ltd., London). Its spectrum, as seen through the chamber window and the different filters used, is given in Fig. 2.4. Photon flux density at the chamber was controlled by means of reflecting neutral density filters. A heat mirror was always used to prevent overheating of the leaf chamber. The spatial distribution of light under the source was such that the photon flux density at any point within the useful area of the chamber was within ±8 % of that measured using the photo-diode permanently affixed inside the chamber (Fig. 2.3).

2.1.4 Measurement of ingoing and outgoing flows

The water-vapour contents of air at the chamber inlet and outlet are measured by means of two dew-point meters (series 3000, Michell Instruments Ltd., Cambridge, U.K.). The molar concentration of CO_2 is measured with an infra-red gas analyser (URAS 3E, Hartmann & Braun AG, Frankfurt, Germany). This analyser can be used in either a differential mode, or an absolute mode. The pressure difference between the inlets to the IRGA cells is monitored with a differential electronic pressure meter (M-10, Mercury Electronics, Glasgow, U.K.). A double water vapour trap (MGK 1 gas cooler, Waltz Mess- und Regeltechnik, Effeltrich, Germany; type 815 temperature controller, Eurotherm Ltd., Durrington, West Sussex, U.K.; and a custom built d.c. power amplifier) is installed on the sample and reference air lines between the dew-point meters and the IRGA[1]. The flow rate of air through these instruments is controlled by means of manually set rotameters (KDG Flowmeters, Burgess Hill, Sussex, U.K.).

2.1.5 Calibration of the IRGA

The sample and reference cells of the IRGA are split into two sections of 0.95 and 0.05 of the total length. These sections are independent with respect to air flow but constitute a single path for the infra-red radiation. This allows calibration of the differential sensitivity of the IRGA with air of normal CO_2 concentration independently of the background CO_2 concentration. Any change in concentration of CO_2 in the short section of the cell is equivalent to a change of 5 % of its magnitude over the whole path. Compressed air from an aluminium cylinder, and dry CO_2-free air pumped through columns filled with 'soda-lime' and silica gel are used as calibration standards.

---

[1]This cold trap was added after some of the experiments had been done.
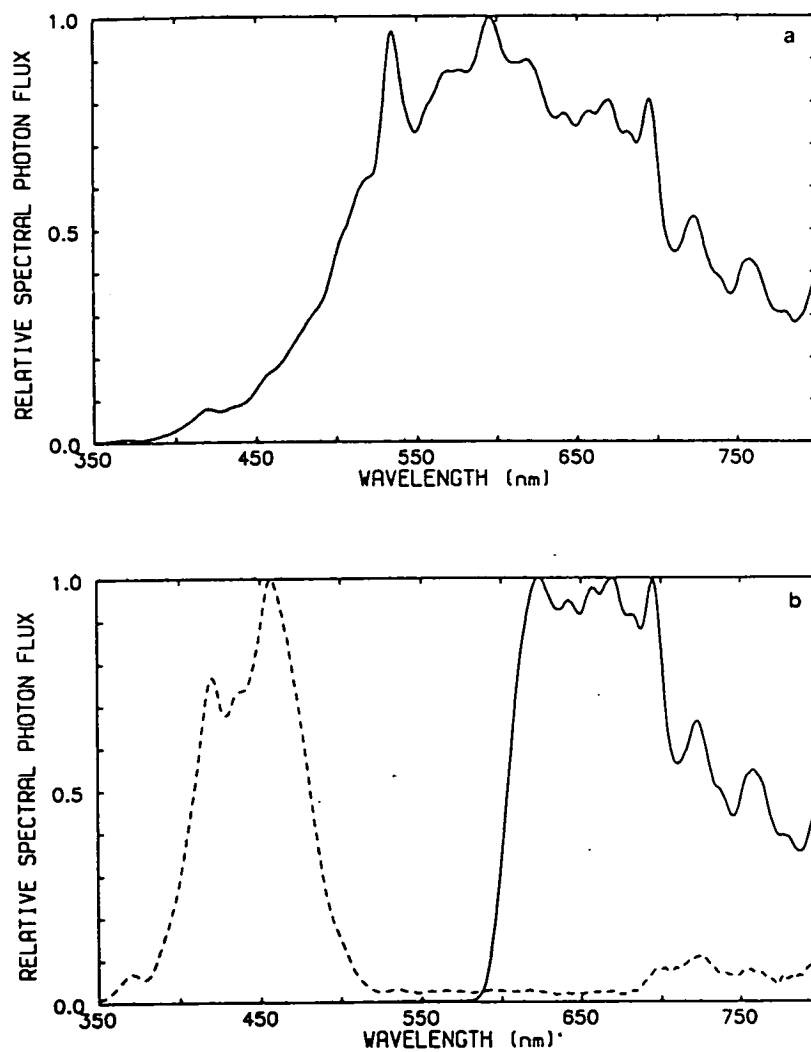
Figure 2.4. Photon spectra of the light sources used in the gas exchange experiments. (a) HQI-R lamp with a heat filter, as seen through the chamber window; (b) with a red filter (——); and with a blue filter (- - - -). Measured with an optical spectrum analyser (model 6800; with a 6100 monochromator, with a 0.9 mm slit installed; and a 6118 photo-tube detector. Monolight Instruments Ltd., Weybridge, Surrey, U.K.).
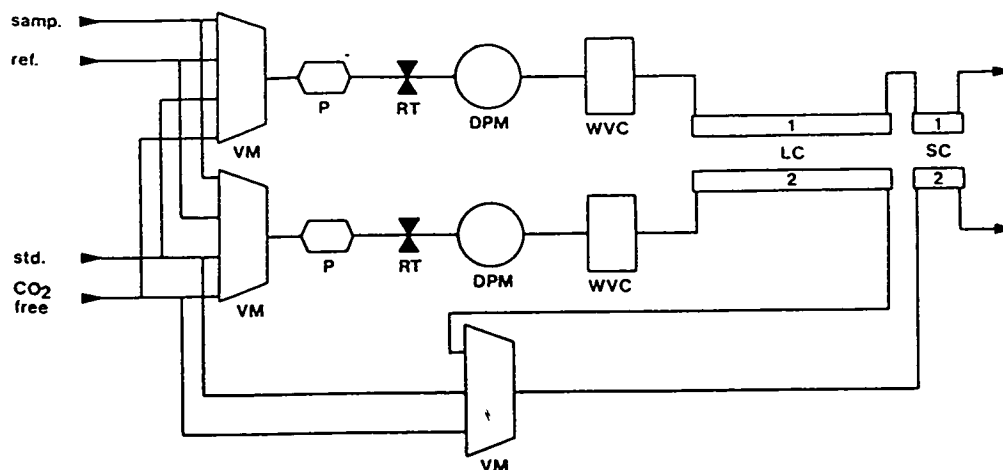
Figure 2.5. Functional diagram of the air circuit used for measurement and calibration. VM: group of valves working as a manifold; P: diaphragm pump; RT: needle valve and rotameter; DPM: dew-point meter; WVC: water vapour condenser; LC1, LC2: long cells of the IRGA; SC1, SC2: short cells of the IRGA. The differential pressure meter, individual solenoid valves, and blow-offs have not been included in the diagram to simplify it. Detailed diagrams are given by Sandford (1987).

The inlets to the cells are switched between the different air sources by means of solenoid valves (Fig. 2.5).

The linearity, sensitivity, and zero offset are checked and adjusted using air of known volume fractions of CO_2. Air of different CO_2 concentrations is obtained by mixing pure CO_2 and dry, CO_2-free air with a set of three gas mixing pumps connected in a cascade (Digamix G27/3F, SA27/3F, and SA18/3F; H. Wösthoff Gmbh, Bochum, Germany).

2.1.6 Data-logging and control

A dedicated personal computer (IBM PC-ATX, IBM United Kingdom International Products Ltd., North Harbour, Portsmouth, U.K.) controls the gas-exchange system using a datalogger (3530B Orion Data Logging System, Solartron Instrumentation Group, Farnborough, Hampshire, U.K.) as an input and output front-end. The datalogger handles both analogue and digital signals, and communicates with the computer through a serial bidirectional data link. Part of the data processing is done on the datalogger (mean of repeated measurements, offset compensation and scaling). The rest of the data processing is done in real-time on the computer. Calculations needed for control also take place in the computer, which sets the outputs of the datalogger that control the mass-flow controllers, valves and pumps.

2.2 Software

I redesigned and rewrote the program that controls the hardware described above with the aim of making it easy to maintain and change. Alterations to the program could be needed to adapt it to changes in the hardware or to the requirements of new experiments. In its use it had to be reliable, fault-tolerant, and provide diagnosis for the most common error conditions arising from hardware faults, software errors and user mistakes. Initially I had no intention of changing data processing or control algorithms. However, during the course of this project I found it necessary to add calculations giving the molar fractions of CO_2 and water vapour at the leaf surface, and the commands for controlling them during experiments. It was also necessary to improve or replace many of the existing control and measurement algorithms.

Two versions of the program exist, one for systems with a water trap before the IRGA, the other for systems in which moist air goes through the gas analyser. The version for systems that include a water trap assumes that when the dew point of the air going through the trap is below the temperature of the trap no humidification occurs. This would be true only if the water trap was bypassed under this condition. In reality what happens is that the air is moistened, but its water content varies depending on the quantity of water remaining inside the trap. When changing from moist to dry air going through the trap, the humidity of the air at its outlet keeps changing for several hours. However, as the saturated molar fraction at the temperature normally used for the trap (1.0 °C) is low, and as this temperature is not far from the maximum cooling of the dew-point meters the error in total molar flow rate is small (<0.5%), even if a bypass is not used.

2.2.1 Algorithms

The design of the program was based on the flow of data. There are two 'kinds' of data: raw data obtained from the sensors, and processed data giving the state of the system and plant leaf. The steps required are (1) acquisition of the raw data from the datalogger, (2) processing of these data to obtain the state of the system, (3) checking the validity of these data, and (4) displaying, printing and storing these data.

In parallel with data acquisition and processing the system must be controlled and calibrated. A calibration is again a data transformation: several sets of raw data acquired after switching valves in different configurations are processed into a set of calibration data expressed at a standard condition. The steps required are then: (1) set valves, (2) acquire raw data, (3) check that data are valid, repeat steps (1) to (3) until all necessary data are available, (4) process the raw data sets into calibration

data, and (5) display, print, and save it.

Control consists of (1) computing the values required for the controlled variables necessary to obtain the requested value of a dependent variable, (2) checking that it is safe to set the values requested, (3) sending the commands to the datalogger. The control algorithm does not use a feedback loop —except through the operator. This decision was made because the response time is long and includes both the response of the measuring system and the measured leaf. Effective control requires intelligence, provided by the human operator.

It is also necessary to prevent conditions dangerous to the integrity of the system or that would affect the validity of data not yet acquired. This is achieved by (1) predicting the danger of an undesirable happening, and by (2) altering the state of the system so as to avert this danger without operator intervention.

Calibration of the dew-point meters

The sensitivity of the dew-point meters is very stable, so only the offset is routinely measured. This calibration is done on its own or concurrently with the IRGA calibration. It is assumed that the offset is a temperature error[2]. The procedure is as follows

- **Zero offset:**
1. Set valves so that both reference and sample DPMs are connected to the reference air stream.
2. *Rebalance the dew-point meters. (Optional.)*
3. Wait long enough to flush air through them and get a steady output.
4. Take a set of readings.
5. The difference between the recorded dew-points gives the zero offset.

During a calibration, when reference air is flowing through both dew point-meters, the mean of the dew-points measured by them is used as the reference to calculate a zero offset for each of them (i.e. half of the total zero offset is attributed to each dew-point meter). When using the calibration data, these offset corrections are applied to T_{in}^{dew} and T_{out}^{dew}. These dew-point temperatures and current atmospheric pressure are used to compute χ_{in}^{w} and χ_{out}^{w}.

---

[2]In the previous version of the program, written by A. P. Sandford, it was assumed to be a water vapour molar fraction error.

Differential IRGA calibration

The following algorithm and equations can only be used with infra-red gas analysers having a split sample cell. This 'short-cell calibration' method is based on that described by Thorpe (1978). Calibration consists of two main steps: the calculation of the zero offset, and the calculation of the sensitivity or gain. As the differential offset and sensitivity of an IRGA depend on the background χ_{in}^c it is necessary either to recalibrate each time χ_{in}^c is altered, or to correct calibration data for this change in χ_{in}^c. To achieve this second option, calibration data are stored expressed at a standard $\chi_{in}^c = 350$ μmol mol^{-1}, and when used, corrected for the actual value of χ_{in}^c. The actual procedure is:

- **Zero offset:**
1. Set valves so that the long and short sections of the reference and sample cells of the IRGA are connected to the reference air stream.
2. Wait long enough to flush the full length of the sample cell.
3. Take a set of readings.
4. The IRGA output is its zero offset (s_{nul}).
- **Sensitivity:**
5. Set valves so that the short sample cell is connected to the CO_2-free air source.
6. Wait long enough to flush the short sample cell.
7. Take a set of readings, getting s_{free}.
8. Set valves so that the short sample cell is connected to a source of air of known CO_2 molar fraction.
9. Wait long enough to flush the short sample cell.
10. Take a set of readings, getting s_{in}.
11. Do sensitivity calculations using equations 2.1 or 2.2–2.4.
12. Compute error of mass flow meters using equation 2.5.
- **Standardize calibration:**
13. Calculate offset at $\chi_{in}^c = 350$ μmol mol^{-1} using equation 2.7.
14. Calculate sensitivity at $\chi_{in}^c = 350$ μmol mol^{-1} using equation 2.9.

If sensitivity is computed from 'standard' air from a cylinder then it is given by:

$$\beta = \frac{s_{in} - s_{free}}{\ell \, \chi_{cyl}^c}. \tag{2.1}$$

However, to compute the sensitivity of the IRGA using the reference air stream as a standard, it is first necessary to calculate the water vapour content of the reference air

at the IRGA:

$$\chi^{w}_{in,IRGA} = \begin{cases} \chi^{w*}_{trap}, & \text{with water trap if } \chi^{w*}_{trap} < \chi^{w}_{in}, \\ \chi^{w}_{in}, & \text{otherwise,} \end{cases} \tag{2.2}$$

and then to get an estimate of the CO_2 concentration from the measured flow rates:

$$\chi^{c}_{in,IRGA} = \frac{J^{c}_{tot}}{(J^{dry}_{tot} + J^{c}_{tot})}(1 - \chi^{w}_{in,IRGA}) \tag{2.3}$$

and finally to obtain the differential sensitivity as:

$$\beta = \frac{s_{in} - s_{free}}{\ell\, \chi^{c}_{in,IRGA}}. \tag{2.4}$$

In this case $s_{in} \equiv s_{nul}$, and steps 8 to 10 of the algorithm are redundant.

If the sensitivity is computed using air from a cylinder then it is possible to measure the error in the mixing ratio of the mass-flow controllers that are used to mix the air going into the chamber:

$$\chi^{c}_{error} = \frac{s_{nul} - s_{free}}{\ell\,\beta} - \chi^{c}_{in,IRGA}, \tag{2.5}$$

for which $\chi^{c}_{in,IRGA}$ is calculated using equations 2.3 and 2.4. If standard air from a cylinder is not used, step 12 of the algorithm must be skipped.

In this case it is also possible to get an absolute value for χ^{c}_{in}:

$$\check{\chi}^{c}_{in} = \frac{s_{nul} - s_{free}}{\ell\,\beta}. \tag{2.6}$$

The dependence of s_{nul} on χ^{c}_{in} is taken into account by means of an empirically measured linear relationship. The following equation is used to standardize the measured offset to $\chi^{c}_{in}=\chi^{c}_{std}$, where $\chi^{c}_{std}=350 \ \mu$mol mol^{-1}:

$$\check{s}_{nul} = s_{nul} + k_o\left(\chi^{c}_{std} - \check{\chi}^{c}_{in}\right) \tag{2.7}$$

and when it is used it is adjusted for the current value of χ^{c}_{in}:

$$s_{nul} = \check{s}_{nul} + k_o\left(\chi^{c}_{in} - \chi^{c}_{std}\right). \tag{2.8}$$

The differential sensitivity or gain of the IRGA also depends on the background χ^{c}_{in} and can be corrected using a method adapted from that proposed by Thorpe (1978).

Standardization to $\chi_{in}^c = 350 \mu$mol mol^{-1} is done as:

$$\tilde{\beta} = \beta \frac{\check{\chi}_{in}^c + k_s}{\chi_{std}^c + k},$$

(2.9)

where k_s and k are empirical constants obtained by measuring the sensitivity at different values of χ_{in}^c. When used, this standardized sensitivity is first adjusted to the current value of χ_{in}^c:

$$\beta = \tilde{\beta} \frac{\chi_{std}^c + k_s}{\chi_{in}^c + k}.$$

(2.10)

- **Using a calibration**
1. Compute offset at current χ_{in}^c.
2. Compute sensitivity at current χ_{in}^c.
3. Compute $\Delta \chi_{IRGA}^c$ from raw voltage reading using equation 2.11.

A differential reading in μmol mol^{-1} is computed as:

$$\Delta \chi_{IRGA}^c = \frac{s_{samp} - s_{nul}}{\beta},$$

(2.11)

where s_{samp} is the current signal from the IRGA, and s_{nul} and β have been computed for the current value of $\chi_{in,IRGA}^c$ from stored calibration data using equation 2.26 below.

Calculations of the leaf and chamber states

The equations used in the calculations in sections 2.2.1 and 2.2.1 are based on those given by von Caemmerer & Farquhar (1981). Some of the equations have been re-arranged for computational reasons. In what follows their presentation follows the program listing and not the original sources.

There are several assumptions involved in the use of these equations:

- The system (leaf + chamber) is in a steady-state.

- Flux densities of water vapour and CO_2 are the same over the leaf surface(s) involved in gas exchange.

- Gradients of water vapour and CO_2 molar fractions are the same over the leaf surface(s) involved in gas exchange.

  These assumptions imply that:

o Stomatal conductance is the same throughout the leaf surface(s).

o Boundary layer conductance is the same throughout the leaf surface(s).

o Temperature is the same in all the leaf.

All the results depend on the first assumption being valid. Non steady-state conditions require more complicated calculations than those described here. Calculations for non steady-state conditions must take into account the dynamic characteristics of the gas-exchange system (time constant, and lag). For a given A and E, these characteristics affect the observed concentration differences, and their rate of change. Using steady-state assumptions under non steady-state conditions leads to the underestimation of the magnitude and speed of changes in A and E.

The time constant of a system depends on the volume of the chamber and the flow rate of air through it, the lag depends on the volume of air in the tubing between the chamber and the measuring instruments and the flow rate through this tubing. Further complications are added by adsorption of water and CO_2 on the walls of the chamber and tubing. In practice, before a gas-exchange system can be used under non steady-state conditions, its dynamic behaviour must be measured.

The second and third assumptions only affect the calculated conductances, and the concentrations internal to the boundary layer. Although these equations assume a *single* gas exchange surface, they can also be applied to amphistomatous leaves if stomatal and boundary layer conductances are the same on both sides. In hyper- or hypostomatous leaves the boundary layer conductance to be used in the calculations is that of the single surface over which gas exchange is taking place. In symmetrical amphistomatous leaves the boundary layer conductance to be used is that of both leaf faces in parallel. These calculations are *not* rigorous for asymmetrical amphistomatous leaves, or leaves having a patchy distribution of stomatal aperture. In practice, these assumptions are seldom true, and so the calculated conductances and molar fractions are only approximations to their mean values over the surface of the leaf. They differ from the true mean because non-linear relationships are involved in their computation.

Flow rates. The total flow rate of dry, CO_2-free air (J_{tot}^{dry}), the dry air flow rate at the humidifier inlet (J_{hum}^{dry}), the CO_2 flow rate (J_{tot}^{c}), and the moist air flow rate at the chamber inlet (J_{in}^{air}) are measured. The diagram in Fig. 2.2 shows the places in the system where the mass-flow controllers used to measure these flow rates are located. The water vapour flow rate evaporating from the humidifier is computed as

$$J_{hum}^{w} = \frac{J_{hum}^{dry} \chi_{hum}^{w*}}{1 - \chi_{hum}^{w*}}$$

(2.12)

and the total moist air flow rate at the outlet of the 'mixing tray' ($J_{\text{tot}}^{\text{air}}$) is calculated from the other flow rates as

$$J_{\text{tot}}^{\text{air}} = J_{\text{tot}}^{\text{dry}} + J_{\text{tot}}^{\text{c}} + J_{\text{hum}}^{\text{w}}. \tag{2.13}$$

Water molar fractions, conductance and molar flux density. The molar fractions of water vapour in the air at the chamber inlet ($\chi_{\text{in}}^{\text{w}}$), and outlet ($\chi_{\text{out}}^{\text{w}}$) are directly calculated from the measured dew-points and ambient pressure. The molar fraction of water vapour in the intercellular air space is computed assuming that it is saturated at the leaf temperature,

$$\chi_{\text{i}}^{\text{w}} = \chi_{\text{l}}^{\text{w*}}. \tag{2.14}$$

The air in the chamber is assumed to be well stirred so,

$$\chi_{\text{a}}^{\text{w}} = \chi_{\text{out}}^{\text{w}}. \tag{2.15}$$

The apparent molar fraction of water vapour in the 'dry CO_2-free' air is computed as:

$$\chi_{\text{dry}}^{\text{w}} = \frac{\chi_{\text{in}}^{\text{w}} J_{\text{tot}}^{\text{air}} - J_{\text{hum}}^{\text{w}}}{J_{\text{tot}}^{\text{dry}}}, \tag{2.16}$$

where no correction is needed for $\chi_{\text{dry}}^{\text{w}}$ because this flow of water vapour is included in the measured $J_{\text{tot}}^{\text{dry}}$. $\chi_{\text{dry}}^{\text{w}}$ reflects both the water vapour content in the dry air, the efficiency of the humidifier, and errors in the calibration of the mass-flow controller used to set $J_{\text{hum}}^{\text{dry}}$. The normal procedure is to calibrate this mass-flow meter for an apparent humidifier efficiency of 100 %.

Relative humidity of the bulk air in the chamber is

$$h_{\text{a}} = \frac{\chi_{\text{a}}^{\text{w}}}{\chi_{\text{a}}^{\text{w*}}} \tag{2.17}$$

and the bulk air to leaf water deficit is

$$D_{\text{a}}^{\text{w}} = \chi_{\text{l}}^{\text{w*}} - \chi_{\text{a}}^{\text{w}}. \tag{2.18}$$

The calculation of the water vapour flux density from the leaf to the air in the chamber takes into account the difference between $J_{\text{in}}^{\text{air}}$ and $J_{\text{out}}^{\text{air}}$ due to the added water vapour:

$$E = \frac{J_{\text{in}}^{\text{air}}(\chi_{\text{out}}^{\text{w}} - \chi_{\text{in}}^{\text{w}})}{(1 - \chi_{\text{out}}^{\text{w}}) S}. \tag{2.19}$$

The total conductance to water vapour is

$$g_t^w = \frac{E[1 - (\chi_a^w + \chi_i^w)/2]}{\chi_i^w - \chi_a^w},\qquad (2.20)$$

where the factor $1 - (\chi_a^w + \chi_i^w)/2$ is a correction for the effect of mass flow.

Leaf conductance to water vapour (stomatal and cuticular conductances in parallel) is computed as

$$g_l^w = \frac{g_t^w \, g_b^w}{g_b^w - g_t^w},\qquad (2.21)$$

where g_b^w is the boundary layer conductance to water vapour previously measured for a replica of the leaf.

The molar fraction of water vapour at the leaf surface is

$$\chi_s^w = \chi_a^w + (\chi_i^w - \chi_a^w)\frac{g_t^w}{g_b^w},\qquad (2.22)$$

the water vapour deficit at the leaf surface is

$$D_s^w = \chi_l^{w*} - \chi_s^w,\qquad (2.23)$$

and the relative humidity at the leaf surface is

$$h_s = \frac{\chi_s^w}{\chi_l^{w*}},\qquad (2.24)$$

assuming that the air at the leaf surface is at the same temperature as the leaf.

CO_2 molar fractions, conductance and molar flux density. The molar fraction of CO_2 in the air at the chamber inlet (χ_{in}^c) is measured only during calibrations[3], otherwise it is computed from the flow rates and the error observed during the calibration as

$$\chi_{in}^c = \frac{J_{tot}^c}{J_{tot}^{air}} + \chi_{error}^c.\qquad (2.25)$$

Any change in water vapour content affects the molar fraction of the other components of the air, so if a water trap is used, the molar fraction of CO_2 at the IRGA is different

---

[3] the program could be easily modified to take both absolute and differential measurements of the CO_2 concentration for every measurement, but this would increase the time necessary for getting each data point.

to that at the chamber inlet.

$$\chi_{in,IRGA}^c = \begin{cases} \chi_{in}^c \frac{1-\chi_{trap}^{w*}}{1-\chi_{in}^w}, & \text{with water trap if } \chi_{trap}^{w*} < \chi_{in}^w, \\ \chi_{in}^c, & \text{otherwise.} \end{cases} \qquad (2.26)$$

The calculation of the molar fraction at the chamber outlet also depends on whether a water trap is used or not.

$$\chi_{out}^c = \begin{cases} (\chi_{in,IRGA}^c + \Delta\chi_{IRGA}^c)\frac{1-\chi_{out}^w}{1-\chi_{trap}^{w*}}, & \text{with water trap if } \chi_{trap}^{w*} < \chi_{out}^w, \\ \chi_{in,IRGA}^c + \Delta\chi_{IRGA}^c, & \text{otherwise.} \end{cases} \qquad (2.27)$$

The difference in molar fraction of CO_2 between the chamber inlet and the chamber outlet ($\Delta\chi_{in-out}^c$), is different to that measured at the IRGA ($\Delta\chi_{IRGA}^c$) when a water trap is used, but can always be calculated as

$$\Delta\chi_{in-out}^c = \chi_{out}^c - \chi_{in}^c. \qquad (2.28)$$

The flux density of CO_2 between the leaf and the air in the chamber is given by

$$A = \frac{-J_{in}^{air}\,\Delta\chi_{in-out}^c\,(1-\chi_{in}^w)}{(1-\chi_{out}^w)\,S} - E\,\chi_{in}^c \qquad (2.29)$$

which includes corrections for both the difference between J_{in}^{air} and J_{out}^{air} and the dilution effect of the flow of water on the molar fraction of CO_2.

The total conductance to CO_2 is calculated from the conductances to water vapour taking into account the different diffusivities of water vapour and CO_2, and the only partially diffusive process in the boundary layer:

$$g_t^c = \left(\frac{1.60}{g_l^w} + \frac{1.37}{g_b^w}\right)^{-1}. \qquad (2.30)$$

The molar fraction of CO_2 in the intercellular space of the leaf must be calculated taking into account the effect of the flow of water on the flow of CO_2, a trace gas:

$$\chi_i^c = \frac{(g_t^c - E/2)\,\chi_a^c - A}{g_t^c + E/2}. \qquad (2.31)$$

The molar fraction of CO_2 at the leaf surface is similarly calculated, using the equation

proposed by Ball (1987):

$$\chi_s^c = \frac{(g_b^c - E/2)\,\chi_a^c - A}{g_b^c + E/2}. \tag{2.32}$$

Control algorithms

As stated above, after using the system for a while it was realized that many of the control algorithms were not working as expected and they were modified to make them more robust with respect to various calibration and operator errors. The possibility of controlling several new variables was added. The algorithms were made as independent from the system hardware configuration as possible. The algorithms used are given below.

Controlling humidity Only the first algorithm from this group assumes an open gas-exchange system. The others are equally suitable for both closed loop and open gas-exchange systems.

- **Control χ_a^w by altering χ_{in}^w**
  1. Check requested χ_a^w against chamber wall temperature and room temperature, and ignore requests that would lead to condensation.
  2. Compute minimum dew-point that can be measured as room temperature minus the maximum cooling that the dew-point meters can achieve.
  3. Check the requested χ_a^w against minimum dew-point that can be measured, and if necessary adjust the requested χ_a^w to keep the dew-point at least 5 °C above this minimum value.
  4. Estimate E under the new condition, and from it, the difference in water vapour molar fraction between the air streams going into, and coming out of the chamber.
  5. Compute required χ_{in}^w as the requested χ_a^w minus the difference resulting from expected transpiration.
  6. Check the required χ_{in}^w against the minimum dew-point that can be measured, and if necessary adjust the air flow rate through the chamber to keep χ_{in}^w at a value that would keep the dew-point at least 2 °C above this minimum.
  7. Compute required change in χ_{in}^w.
  8. If this change is small request a relative change in the value of χ_{in}^w, otherwise request an absolute value for χ_{in}^w.

- **Control χ_s^w by altering χ_a^w**
  1. Compute required χ_a^w assuming that χ_a^w/χ_s^w remains unchanged.
  2. Request required χ_a^w.

- **Control h_a by altering χ_a^w**
1. Compute required χ_a^w from requested h_a and χ_a^{w*} at current P_{atm} and T_a.
2. Request required χ_a^w.

- **Control h_s by altering χ_s^w**
1. Compute required χ_s^w from requested h_s and χ_l^{w*} at current P_{atm} and T_l.
2. Request required χ_s^w.

- **Control D_a^w by altering χ_a^w**
1. Compute required χ_a^w from requested D_a^w and χ_l^{w*} at current P_{atm} and T_l.
2. Request required χ_a^w.

- **Control D_s^w by altering χ_s^w**
1. Compute required χ_s^w from requested D_s^w and χ_l^{w*} at current P_{atm} and T_l.
2. Request required χ_s^w.

- **Control E by altering χ_a^w**
1. Compute required χ_a^w from requested E, χ_l^{w*} at current P_{atm} and T_l, current $\chi_{in}^w - \chi_{out}^w$, and current E, i.e. assuming no change in g_l^w.
2. Request required χ_a^w.

Control of CO_2 molar fraction

- **Control χ_a^c by changing χ_{in}^c**
1. Guess what the value of A will be after the change in χ_a^c takes place: if requested $\chi_a^c > 60$ μmol mol^{-1} and $A > 0.5$ μmol m^{-2} s^{-1} then assume that A is a linear function of χ_a^c, otherwise assume that A is not going to change.
2. Check whether expected value of A is negative, and if so set it to zero.
3. Compute J_{out}^{air} from J_{in}^{air}, expected A, current E, and leaf area.
4. Compute required χ_{in}^c to get the requested χ_a^c taking into account the change in total flow ($J_{out}^{air} - J_{in}^{air}$).
5. *If $\chi_{out}^c - \chi_{in}^c$ would be out of the IRGA sensitivity range, then adjust J_{in}^{air} (NOT IMPLEMENTED).*
6. Compute required change in χ_{in}^c.
7. If this change is small request a relative change in the value of χ_{in}^c, otherwise request an absolute value for χ_{in}^c.

- **Control χ_i^c by changing χ_{in}^c**

1. Check whether current g_l^w is high enough to yield a reliable estimate of χ_i^c. If not ignore the request to change χ_i^c.

2. Guess what the value of A will be after the change in χ_i^c takes place: if 50 μmol mol^{-1} > requested χ_i^c > 280 μmol mol^{-1} and A > 0 then assume that A is a linear function of χ_i^c, otherwise assume that A is not going to change.

3. Compute total conductance to CO_2.

4. Compute required χ_a^c taking into account the effect of E on χ_i^c.

5. Check whether expected value of A is negative, and if so set it to zero.

6. Compute J_{out}^{air} from J_{in}^{air}, expected A, current E, and leaf area.

7. Compute required χ_{in}^c to get the requested χ_a^c taking into account the change in total flow ($J_{out}^{air} - J_{in}^{air}$).

8. *If $\chi_{out}^c - \chi_{in}^c$ would be out of the IRGA sensitivity range, then adjust J_{in}^{air} (NOT IMPLEMENTED).*

9. Compute required change in χ_{in}^c.

10. If this change is small request a relative change in the value of χ_{in}^c, otherwise request an absolute value for χ_{in}^c.

- **Control χ_s^c by changing χ_a^c**

1. Compute required χ_a^c, assuming that χ_s^c/χ_a^c is not going to change.

2. Request required χ_a^c.

Runtime error checking

Data are checked for the following conditions: water condensation, wrong CO_2 flow rate, wrong dry air flow rate, wrong air flow rate through the humidifier, wrong air flow rate through the chamber, humidifier temperature too low, chamber temperature too hot, pressure imbalance between IRGA cells, no wind in chamber, moist 'dry air', and data set not valid. Of these conditions the only one that is dealt with automatically is water condensation.

- **Test for error conditions**

1. Check that the data set is valid (not marked as not valid because of problems during data acquisition or calculation).

2. Compare dew-point at χ_a^w with the temperature of the chamber wall and room temperature, using a safety margin of 2.5 mmol mol^{-1}.

3. Compare measured flow rates against those requested.

4. Check that water temperature in the humidifier is close to the set point.

5. Check that chamber air temperature is not too high.

6. Check that air temperature inside the measuring rack is not too high.

7. Check that there is no pressure difference between the cells of the IRGA.

8. Infer whether the internal chamber fan is working or not by comparing the air temperature and wall temperature in the chamber.

9. Check that 'dry air' is not moist.

When danger of, or actual, condensation is detected the following algorithm is used to recover:

1. Select the lowest temperature from room or chamber wall temperature.

2. Use this temperature to find out whether there is a danger of water condensation, or that condensation has already occurred.

3. If there has been condensation then set the air flow rate through the humidifier to zero to get very dry air to remove liquid water from the system, otherwise decrease χ_{in}^{w} just enough to get a value of χ_{a}^{w} slightly less than that which would trigger a 'danger of condensation' state.

2.2.2 Implementation

The software includes two programs: runexper and lookdata. The first one is used to control the system, and acquire and process data in 'real time'. The second one can be used to reprocess and look at data previously saved to a disk file. There are two programs because I decided that the best approach was to save the raw data instead of the processed data, in contrast to what was done in the program written by A. P. Sandford. The rationale is that doing so adds both flexibility and safety, without increasing the store space required. It is safer because it allows the errors in the calculations to be fixed. It is more flexible because it allows, in some experiments, the measurement of g_{b}^{w} and leaf area after taking gas-exchange data. It also makes it possible to measure the sensitivity of the results to errors in the measurement of g_{b}^{w} and leaf area, or in the calibrations.

The programs were written in Modula-2 (Logitech Modula-2 Development System, Version 3.0; Logitech Inc., Fremont, California, U.S.A.). This was done because it is a language closely related to Pascal which was used in the original program written by A. P. Sandford. The program was totally rewritten, and redesigned. The old program was badly structured and had too many global variables. The data variables in the new programs are structured according to the data flow, and the procedures are grouped in modules according to the position of their use in the data flow and their degree of independence from the hardware configuration of the system. All the code that depends

on the actual data-logger is in a few modules and is not spread all over the program listing. The same is true for those parts that depend on the gas-exchange system being of an open design. Output is handled independently from data processing. Having followed a modular design, all code common to both programs is not duplicated. In this way both programs are simultaneously updated when changes are introduced.

A very simple change that had a very important effect on the quality of the data obtained from the system was to use in the calculations the median of three consecutive raw data measurements, or of five measurements in the case of calibrations. This greatly reduced random errors, and, as data transmission rate between the computer and datalogger was increased, it had only a small effect on the total time required to get a set of measured values.

The listings were written using meaningful variable names, and further comments have been added when the text of the program was not clear enough. Each file has a header where a record of its history is kept. When several versions of the same module exist, they coexist in a single file as comments. These modules can be interconverted between different versions by means of the program M2VERS. Some versions are useful for debugging or testing, others reflect the changes necessary for different hardware, such as the presence or absence of a water trap before the IRGA.

The source code of the programs is provided in the diskette attached to this thesis. Table 2.1 gives a brief description of the contents of the modules specific to this program. The listings of these modules add up to more than 5500 lines of text. Several other 'library' modules were written or adapted to be used in these programs, but their use is not limited to them.

2.3 Performance

Having described the hardware and software of the gas-exchange system I am now going to give some data on its performance. The steady-state performance of the system is shown in Fig. 2.6. These data were measured with an empty gas-exchange chamber with the system running without intervention of an operator and they show the stability of χ_a^w and χ_a^c. χ_a^c displayed oscillations with an amplitude of less than 1 μmol mol^{-1}, while χ_a^w drifted approximately 0.2 mmol mol^{-1} in 5 h.

The dynamic response of the gas-exchange system was measured by following the time course of the IRGA output signal after a step change in concentration. As the volume of air in the reference and sample branches of the system's air circuit is different, a step change in χ_{in}^c reaches the IRGA cells out of phase, and produces a huge swing in the differential output. In a test done by changing χ_{in}^c from 350 to 600 μmol mol^{-1} a

Table 2.1. Partial list of modules from the program used to control the gas-exchange system (`runexper`), and from that used to reprocess data (`lookdata`).

| MODULE	Description	Versions
RunExperiment	Main (program) module of program used to control the system during an experiment and to acquire data. Main time loop and menu.	—
LookData	Main (program) module of program used to reprocess raw data saved during an experiment.	—
DataTypes	Declarations of data TYPES used in more than one module.	—
Logger	Communications with the data-logger.	Normal, Testing
DataAcquisition	Measurement of raw data.	NoTrap, WaterTrap
DataProcesing	Computation of system state from raw data and calibration data.	NoTrap, WaterTrap
Calibration	Calibration of IRGA and dew-point meters.	NoTrap, WaterTrap
StandariseIRGA	Correction of differential IRGA calibrations for differences in the background CO_2 concentration.	—
PressureBalancing	Rebalancing of air flow rate through IRGA cells to keep a null pressure difference between them.	—
SystemControl	Control of mass-flow controllers, valves, and pumps.	Normal, Testing
RefControl	Control of molar fractions of the air going into the chamber.	—
ExpControl	Control of derived variables.	—
Check	Test system state data for error conditions, and provide automatic recovery for some of them.	Run, Look
ErrorHandler	Display error messages and warnings, and emergency shut-down.	Run, Look
DataIO	Input and output of raw data to/from disk files.	—
CalibIO	Input and output of calibration data to/from disk files.	—
Screens	Data output to the CRT screen and printer.	—
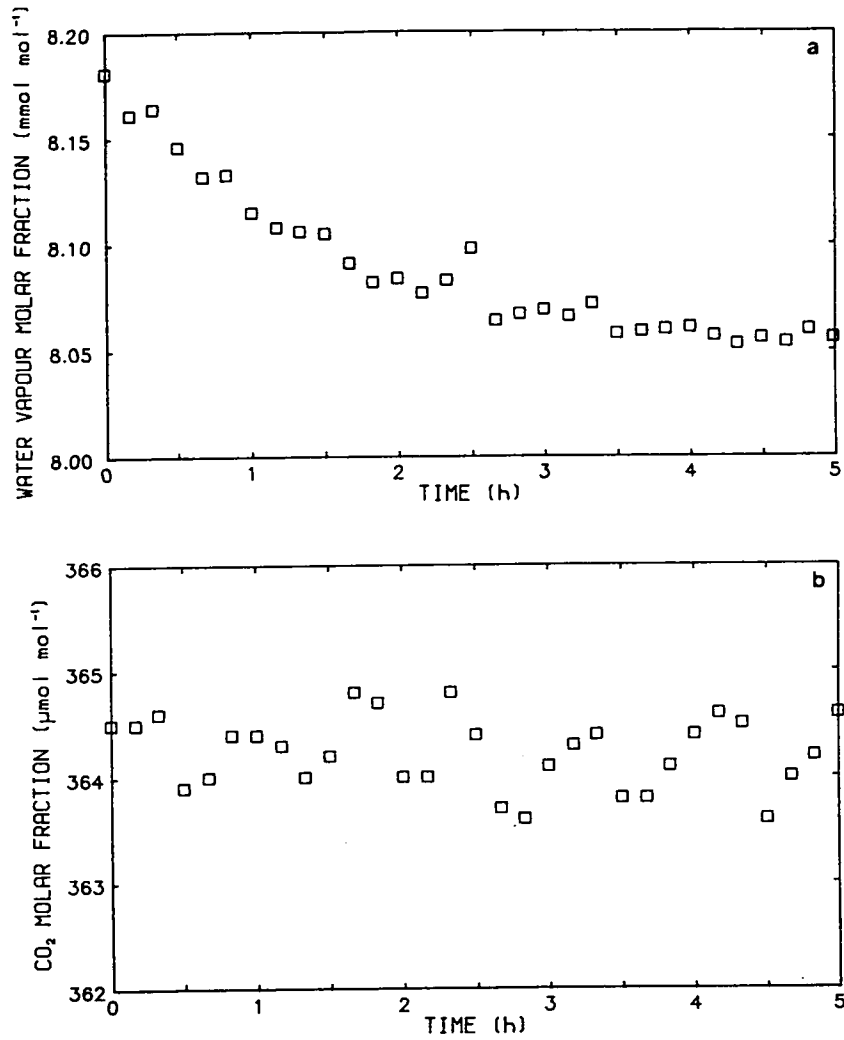
Figure 2.6. Steady-state performance of the gas-exchange system running without intervention of an operator and with an empty leaf chamber. Time course of (a) water vapour molar fraction (χ_a^w), and (b) CO_2 molar fraction (χ_a^c).

new steady-state was reached 5 min after a step change in CO_2 concentration, and the lag before any change was observed in the output was 23 s ($J_{in}^{air} = 2$ mmol s^{-1}, $J_{tot}^{air} = 4$ mmol s^{-1}). The raw output also displayed a slight change in the differential offset of the IRGA caused by the change in background CO_2 concentration.

The errors in the measurements of A and E depend on the area of the leaf or leaves enclosed in the chamber, and on the flow rate of air through the chamber (J_{in}^{air}). The short term noise, measured as the spread of 5 consecutive readings taken within 5 min, for a leaf with an area of 50 cm^2 and $J_{in}^{air} = 2$ mmol s^{-1} was for A approximately 0.2 μmol m^{-2} s^{-1}, and for E approximately 0.01 mmol m^{-2} s^{-1} ($T_l = 20$ °C, $D_a^w \approx 8$ mmol mol^{-1}, and $\chi_a^c \approx 350$ μmol mol^{-1}). This short term random noise can be easily removed from the data by smoothing it using the median of 3 or 5 measurements instead of individual data points. In contrast, measurement errors caused by errors in the calibrations of the IRGA and dew-point meters cannot be eliminated in this way.

The coefficients of variability, from a set of 19 IRGA calibrations done during a single day and under constant background CO_2 concentrations, were 0.64 % for the sensitivity or gain, and 1.18 % for the offset. But a closer look at the data as displayed in the box diagrams in Fig. 2.7 shows that errors are not normally distributed —there were outliers, and the distribution for the sensitivity was skewed. This variability includes the drift of the IRGA throughout a day and measurement errors during calibration.

When altering χ_{in}^c, whether we have to recalibrate the IRGA or not depends on how well the corrections incorporated in the program are able to compensate for the effects of the background CO_2 molar fraction. For a set of 27 calibrations measured at different values of χ_{in}^c, the standardized differential gain of the IRGA ($\tilde{\beta}$) was insensitive to χ_{in}^c, and the standardized differential offset ($\tilde{s}_{nul}$) decreased less than 2 % of the full-scale signal for a change in χ_{in}^c of 600 μmol mol^{-1} (Fig. 2.8). These results were obtained using values measured more than four years earlier for the coefficients in Equation 2.9, and for that in Equation 2.7 a value measured 18 months earlier. The decrease of $\tilde{s}_{nul}$ with χ_{in}^c can be corrected by updating the value of the constant used in the calculations. However, the error observed represents an error of only 0.33 μmol mol^{-1} per 100 μmol mol^{-1} of change in χ_{in}^c.

During the course of the experiments, the IRGA was recalibrated when χ_{in}^c was altered by more than 50 μmol mol^{-1} because, in this case, the standardization procedure would not be able to completely correct for the sensitivity of the IRGA to χ_{in}^c. The IRGA was also recalibrated whenever the room temperature changed by more than 5 °C. The dew-point meters were recalibrated (offset only) when T_{in}^{dew} changed by more than 5 °C. If χ_{in}^c and χ_{in}^w were not altered significantly, calibrations were repeated at least every six hours to compensate for the usually very small drift of the IRGA and

a

DIFFERENTIAL OFFSET (V)

b

DIFFERENTIAL GAIN (V/mol)
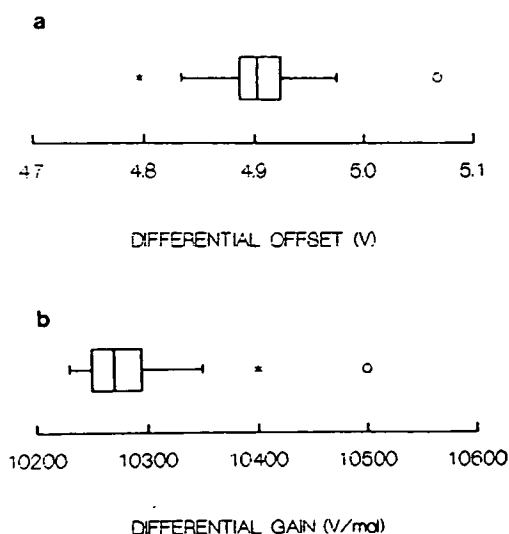
Figure 2.7. Box diagrams for the IRGA calibration data measured during a single day, and under the same reference CO_2 molar fraction (χ_{in}^c=365 μmol mol^{-1}). (a) standardized differential offset ($\tilde{s}_{nul}$), and (b) standardized differential gain ($\tilde{\beta}$) of the IRGA. In a box diagram the crossbar at the center of the box is the *median*, the length of the box is the *fourth spread*, the lines extending from the end of the box give the *tail length*, and * or o indicate the location of *outliers* (see Emerson & Strenio, 1983).

dew-point meters.

The performance of the gas-exchange system is satisfactory but it could be further improved. The dynamic response of the system to changes in the molar fractions in the reference air could be improved by putting a flask in the reference branch of the air circuit to balance the volume of the chamber, and by keeping a fixed ratio between the air flow rates through the chamber and this flask. This would make differential measurements insensitive to step changes in χ_{in}^c and χ_{in}^w which would allow much easier control of the system, and with some limitations would also allow the measurement of the dynamics of plant response to these changes. This change would also improve the rejection of noise in χ_{in}^c by making the whole gas-exchange system truly differential.

Another significant improvement would be to have an environmental chamber to control the conditions (I, χ_a^w, χ_a^c, and T_a) in which the whole plant is kept independently of those in the room were the measuring instruments are located. This would make it possible to use extreme environmental conditions without affecting the instruments, and what is more important, to keep the whole plant in a homogeneous and known environment.
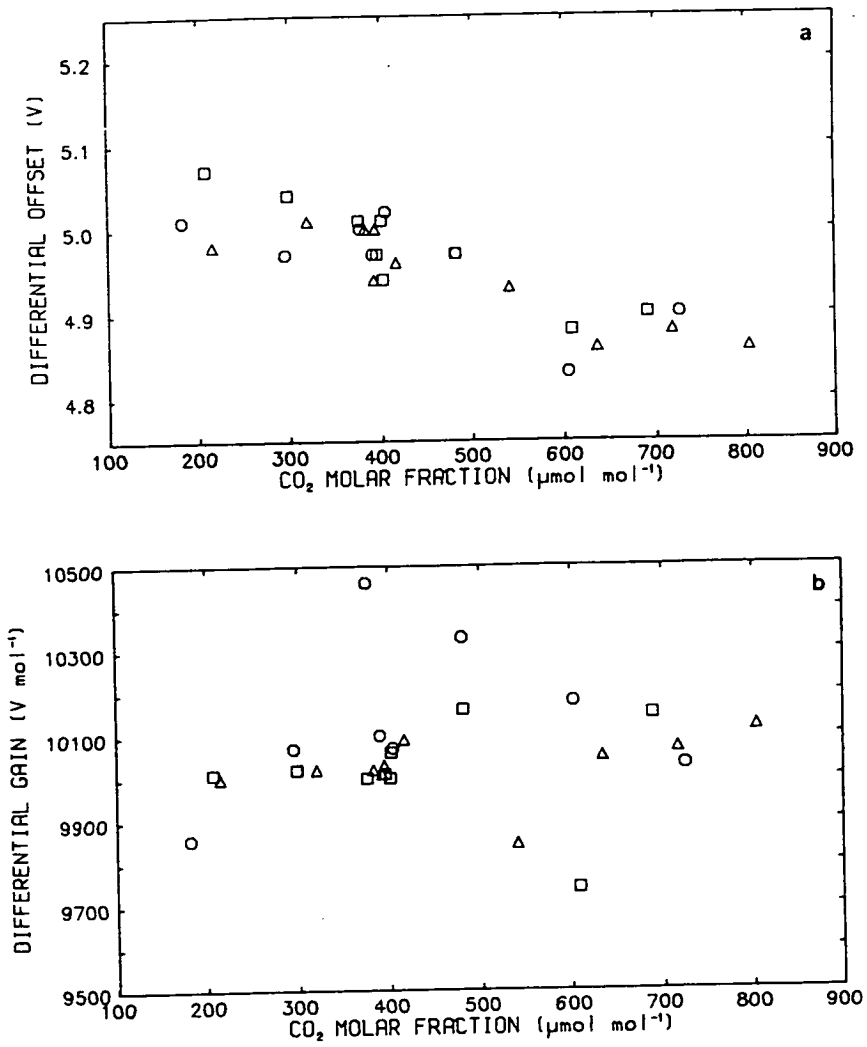
Figure 2.8. Sensitivity of the standardized IRGA calibration to the background CO_2 concentration. Plots of (a) the differential offset ($\tilde{s}_{nul}$), and (b) the differential gain or sensitivity ($\tilde{\beta}$) of the IRGA vs. the reference molar fraction of CO_2 (χ_{in}^c). Values shown were standardized to $\chi_{in}^c = 350$ μmol mol^{-1}. Data from 27 calibrations done on three different days (indicated with different symbols).

Chapter 3

Plants

3.1 Taxonomy and plant culture

The experiments were carried out on ivy [*Hedera helix* subsp. *canariensis* (Willd.) Coutinho] plants. Ivy has two different phases: adult and juvenile. Only the juvenile phase was used. Ivy is a common garden plant with numerous horticultural forms, both with normal and variegated leaves. Plants from a non-variegated clone were used in the gas-exchange experiments. Plants were identified using Rose (1980) as a guide, but for the Latin name Tutin *et al.* (1968) was followed. *Hedera helix* has a wide distribution —from Norway to Southern Europe and N. Iran (Tutin *et al.*, 1968). Grime *et al.* (1988) describe it as a long-lived evergreen woody species, most characteristic of shaded habitats, and commonly occurring in woodlands and hedgerows, either carpeting the ground or growing vertically up the trunks of trees. They classify ivy, according to its established strategy, as a stress-tolerant competitor. The subspecies used has large flat leaves with long petioles which makes it suitable for gas exchange experiments. Leaves are long lived (i.e. several years).

The plants were grown in a heated greenhouse from cuttings collected in the gardens of the University of Edinburgh at King's Buildings, Edinburgh, U.K. They were grown in 12, 16 or 18 cm diameter plastic pots filled with a peat-perlite-vermiculite mix. Plants were repotted at least once a year, and when they became too big to handle (branches longer than 1.5m) they were cut back. Before the beginning of the experiments the plants were transferred to growth chambers. At this time they were fertilized with slow release granules (Fisons plc, Ipswich, U.K.; N=14 %, P=6.1 %, and K=11.6 %, w/w) at 2.5 g per pot. Afterwards they were fertilized weekly with liquid fertilizer (Liquinure, Fisons plc, Ipswich, U.K.; N=8 %, P=1.7 %, K=11.6 %, w/w, and micronutrients) at 0.5 cm^3 per pot. Further details about plant growth conditions are given in later.

chapters.

3.2 Microscopic description of the leaves

Leaves similar to those used in the experiments were observed microscopically. Both the surface of the leaves and their internal structure were observed. In the first case the samples were gold sputtered, and then observed at 3 kv with a S-90 B scanning electron microscope (SEM) (Cambridge Instruments Ltd., Cambridge, U.K.). In the second case the samples were cryofixed: they were first glued to stubs with an embedding medium (Tissue Tek II O.C.T. compound, Emscope Laboratories, Ashford, Kent, U.K.), they were then frozen in liquid N_2, once frozen the specimens were fractured under vacuum, gold coated in an argon atmosphere, and finally transferred under vacuum to the SEM. The fixation procedure was carried out in a cryo- preparation system (Emscope SP2000, Emscope Laboratories, Ashford, Kent, U.K.), and the observations done with a SEM fitted with a cold stage (Stereoscan 250, Cambridge Instruments Ltd., Cambridge, U.K.). In both cases photomicrographs were taken on T-Max 100 film (Kodak Limited, Hemel Hempstead, U.K.). Additional observations of imprints of the leaf surface were done with an optical microscope. The imprints were made with Loctite super glue 3 (Loctite UK, Welwyn Garden City, Herts., U.K.) using the method of Wilson *et al.* (1981).

The surface of the leaves, as seen with the SEM, was smooth, with stomata in the abaxial epidermis, and the location of the anticlinal walls of epidermal cells just visible in the adaxial epidermis (Figs. 3.1 and 3.2). Imprints, observed through a light microscope, confirmed these results, but the image had a shallower depth of focus than with the SEM. Stomatal frequency in Fig. 3.2 is 188 stomata mm^{-2}, which is similar to the 150 stomata mm^{-2} observed by Aphalo & Sánchez (1986) in this species. The length of the stomata was approximately 30 μm, and their width 28 μm.

A thick cuticle covers the outer walls of the epidermis and a ridge borders the antechamber of the stomatal pore (Figs. 3.3 & 3.4). In the lengthwise fracture of the guard cell the outer walls are very thick, but this could be because the fracture is close to the anticlinal walls of the guard cell. The walls of the guard cells are lignified (Ziegler, 1987), something that is not frequent in angiosperms.

Ivy leaves have a clearly defined palisade parenchyma adjacent to the adaxial epidermis (Fig. 3.5). In the section shown in this figure there were two layers of well differentiated palisade cells, and a third layer with less elongated cells. Other leaves, used as replicates, had either two or three layers of palisade parenchyma. The spongy parenchyma had a compact honeycomb structure (Fig. 3.5). In ivy the thickness of

the palisade parenchyma depends on the quantum flux density during growth (Bauer & Thöni, 1988) and on the growth phase (Bauer & Bauer, 1980).

Figure 3.1. SEM photograph of the surface of the adaxial epidermis of an ivy leaf. The arrowhead points to one of the shallow groves on the surface, that show the position of anticlinal walls underneath.
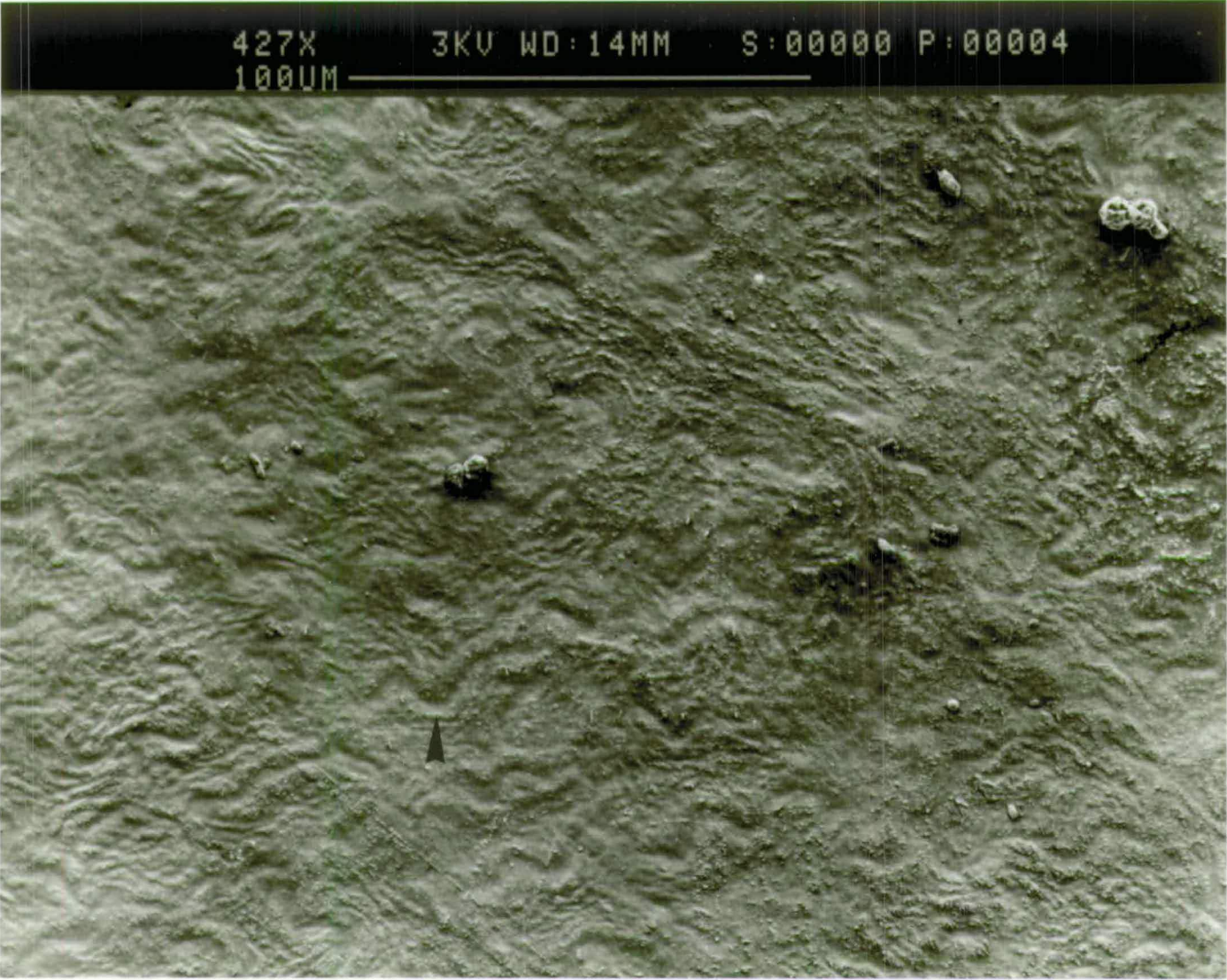
Figure 3.2. SEM photograph of the surface of the abaxial epidermis of an ivy leaf.

105X 3KV WD:14MM S:00000 P:00001
200UM

44
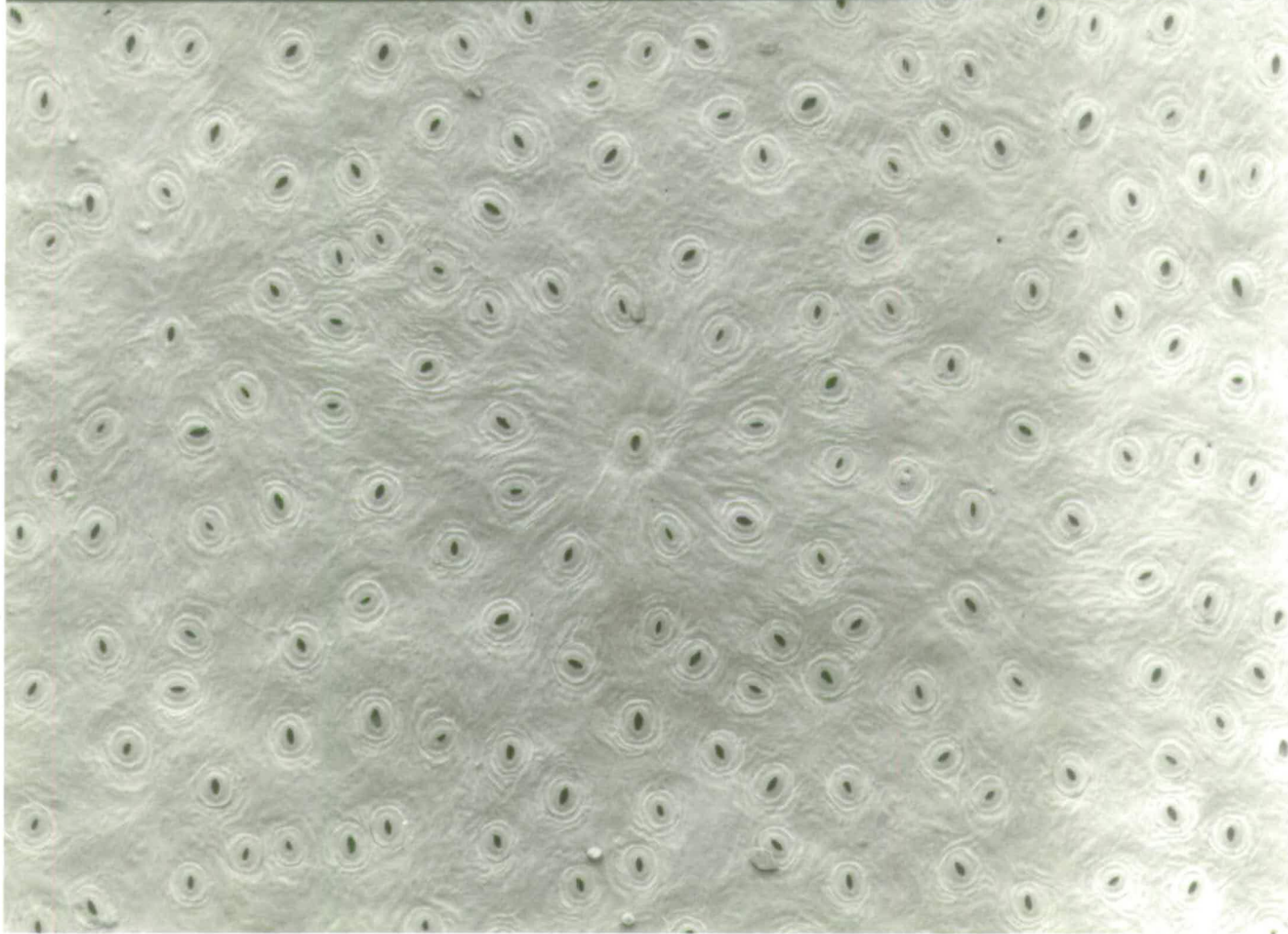
Figure 3.3. SEM photograph of the of the abaxial epidermis of an ivy leaf showing one stoma. The throat of the stoma is indicated by an arrowhead.
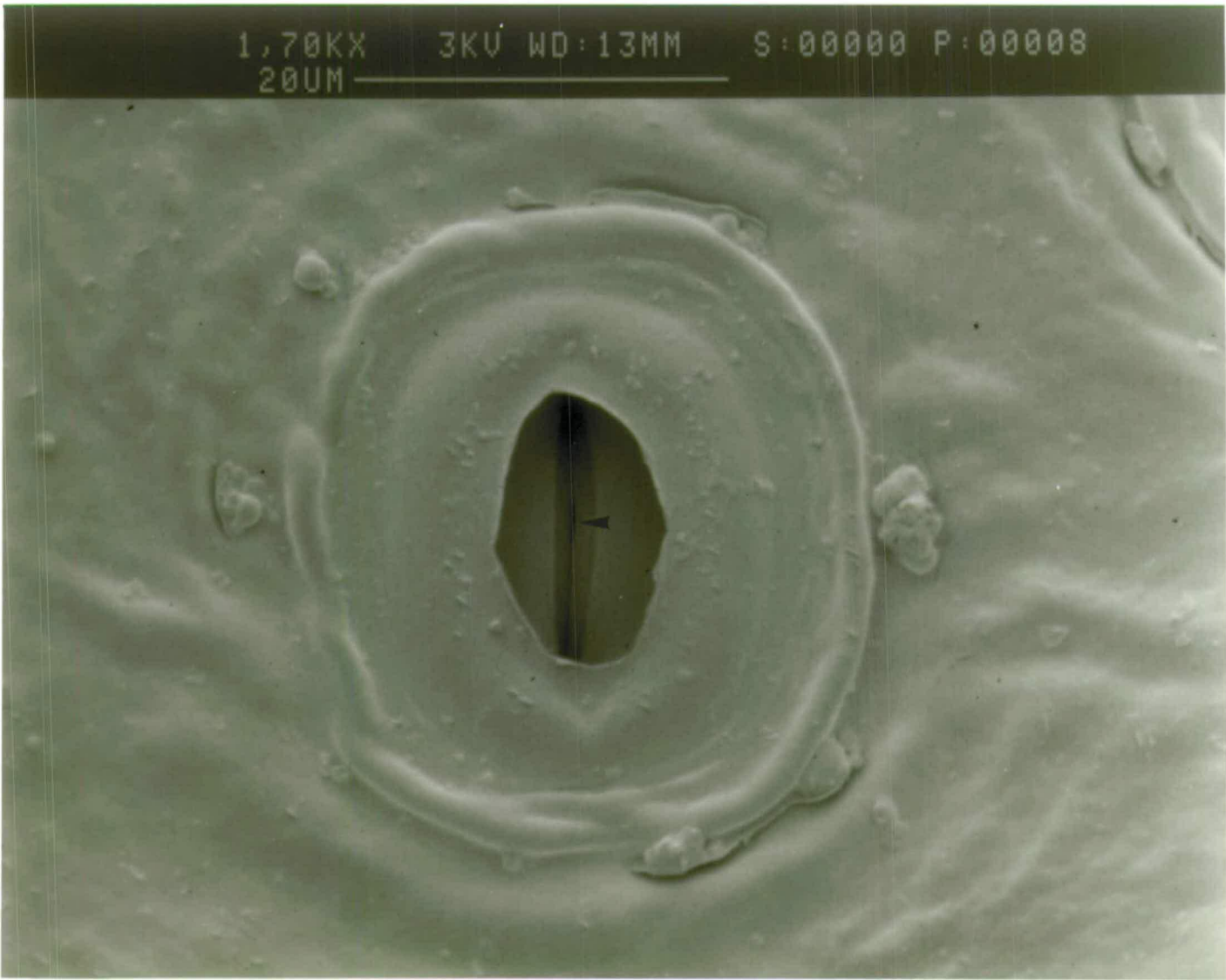
Figure 3.4. Lengthwise transverse fracture of an ivy stoma. Cy: cytoplasm, W: cell wall, Cu: cuticle, r: ridge.
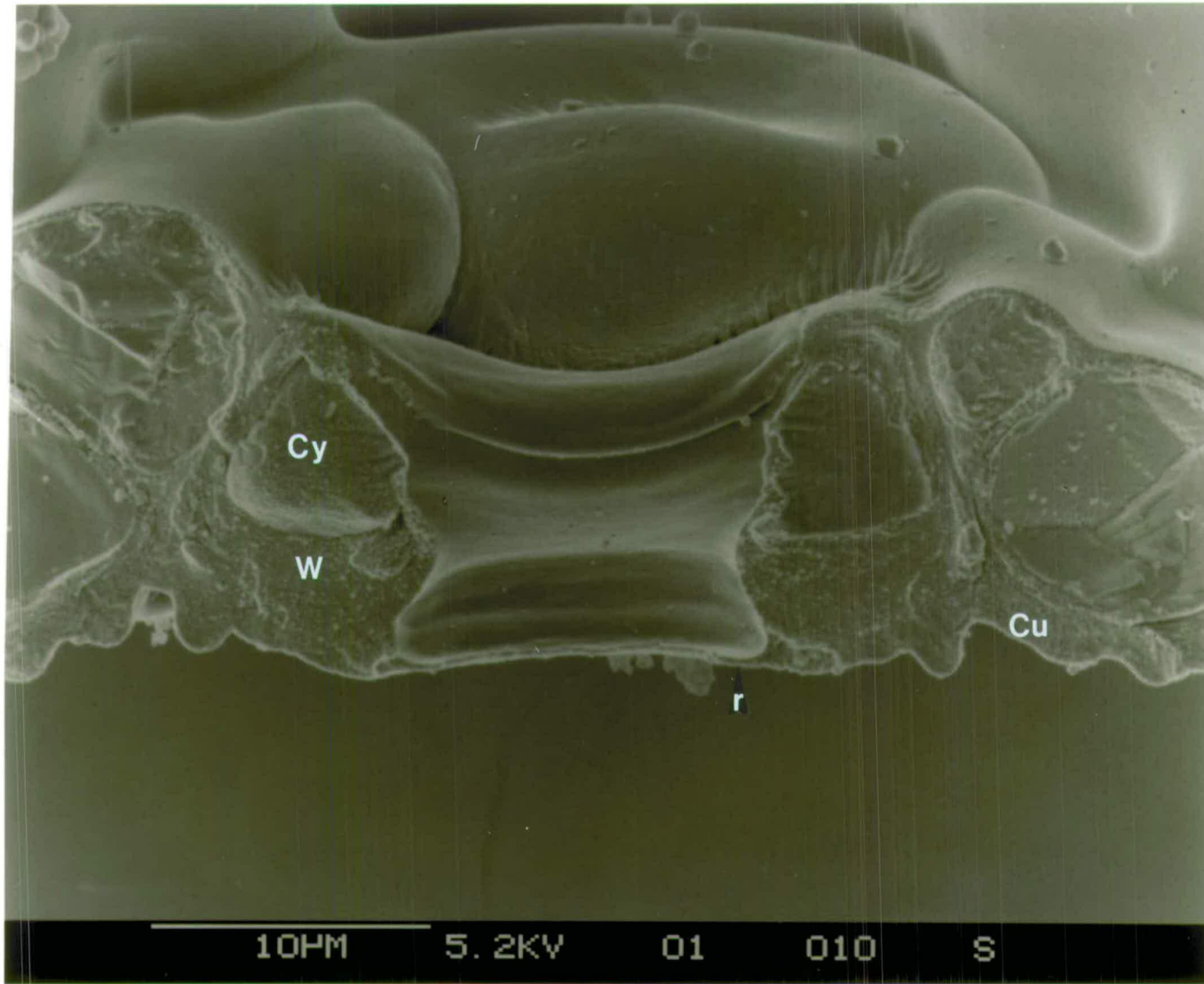
Figure 3.5. Transverse fracture of an ivy leaf. The numbers indicate the cell layers in the palisade parenchyma, and the arrowhead with an s indicates an stoma.
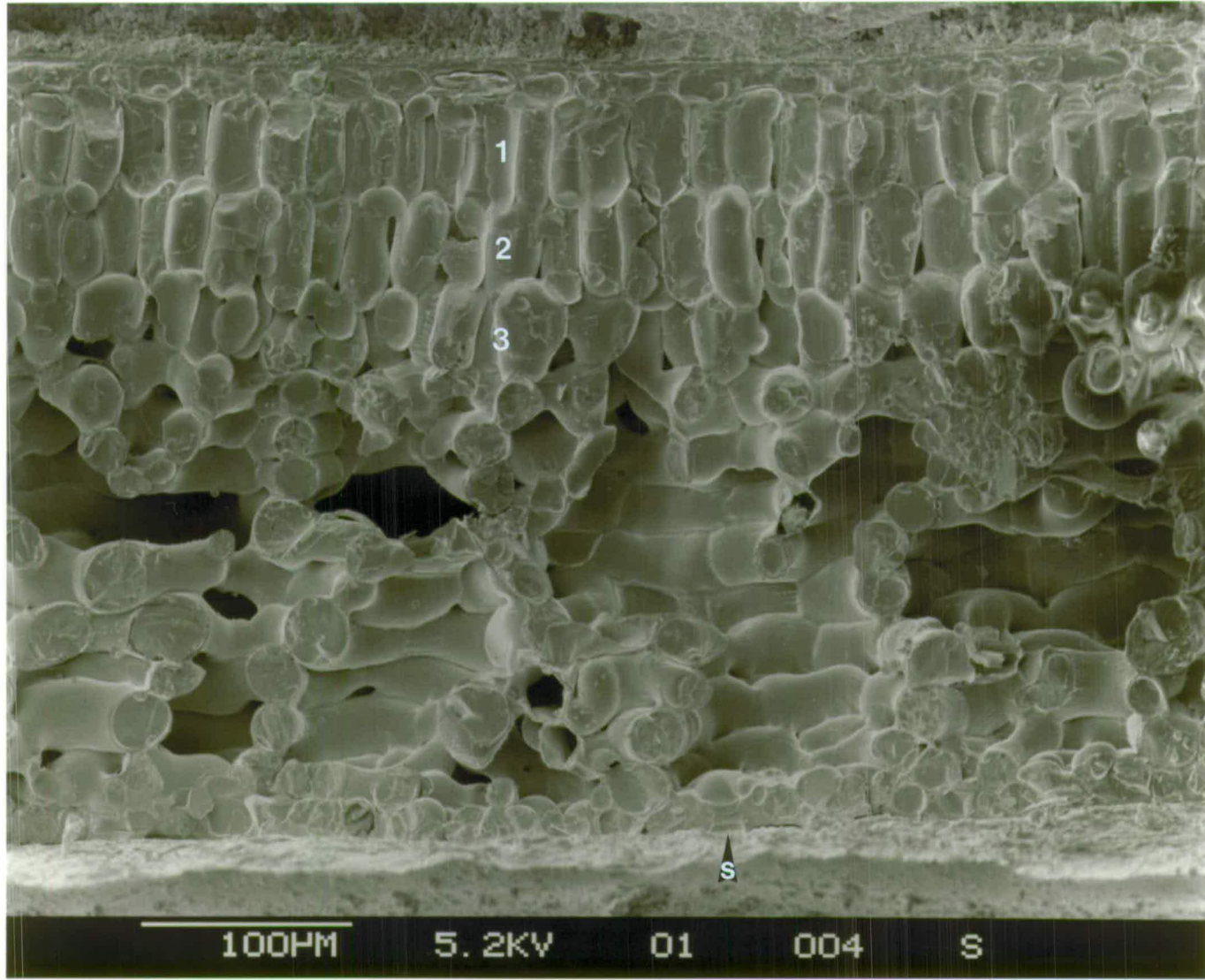
3.3 Optical characteristics of the leaves

The optical properties of ivy leaves similar to those used in the gas exchange experiments were studied by means of a spectroradiometer fitted with an integrating sphere (Optical spectrum analyser model 6800; with a 6100 monochromator, with a 0.9 mm slit installed; a 6118 photo-tube detector; and a 6190 integrating sphere. Monolight Instruments Ltd., Weybridge, Surrey, U.K.). Transmittance (normal/diffuse)[1] and reflectance (normal/diffuse) were measured for both sides of three replicate green leaves and one white leaf, absorptance was calculated from these measurements.

A typical spectrum showing the proportions of the incident radiation that are absorbed, reflected, and transmitted is given in Fig. 3.6, and the values integrated over PAR are given in Table 3.1. The adaxial surface had very low values of reflectance and transmittance in the photosynthetically active part of the spectrum, even in the green region —to the eye this surface of the leaves looked almost black. PAR absorptance for this surface was 95 % (Table 3.1). In the far-red and near infrared region ($\lambda \geq 750$ nm) the transmittance and reflectance each increased to nearly 50 %. The transmittance, and especially the reflectance, were higher for the abaxial surface, with a shallow peak of reflectance in the green —to the eye this surface looked green. PAR absorptance of the abaxial surface was 87 % which is 8 % lower than that of the adaxial surface. In the far-red ($\lambda = 700$–750 nm) region the increase in reflectance of the abaxial surface started at a shorter wavelength than for the adaxial surface. Except for the very low reflectance and transmittance in the green region of the spectrum for the adaxial surface, and the lower transmittance over the whole visible part of the spectrum in both surfaces, these spectra did not differ much from those reported for soybean (Woolley, 1971, Figs. 14 and 16).

The different reflectance of the abaxial and adaxial epidermes can be explained by the structure of the underlying mesophyll tissue. Ivy leaves are dorsiventral with clearly differentiated palisade and spongy regions (Fig. 3.5), and it has been observed that spongy mesophyll scatters light more effectively than the palisade mesophyll (Knapp *et al.*, 1988; Vogelman *et al.*, 1988). That the main effect is internal scattering at the air-water interface can be easily demonstrated by infiltrating albino portions of variegated leaves with water: they become almost clear. The transmittance and reflectance of these white parts are nearly 50 % for most of the visible region of the spectrum (Fig. 3.7).

---

[1] As defined in Commission Internationale de L'Éclaraige (1982).
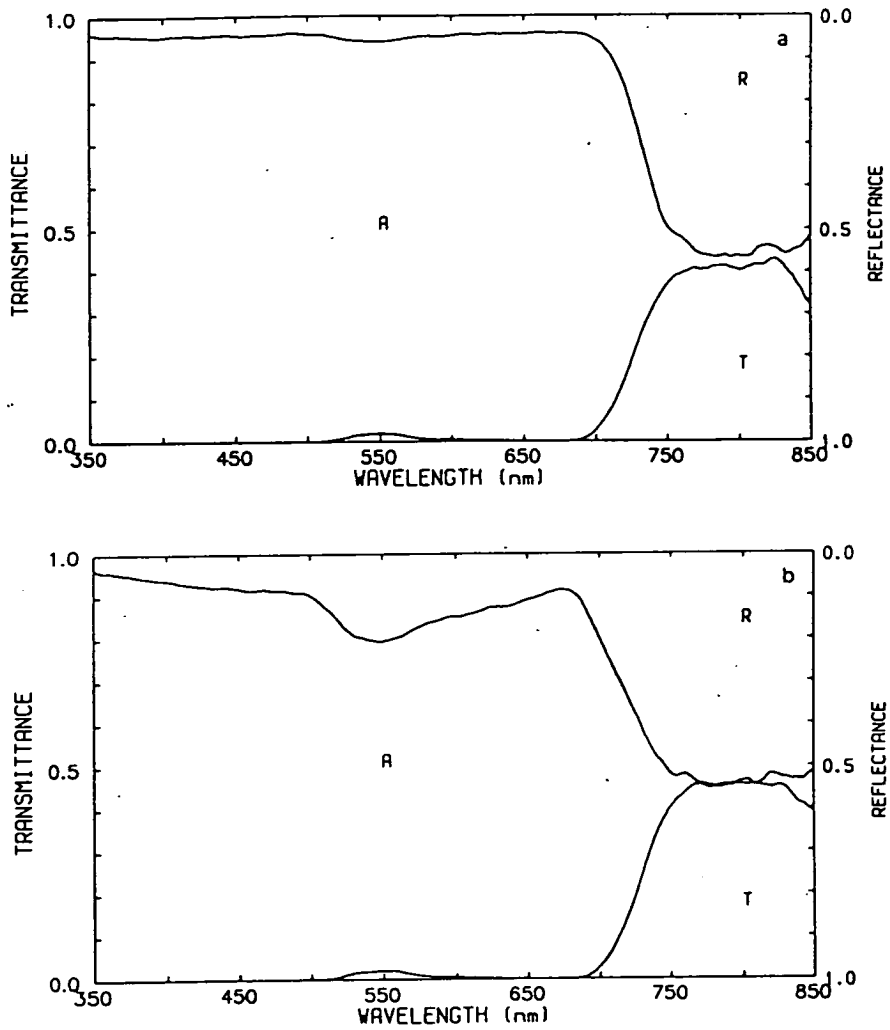
Figure 3.6. Transmittance and reflectance spectra of a typical green ivy leaf. (a) Adaxial surface, (b) abaxial surface. T: transmittance, R: reflectance, A: absorptance.
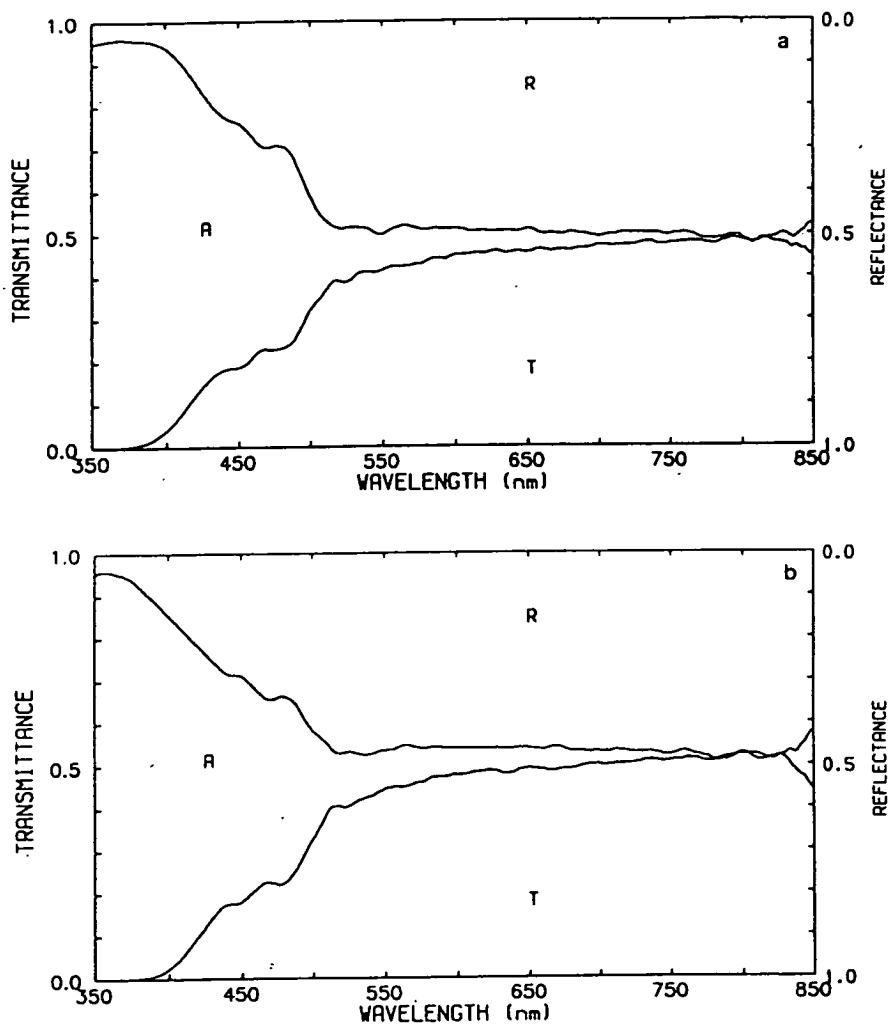
Figure 3.7. Transmittance and reflectance spectra of a white ivy leaf. (a) Adaxial surface, (b) abaxial surface. T: transmittance, R: reflectance, A: absorptance.

Table 3.1. Absorptance, reflectance, and transmittance of photosynthetically active radiation (λ =400–700 nm) for the abaxial and adaxial surfaces of ivy leaves. Values are means of measurements from three green leaves, with the standard error of the mean in brackets, and data from one white leaf.

	green leaves		white leaf	
	abaxial	adaxial	abaxial	adaxial
absorptance (%)	87.3 (0.10)	94.7 (0.17)	23.1	24.5
reflectance (%)	12.3 (0.06)	4.9 (0.17)	40.3	40.4
transmittance (%)	0.4 (0.11)	0.5 (0.22)	36.6	35.1

3.4 Test of assumptions concerning g_s^w and g_c^w

An upper limit to g_c^w was obtained by measuring the water exchange of a detached leaf kept in darkness. The same gas-exchange system was used as in other experiments[2], but to increase the sensitivity a very low air flow rate was used (0.5 mmol s^{-1}). From Equation 1.2 it follows that if $g_s^w \approx 0$ then $g_l^w \approx g_c^w$. The lowest value of g_l^w observed during 6 h in darkness was assumed to be equal to g_c^w. In leaves similar to those used in the stomatal conductance experiments, g_c^w, for both epidermes in parallel, and expressed per unit of projected leaf area, was less than 2 mmol m^{-2} s^{-1}(n=3; T_l=20 °C, $D_s^w \approx$10 mmol mol^{-1}) . A g_c^w of this order of magnitude is common in xerophytes (Weyers & Meidner, 1990, Table 2.3). The g_c^w observed in *Hedera helix* was so low that in discussions elsewhere in this thesis g_l^w measurements were considered equivalent to g_s^w values.

Another important issue is to prevent circadian rhythms from affecting the results when other variables are under study. The approach taken was to measure g_s^w under two different constant sets of conditions throughout a day: darkness, and non-saturating light. An example of the results under light is given in Figure 3.8. No stomatal opening was observed in darkness, even during the daytime. From the results obtained under illumination it was assumed that the safe working period was from 2.5 h after the start of the normal photoperiod to 1 h before its end. Measurements in all other experiments were restricted to this period.

A transient oscillation of g_s^w was observed at the start of the day (Fig. 3.8). This kind of transient response has been described more frequently for grasses than non-grasses (e.g. Johnsson *et al.*, 1976). In the time course of g_s^w in Fig. 3.8 environmental

---

[2]The gas-exchange system is described in Chapter 2.
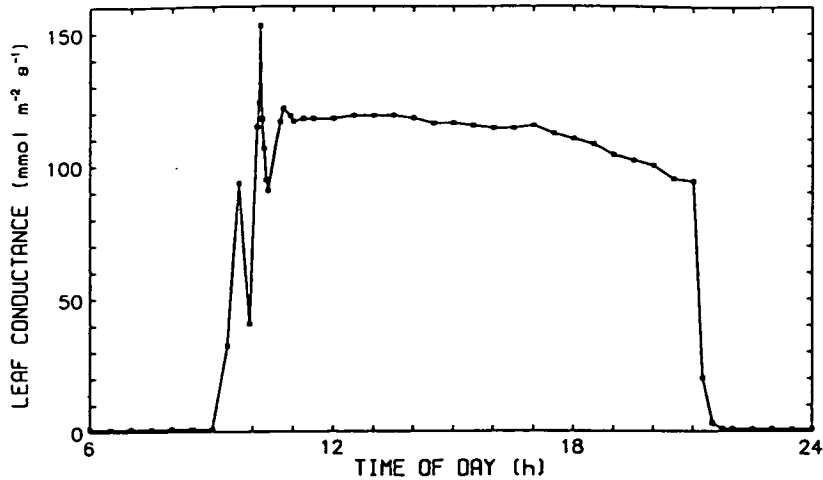
Figure 3.8. Leaf conductance of an ivy leaf throughout a day under constant conditions. Typical response under 340 μmol m^{-2} s^{-1} of white light. D_s^w=10 mmol mol^{-1}, T_l=20 °C, χ_a^c=350 μmol mol^{-1}. The photoperiod was from 9:00 to 21:00.

conditions were not completely stable in the gas-exchange chamber between 9:00 and 11:00 because E and A were changing very fast, and this instability could have reinforced this effect. However, under background red illumination this fast transient has been shown to be a blue light response (Karlsson & Assmann, 1990). *Hedera helix* is the only known dicotyledon capable of fast stomatal opening[3] (Karlsson & Assmann, 1990), a type of response previously thought to be restricted to plants with grass-like stomata (Johnsson *et al.*, 1976).

---

[3] As defined by the rise time and the delay time, and the ratio of their values under red and blue light (see Johnsson *et al.*, 1976).

Chapter 4

Stomatal responses to light

4.1 Introduction

Stomatal responses to light are complex: several photoreceptors and transduction chains are involved. The responses are called either *direct* or *indirect* according to the location of the light receptor. In direct responses light is sensed in the guard cells, in indirect ones in other cells (i.e. in the mesophyll). Direct responses have been postulated to take place through (1) an unidentified, blue absorbing photoreceptor, (2) chlorophyll in guard cell chloroplasts, and (3) phytochrome(?); the indirect response takes place mainly through mesophyll chlorophyll. Light absorbed in the mesophyll drives photosynthesis which, by altering the internal environment of the leaf, indirectly affects stomata. The three different receptors involved in direct responses to light differ in their spectral sensitivity. They also differ in their sensitivity to photon flux density. The blue light response is direct, that to PAR can be direct and/or indirect. It will not be fruitful to discuss further the poorly understood response through phytochrome.

Experimenters have used various procedures to distinguish between the different responses: monochromatic light (e.g. Johnsson *et al.*, 1976; Aphalo & Sánchez, 1986), variegated chimeras (e.g. Virgin, 1957; Aphalo & Sánchez, 1986) or chlorophyll deficient mutants (e.g. Virgin, 1957; Skaar & Johnsson, 1980), species with uncommon characteristics (e.g. Nelson & Mayo, 1975) and chemicals affecting chlorophyll content (e.g. Karlsson *et al.*, 1983). To separate direct from indirect light responses in whole leaves both chimeras (e.g. Aphalo & Sánchez, 1986), and leaf inversion experiments (e.g. Turner, 1970; Raschke *et al.*, 1978; Aphalo & Sánchez, 1986) have been used.

Stomata are usually more sensitive to blue than to red light (Kuiper, 1964; Sharkey & Raschke, 1981a). However, not all species share the same high sensitivity to blue light: in *Fuchsia magellanica* g_s^w is equally sensitive to blue and red light (Aphalo *et al.*,

1991) while in *Hedera helix* g_s^w is nearly 100 times more sensitive to blue than to red light (Aphalo & Sánchez, 1986), and in *Pinus sylvestris* it is approximately 10 times more sensitive to blue than to red light (Morison & Jarvis, 1983a). In some species responses to blue light are also faster (Johnsson *et al.*, 1976).

The role proposed for the blue light-dependent system is to provide the plant with a means for opening stomata in the early morning and to respond quickly to sunflecks (Meidner & Mansfield, 1968; Zeiger *et al.*, 1981; Aphalo & Sánchez, 1986; Zeiger, 1990). It has also been proposed that by modulating the sensitivity of this photosystem, plants tune stomatal behaviour to prevailing environmental conditions such as drought stress (Aphalo & Sánchez, 1986). It is still not clear which are the roles fulfilled by direct and indirect responses to PAR. Some species, such as *Petunia axillaris* and *Petunia hybrida*, seem to rely on endogenous rhythms regulating aperture in darkness and modulating sensitivity to light, for early morning aperture and midday closure (P. J. Aphalo, unpublished). In many species the speed with which stomata open in response to light depends on the phase of the circadian rhythm (Weyers & Meidner, 1990, give examples and primary references). It has also been shown that in *Avena sativa* the maximum amplitude of rapid (blue light-dependent) and slow (PAR-dependent) stomatal responses occur during opposite phases of the circadian rhythm (Brogårdh & Johnsson, 1975). In *Hedera helix* the effect of endogenous rhythms on g_s^w is very small during the normal photoperiod (see Section 3.4), and response to blue light is rapid (Karlsson & Assmann, 1990).

Scarth (1932) was the first to suggest that light-induced stomatal opening was caused by photosynthetic removal of CO_2 from the intercellular spaces. Stomata are sensitive to CO_2 in light and darkness, and in whole leaves and epidermal strips (Heath, 1950; Heath & Milthorpe, 1950; Meidner & Mansfield, 1968; Morison, 1987). In whole leaves stomata are sensitive to χ_i^c (Mott, 1988). As A is dependent on, but also affects, χ_i^c, a feedback loop is generated between both processes. In some species or conditions stomata can be insensitive to CO_2 (Morison, 1987), and in many situations light responses independent of χ_i^c make a larger contribution to the total response to light than those dependent on χ_i^c (Dubbe *et al.*, 1978; Sharkey & Raschke, 1981b).

Aphalo & Sánchez (1986) have suggested, based on the results of leaf inversion experiments, that in *Hedera helix* the blue light-dependent response of g_s^w is direct, and the PAR-dependent one is indirect. This is in contrast to what Sharkey & Raschke (1981a) observed in *Xanthium strumarium*, a species in which both blue light and PAR-dependent responses were found to be mainly direct.

When I is changed A and g_s^w are usually linearly correlated, if χ_a^c is kept constant

(e.g. Wong *et al.*, 1979; Louwerse, 1980; Ramos & Hall, 1982). However this relationship cannot always be explained by the response of g_s^w to χ_i^c (Wong *et al.*, 1979). Even though this correlation can be experimentally broken, Wong *et al.* (1979) have proposed that it could depend on metabolites other than CO_2 conveying to the stomata information about the rate of photosynthesis in the mesophyll. Cowan *et al.* (1982) proposed that abscisic acid coordinates A and g_s^w even in responses to light. Although it has been shown that these hypotheses are not the main basis for this correlation, they could in some species be part of a more complex mechanism, and so need to be further investigated.

Two different experiments were done with the objective of elucidating the mechanism behind the coordination of changes in A and g_s^w. In the first experiment, the responses of A and g_s^w to I were measured under constant χ_s^c to describe the correlation between the effects of I on A and g_s^w. In the second experiment, irradiation with light of different wavelengths, and of either the abaxial or adaxial epidermis, was used to alter A and g_s^w. Leaf inversion increases the I received by the guard cells, and also affects the distribution of light within the leaf mesophyll. By keeping χ_i^c constant any effect of CO_2 on either A or g_s^w was prevented. This was intended to make any CO_2-independent correlation between A and g_s^w observable.

4.2 Materials and methods

4.2.1 Plant material

Ivy plants were grown in a heated greenhouse. Three different sets of plants were used, two in two replicates of one experiment, and the third one in a second experiment. The plants were grown in 12 or 18 cm diameter plastic pots filled with a peat-perlite-vermiculite mix, watered every other day, and fertilized weekly (See Chapter 3 for details).

One set of plants —henceforth called set A— was kept for 4 months in a growth chamber at 20 °C, h=30–60 %, and a photoperiod of 12 h at 400 μmol m^{-2} s^{-1} at leaf level from metal halide lamps (Wotan 'Power Star' HQI-R 250 W/NDL, Wotan Lamps Ltd., London).

The second set of plants —set B— was kept in the same chamber and under similar conditions for 3 months.

The third set of plants —set C— was kept for more than 26 d in a growth room at 20 °C, h=50–70 %, and a photoperiod of 12 h at 500 μmol m^{-2} s^{-1} at leaf level from metal halide lamps (Kolorarc 400W MBIF/BU, Thorn Lighting Ltd., London, U.K.).

4.2.2 Gas exchange measurements

The computer-controlled gas-exchange system described in Chapter 2 was used. Boundary layer conductance was measured by means of leaf replicas of Whatman No. 3 filter paper covered with aluminium foil on the upper or lower side, according to the position of the leaf, and wetted with distilled water. g_b^w was 650-700 mmol m^{-2} s^{-1} for the leaves used, and not affected by the position of the evaporating surface. The temperature of leaves and leaf replicas was measured with thermojunctions in contact with their shaded face. Steady-state measurements were made, and no data taken during the first hour after a change in conditions were used. However, the data were checked to see whether a steady state had been reached and this period was extended if necessary. The leaves to be measured the next day were placed overnight in the gas-exchange chamber in darkness with χ_s^c=350 μmol mol^{-1}, D_s^w=10 mmol mol^{-1}, and T_l=20 °C. Attached non-senescent fully expanded leaves were used in the experiments.

4.2.3 Experiments

The first experiment consisted of measuring the response of g_s^w, A, and χ_i^c to I of white light under constant conditions of χ_s^c=350 μmol mol^{-1}, D_s^w=10 mmol mol^{-1}, and T_l=20 °C. This experiment was done using three plants from set A and was then replicated with another two plants from set B.

The second experiment consisted of measuring g_s^w and A under constant conditions of χ_i^c=220 μmol mol^{-1} and I=500 μmol m^{-2} s^{-1} of white light, I=18 μmol m^{-2} s^{-1} of blue light, or I=120 μmol m^{-2} s^{-1} of red light, in leaves in an inverted position as compared to the same leaves in normal position. The photon flux densities of red and blue light were selected so as to give approximately the same g_s^w. The plants were kept in darkness for 1 h after changing the position of the leaf only when blue or red light was used. These treatments were applied in a random order. Three plants from set C were used.

4.3 Results

4.3.1 Responses of g_s^w and A to quantum flux density

In most of the plants from both sets, the response of g_s^w to I did not saturate in the range of values tested (Fig. 4.1). The threshold for stomatal opening in white light was approximately 2 μmol m^{-2} s^{-1} in set A, and 7 μmol m^{-2} s^{-1} in set B. CO$_2$ flux density saturated at a lower I than stomatal aperture, and light compensation occurred at 5 μmol m^{-2} s^{-1} (Fig. 4.2). In both sets of plants the initial slope was 0.05 mol of CO$_2$
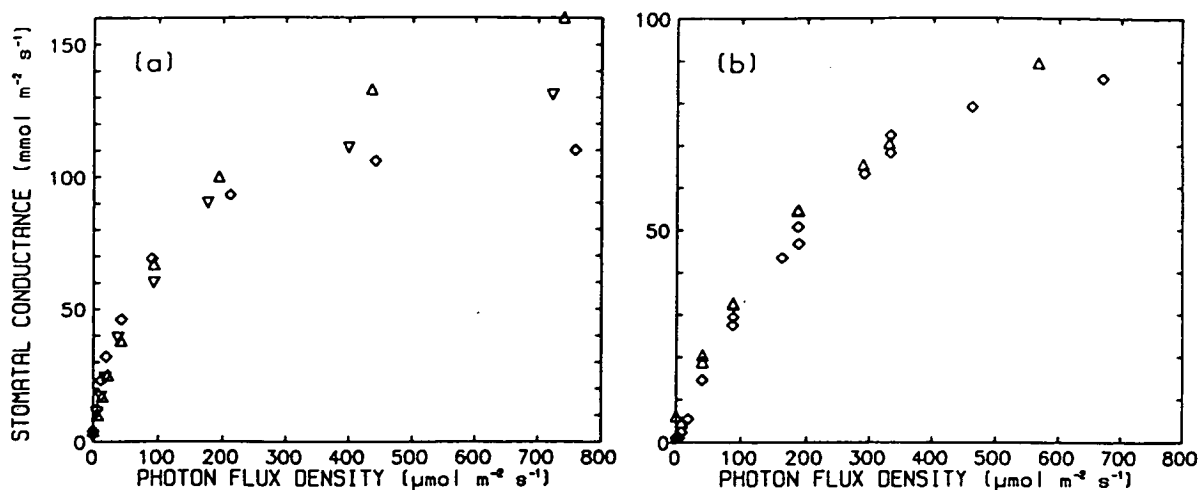
Figure 4.1. Stomatal conductance *vs.* photon flux density of white light. D_s^w=10 mmol mol^{-1}, χ_s^c=350 μmol mol^{-1}, T_l=20 °C. (a) Three plants from set A, (b) two plants from set B. Symbols indicate data from different plants.

per mol of photons. χ_i^c showed a minimum at 300 μmol m^{-2} s^{-1} in plants from set A, and at 200 μmol m^{-2} s^{-1} in those from set B (Fig. 4.3). g_s^w, A and χ_i^c were higher in plants from set A than in plants from set B (Figs. 4.1, 4.2 & 4.3).

If A is plotted *vs.* g_s^w a good linear fit is achieved, except for the data measured at very low or very high irradiances (Fig. 4.4, Table 4.1). The slopes (P=0.047) and intercepts (P=0.073) were slightly different in the two sets of plants. When g_s^w is plotted *vs.* χ_i^c the relationship is not as clear as with light, especially for data from set B (Fig. 4.5), and the relationship is not monotonic —i.e. there is more than one value of g_s^w for a given χ_i^c.

4.3.2 Leaf inversion experiment

The effects of leaf inversion on g_s^w and A were very different. Under 500 μmol mol^{-1} of white light g_s^w did not change, and A decreased to 0.58 of its original value (Table 4.2). The effect on A was readily reversible (data not shown). Increasing I in inverted leaves under these conditions did not alter the steady-state g_s^w even though A increased somewhat; decreasing χ_i^c decreased A and increased g_s^w (Fig. 4.6). Under non-saturating red light g_s^w more than doubled in response to leaf inversion, while A decreased to 0.58 of that before inversion (Table 4.2). Under low I of blue light g_s^w doubled with leaf inversion, while A remained almost unchanged and near zero (Table 4.2). As
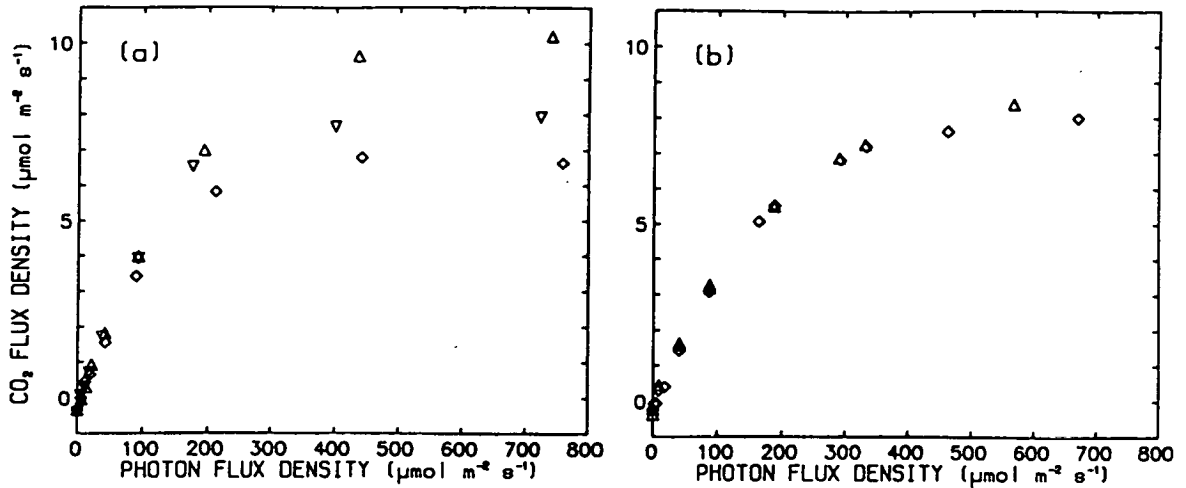
Figure 4.2. CO_2 flux density *vs.* photon flux density of white light. $D_s^w=10$ mmol mol^{-1}, $\chi_s^c=350$ μmol mol^{-1}, $T_l=20$ °C. (a) Three plants from set A, (b) two plants from set B. Symbols indicate data from different plants.
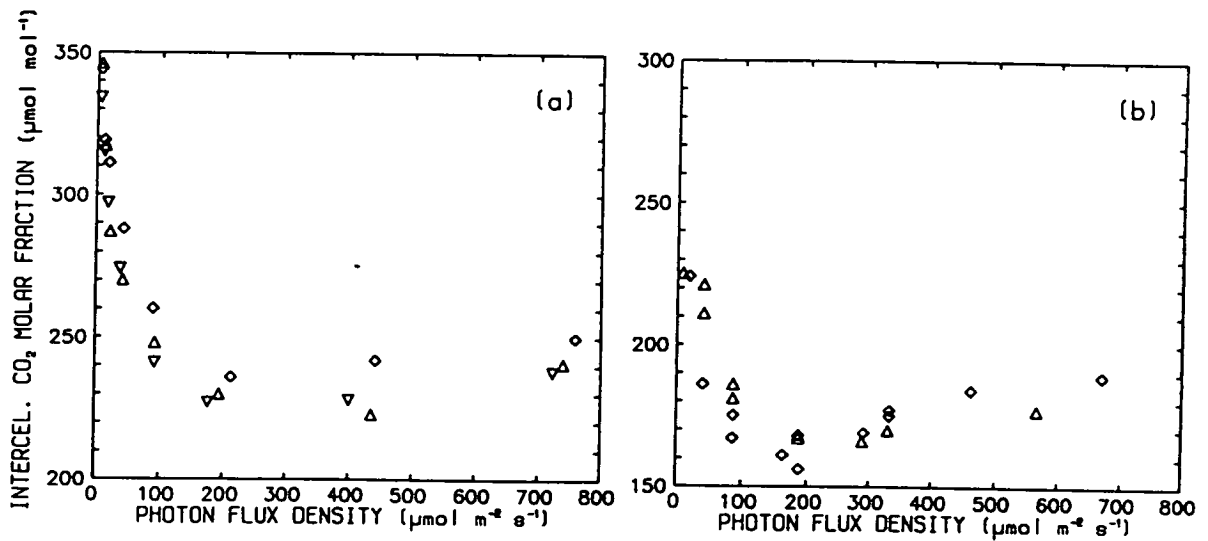
Figure 4.3. Intercellular CO_2 concentration *vs.* photon flux density of white light. $D_s^w=10$ mmol mol^{-1}, $\chi_s^c=350$ μmol mol^{-1}, $T_l=20$ °C. Data from the same experiment as that in Fig. 4.2. (a) Three plants from set A, (b) two plants from set B. Symbols indicate data from different plants.
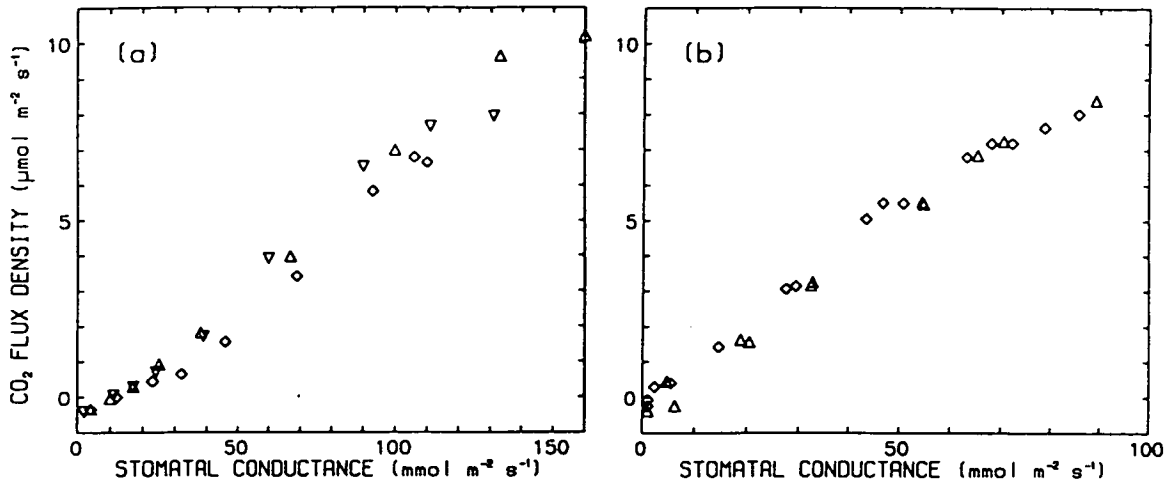
Figure 4.4. CO_2 flux density *vs.* stomatal conductance, measured under changing photon flux densities. Same data as in Figs. 4.2 & 4.1. $D_s^w = 10$ mmol mol^{-1}, $\chi_s^c = 350$ μmol mol^{-1}, $T_l = 20$ °C. (a) Three plants from set A, (b) two plants from set B. Symbols indicate data from different plants.

Table 4.1. Regression of CO_2 flux density on stomatal conductance in leaves of *Hedera helix*. $I = 35$–500 μmol m^{-2} s^{-1}(white light), $D_s^w = 10$ mmol mol^{-1}, $\chi_s^c = 350$ μmol mol^{-1}, $T_l = 20$ °C. A subset of the data in Fig. 4.4 was used in the calculations, and regression lines were fitted to data from single leaves for a restricted range of I.

Plant	intercept (μmol m^{-2} s^{-1})	slope (μmol mol^{-1})	R^2	n
A1	-2.59	89	0.998	4
A2	-1.47	83	0.999	4
A3	-1.28	83	0.986	4
B1	0.43	97	0.974	10
B2	-0.53	111	0.997	8
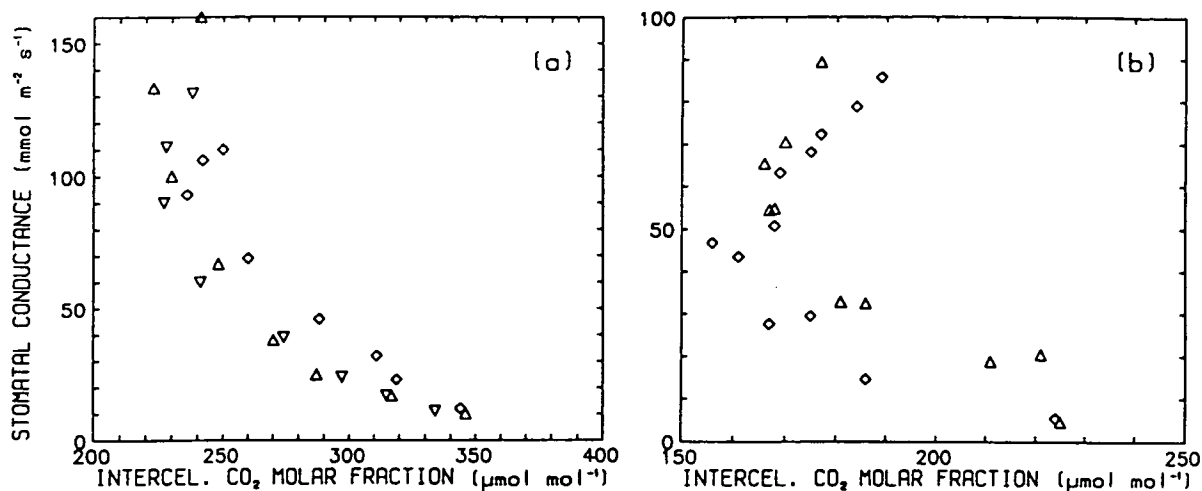
Figure 4.5. Stomatal conductance vs. intercellular CO_2 concentration, measured under changing photon flux densities. Same data as in Figs. 4.1 & 4.3. $D_s^w=10$ mmol mol^{-1}, $\chi_s^c=350$ μmol mol^{-1}, $T_l=20$ °C. (a) plants from set A, (b) from set B. Symbols indicate data from different plants.

previously stated, the I values of blue and red light were selected so that g_s^w was similar, and this resulted in very different values of A. Leaf inversion had a significant effect on χ_i^c/χ_s^c under both white and red light (Table 4.2).

4.4 Discussion

An important, and unsolved, question in plant physiology is: What is the mechanism behind the correlation between A and g_s^w? This correlation has been observed in several experiments when A and g_s^w changed in response to different variables including light (Wong et al., 1979, 1985a, 1985b, 1985c; Louwerse, 1980; Ramos & Hall, 1982). It has also been observed that, in the case of responses to light, this correlation can be broken experimentally (Jarvis & Morison, 1981; Aphalo & Sánchez, 1986). The competing hypotheses to explain this correlation are (1) feedback through χ_i^c, (2) feedback through another metabolite of A, and (3) parallel, but independent, responses to light of g_s^w and A. Different researchers, using different species and conditions have found evidence bearing out hypotheses (1) and (3): the gain of the feedback loop through χ_i^c has been measured (Farquhar et al., 1978; Dubbe et al., 1978), and direct responses of stomata to light have been observed (e.g. Jarvis & Morison, 1981; Aphalo & Sánchez, 1986). Evidence in favour of hypothesis (2) is weak: Wong et al. (1979, 1985b, 1985c)

Table 4.2. Stomatal conductance (g_s^w), CO_2 flux density (A), and ratio of intercellular to surface CO_2 molar fractions (χ_i^c/χ_s^c) in leaves of *Hedera helix* in inverted and normal positions. $D_s^w=7$ mmol mol^{-1}, $\chi_i^c=220$ μmol mol^{-1}, $T_l=20$ °C. Data from three plants from set C. **Part A:** means and standard errors of the means (in brackets). W: white light, R: red light, B: blue light. **Part B:** summary table of analysis of variance. A complete randomized blocks design was used, the plants being the blocks. Orthogonal contrasts were done to find out the origin of significant interactions (e.g. position(white) is the effect of normal *vs.* inverted position under white light). M.S.: mean square, *P:* probability.

Part A: means and standard errors			
Position	I	g_s^w	A	χ_i^c/χ_s^c
	(μmol m^{-2} s^{-1})	(mmol m^{-2} s^{-1})	(μmol m^{-2} s^{-1})	(mol mol^{-1})
Normal	500 (W)	122(5.3)	8.8(0.43)	0.65(0.01)
Inverted	500 (W)	129(9.6)	5.1(0.21)	0.77(0.01)
Normal	120 (R)	52(6.9)	5.3(0.46)	0.55(0.07)
Inverted	120 (R)	117(8.5)	3.1(0.07)	0.82(0.02)
Normal	18 (B)	60(11.9)	0.5(0.05)	0.93(0.02)
Inverted	18 (B)	118(22.6)	0.5(0.13)	0.96(0.01)

Part B: analysis of variance						
Source of variation	d.f.	g_s^w M.S.	g_s^w P	A M.S.	A P	χ_i^c/χ_s^c M.S.	χ_i^c/χ_s^c P
Light	2	3210	<0.001	62.33	<0.001	0.121	<0.001
red−blue	1	136	0.396	41.40	<0.001	0.195	<0.001
Position	1	7904	<0.001	17.15	<0.001	0.090	<0.001
position(white)	1	74	0.529	20.54	<0.001	0.023	0.007
position(red)	1	5436	<0.001	7.37	<0.001	0.113	<0.001
position(blue)	1	5139	<0.001	0.005	0.874	0.0012	0.460
Light × position	2	1372	0.009	5.38	<0.001	0.0231	0.003
(red−blue) × pos.	1	2	0.915	3.89	0.001	0.0454	0.001
Plants	2	2052	0.002	0.354	0.226	0.0062	0.092
Error	10	173	—	0.205	—	0.0020	—
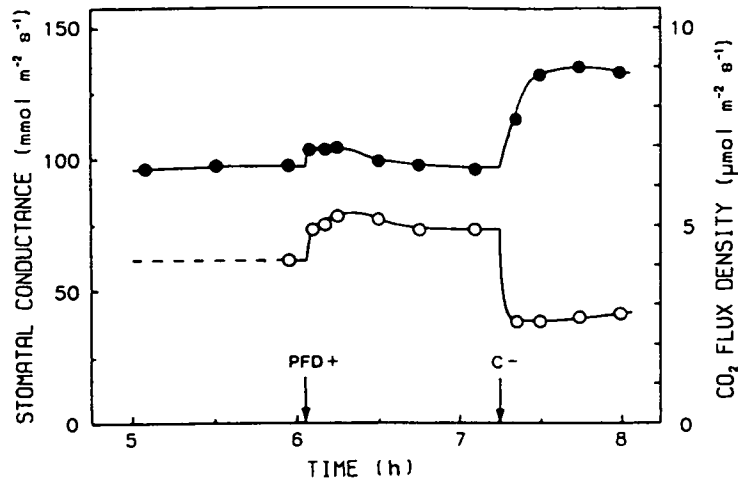
Figure 4.6. Responses of stomatal conductance ($\bullet$) and CO_2 flux density ($\circ$) to increased photon flux density (I) and decreased intercellular CO_2 concentration (χ_i^c) in a leaf in inverted position. Starting conditions: $\chi_i^c=220$ μmol mol^{-1}, $I=500$ μmol m^{-2}s^{-1} (white light), $D_s^w=7$ mmol mol^{-1}, $T_l=20$ °C. C-: χ_i^c reduced to 120 μmol mol^{-1}; PFD+: I increased to 750 μmol m^{-2} s^{-1}.

provided some evidence suggesting that there is something else that is conveying information about A to the stomata, their main argument being that the highly constant proportionality between A and g_s^w cannot be explained by feedback through χ_i^c. Most of the evidence supporting hypotheses (1) and (3) does not rule out hypothesis (2).

In *Hedera helix* A and g_s^w were linearly correlated under constant χ_s^c, but, having used a very wide range of I (2–760 μmol m^{-2} s^{-1}), this correlation tended to break down at low and high I —high for a shade loving species. For I in the range 35–500 μmol m^{-2} s^{-1} correlations for individual leaves were very high but the slopes and intercepts differed slightly between the two sets of plants.

This correlation can be easily broken through manipulation of the experimental conditions. Stomatal conductance was almost the same in inverted leaves under white, red and blue light, and in leaves in a normal position under white light. In these same treatments A varied between 0.5 to 8.8 μmol m^{-2} s^{-1}. In leaves in a normal position g_s^w was similar under 120 μmol m^{-2} s^{-1} of red and 18 μmol m^{-2} s^{-1} of blue light, while A was 10 times higher under red light than under blue light.

At high I stomata continued to open with increasing I even though A was almost light saturated, leading to an increase in χ_i^c (Figs. 4.1, 4.2 & 4.5), as also observed in *Phaseolus vulgaris* plants grown at low I (Wong et al., 1985b). Under constant χ_s^c,

this behaviour was reflected in a poor relationship between g_s^w and χ_i^c, indicating that the main effect of light on stomata is not through χ_i^c. However, as stomata of ivy are sensitive to χ_i^c (see Chapter 6 and Fig. 4.6) part of the effect of light under constant χ_s^c must occur indirectly through χ_i^c.

Under constant χ_s^c and saturating I, g_s^w did not differ when stomata were directly illuminated, or shaded by the mesophyll, even though A was higher in the latter than in the former case (Table 4.2). Under non-saturating blue or red light, inverting the leaves, and thus increasing I on the guard cells, increased g_s^w, and either did not affect or decreased A, indicating that ivy stomata respond directly to both red and blue light.

Under red light χ_i^c/χ_s^c increased from 0.56 to 0.82 in response to leaf inversion. Had χ_s^c not been decreased to keep χ_i^c constant, χ_i^c would have increased. Under red light Aphalo & Sánchez (1986) did not find an effect of leaf inversion on g_s^w. However, as they did not control χ_i^c, a possible explanation for their results is that the direct effect of red light was masked by the increase in χ_i^c caused by the decrease in A.

Under blue light there was almost no effect of leaf inversion on χ_i^c/χ_s^c because, as A was very low, the change in g_s^w had little effect on χ_i^c. Aphalo & Sánchez (1986) did observe, under blue light, a big effect of leaf inversion on g_s^w, probably because under low I and high g_s^w there was no masking effect through χ_i^c. A response of g_s^w to blue light has been observed in the white portions of variegated leaves of *Hedera helix* (Aphalo & Sánchez, 1986).

In inverted leaves g_s^w was light saturated at 500 μmol m^{-2}s^{-1} of white light (Fig. 4.6), which explains the lack of an effect of leaf inversion on g_s^w under this condition. Even though g_s^w was light saturated, it was not at its maximum, as under this value of I it increased in response to a decrease in χ_i^c. This indicates that aperture was not mechanically limited, it was limited by the capacity of the photosensors or by the transduction chain.

If the correlation between g_s^w and A was caused by a metabolite of photosynthesis different to CO_2, then it would not be possible to break this correlation by experimentally manipulating χ_i^c —i.e. If the messenger is not affected then the relationship between A and g_s^w should not change. However, an increase in χ_i^c under white light led to an increase in A, and to a decrease in g_s^w, an effect opposite to what would be expected from the relationship between A and g_s^w under changing I (Fig. 4.6). This information could be consistent with the hypothesis that this messenger is, or is dependent on, the surplus electron transport capacity in the mesophyll, but this hypothesis has to be rejected because it has been observed that stomata are sensitive to χ_i^c in darkness. So it can be concluded that CO_2 is the main 'messenger' for the indirect response of g_s^w to light.

An opposite effect of CO_2 on A and g_s^w, as observed in ivy, has been seen in other species, together with a lack of response of g_s^w to CO_2, e.g. *Pinus sylvestris* (Jarvis & Morison, 1981). The degree of control of g_s^w by the χ_i^c feedback loop varies with species and conditions (Dubbe *et al.*, 1978; Sharkey & Raschke, 1981b).

In white and red light, A was lower in inverted leaves than in those in a normal position, even though χ_i^c was kept constant. The decrease in A is probably due to the dorsiventral structure of the leaves (described in Section 3.2), which, when a leaf is inverted, leads to a different distribution of light within the mesophyll. Only a small part of the decrease in A can be explained by the difference in light absorptance of the two leaf surfaces (see Section 3.3). A similar effect of leaf inversion on A has been observed in *Calopogonium mucunoides*, a legume (Ludlow & Wilson, 1971), and in *Picea sitchensis* (Leverenz & Jarvis, 1979), but not in *Pennisetum purpureum*, a grass (Ludlow & Wilson, 1971). In blue light, A was very low, and no effect of leaf inversion on A was observed probably because of a proportionally larger experimental error.

The results presented here are a confirmation of previous results that have indicated that most of the effect of light on stomata is direct (e.g. Sharkey & Raschke, 1981b; Morison & Jarvis, 1983a; Morison & Jarvis, 1983b). In ivy, if there is a messenger other than CO_2 involved in the coordination of g_s^w with A, any effect of such a messenger must be quantitatively very small. The direct responses plus the response through χ_i^c are able to explain all the observed stomatal responses to light, even the apparent inconsistency between leaf inversion experiments done under constant χ_i^c and constant χ_a^c. Not only it is unnecessary to postulate that some unknown messenger conveys information to the stomata about the rate of CO_2 assimilation in the mesophyll, but what is more important, such a messenger would be incompatible with the experimental results.

Chapter 5

Stomatal responses to humidity and temperature[1]

5.1 Introduction

Humidity includes information on both the water vapour and energy content of air. A difficult and important question in biology is selecting an appropriate measure of humidity for studying a response because the relation between different ways of expressing humidity is not linear. Hall *et al.* (1976) have said that the mechanism for "direct" stomatal response to humidity is not known, and that the use of D_a^w as the driving force, rather than other variables such as relative humidity, should be examined. According to Grantz (1990), this question is still open. It has been said both that '...stomata respond to relative humidity' (Ball *et al.*, 1987), and that '...a fall in humidity increases evaporation from the epidermis, and that stomata respond to the consequent fall in water potential' (Sheriff, 1984). The assertion that stomata respond to relative humidity was mainly based on the good fit of data to the empirical model proposed by Ball *et al.* (1987), $g_s^w = kAh_s/\chi_s^c$, but there are two big problems in arriving at this conclusion. Firstly, correlation is being equated with causation, and secondly, any combined response of A and g_s^w to temperature that keeps χ_i^c/χ_s^c constant under constant h_s can fit this model. (See chapter 7.) It must also be stressed that a mechanistic interpretation of this model implies the lack of any direct response of g_s^w to temperature.

I start by considering the question 'Do stomata respond to relative humidity?'. In some respects, this is a misleading question simply because h_s reflects simultaneously

---

[1]This chapter is based on the article: Aphalo, P. J., & Jarvis, P. G. 1991. Do stomata respond to relative humidity? *Plant Cell and Environment* 14, 127–132.

change in the two variables, temperature and air water vapour content. D_s^w and h_s are related according to $h_s = 1 - (D_s^w/\chi_s^{w*})$, where χ_s^{w*} is a function of T_l. At any particular T_l this relationship is linear. Two, more explicit questions which define the problem are:

1. Do stomata respond to both air water vapour content and temperature?

2. Do the responses of stomata to air water vapour content and temperature interact in such a way that h_s is a more appropriate variable than χ_s^w and yields a simpler description of the compound response?

What is known about stomatal responses to humidity and temperature? In a large number of species it has been observed that there is a response of g_s^w to both temperature and humidity (e.g. Lösch & Tenhunen, 1981). In such studies the 'humidity driving variable' has usually been described as the difference between the water vapour concentration or partial pressure in the air outside the boundary layer and the saturated vapour pressure at the temperature of the leaf, and often expressed as a vapour pressure or an absolute humidity *difference*. This difference is the driving force for transpiration and consequently expression in this form implies that the response to humidity is a response to transpiration rate, i.e. evaporation of water in the cell walls of the leaf and its diffusion to the atmosphere.

However, it has been proposed that humidity is sensed at the leaf surface, and not through the rate of evaporation from the mesophyll. Lange *et al.* (1971) observed that in epidermal strips taken from *Polypodium vulgare* leaves, stomata responded to the water vapour content of the air at the leaf surface. By manipulating boundary layer thickness it has been shown that g_s^w is dependent on D_s^w (Bunce, 1985). The information available on the time course of the relationships between g_s^w, or transpiration, and leaf water status (epidermal cell turgor, and xylem water potential) induced by changes in D_a^w (Shackel & Brinckmann, 1985), is also consistent with this hypothesis.

In gas-exchange experiments comparing stomatal response to humidity in air and helox[2] it was found that stomatal aperture was related to the rate of transpiration, rather than to the molar fraction or relative humidity (Mott & Parkhurst, 1991). These experiments with helox give information about the process involved in sensing humidity, but not about the place where sensing takes place.

The relationship between g_s^w and temperature that is observed under constant D_a^w usually shows an optimum (e.g. Neilson & Jarvis, 1975; Osonubi & Davies, 1980). This

---

[2]Helox is a mix of helium and oxygen, that has different physical properties to those of air because of the lower molecular weight of helium compared to nitrogen. The higher diffusivity of water vapour in helox than in air was used as a tool to increase conductances.

optimum can be broad-topped, especially under low I (Osonubi & Davies, 1980). The response of g_s^w to T_l is thought to be mainly the result of the effects of temperature on the energy metabolism of the guard cells, but the question of whether there is a specific temperature sensor in guard cells remains open (e.g. Zeiger, 1983).

Why is it important to know whether stomata respond to h_s or D_s^w? From a practical point of view it is essential to control the correct variable in experimentation, especially in controlled environments. Keeping the wrong humidity variable constant in an experiment to study the response of g_s^w to temperature would result in almost useless data that would show the confounded effects of temperature and humidity. Secondly, using the wrong variable in a model to interpret values of g_s^w measured in the field, must ultimately lead to the model breaking down. From a conceptual point of view, appreciation of the correct variable has a strong influence on hypotheses about the mechanism of stomatal action, and, in this case, has led to the development of the "feed-forward" hypothesis (Cowan, 1977).

I have carried out experiments to test (a) whether g_s^w responds linearly to D_s^w and h_s at a fixed temperature, and (b) whether g_s^w changes with T_l, and thus whether h_s is a more appropriate measure of humidity than D_s^w. This was done by altering leaf temperature and ambient air humidity so as to maintain either h_s or D_s^w constant, whilst observing g_s^w.

5.2 Materials and methods

5.2.1 Plant material

Hedera helix subsp. *canariensis* (Willd.) Coutinho plants were grown in a heated greenhouse. Two different sets of plants were used, in two replicates of the whole experiment. The plants were grown in 12 cm diameter plastic pots filled with a peat-perlite-vermiculite mix, watered every other day, and fertilized weekly (See Chapter 3 for details).

One set of plants —henceforth called set A— was moved 10 days before the beginning of the experiments from the greenhouse to a growth cabinet at 20 °C, with no humidity control ($h \approx 50$ %), and a photoperiod of 12 h at 200 μmol m^{-2} s^{-1} at leaf level from fluorescent tubes (Sylvania 'Powertube' F48T12-CW-VHO).

The second set of plants —set B— was kept for 2.5 months in a growth chamber at 20 °C, h=30–60 %, and a photoperiod of 12 h at 400 μmol m^{-2} s^{-1} at leaf level from metal halide lamps (Wotan 'Power Star' HQI-R 250 W/NDL, Wotan Lamps Ltd., London).

5.2.2 Gas exchange measurements

We used the computer-controlled, open path gas-exchange system described in Chapter 2. The equations used assume a single transpiring surface with uniform spatial distribution of temperature and conductance (see Section 2.2.1). By using a wind speed that gave a g_b^w at least six times the maximum g_s^w and a species with hypostomatous leaves, we attempted to keep the conditions of measurement close to those assumed in the calculations. g_b^w was measured by means of leaf replicas of Whatman No. 3 filter paper covered on the upper side with aluminium foil and wetted with distilled water, and was within the range 650 to 750 mmol m^{-2} s^{-1} for the different leaves used.

Steady-state measurements were made. A new steady value of g_s^w was reached sooner after a change in humidity than after a change in temperature. In the first case no data taken during the first hour after a change in conditions were used; in the second case this time was doubled. However, the data were checked to see whether a steady state had been reached and these periods were extended if necessary.

The leaves to be measured the next day were placed overnight in the gas-exchange chamber in darkness with χ_s^c=350 μmol mol^{-1}, D_s^w=10 mmol mol^{-1}, T_l=20 °C for humidity response experiments, and T_l=15 °C for temperature response experiments.

5.2.3 Experiments

We measured the response of g_s^w to either h_s or D_s^w at a constant T_l of 20 °C, and to increasing temperature at either a constant h_s of 60 % or a constant D_s^w of 10 mmol mol^{-1}. Humidity response was measured by changing the humidity in the gas-exchange chamber so that D_s^w varied over the range 4–17 mmol mol^{-1}, but the environment of the rest of the plant was kept unchanged. In the temperature response experiment, the temperature of the leaf inside the chamber and room air temperature were increased simultaneously over the range 15–29 °C, and in one case 10–29 °C, keeping room air temperature within ±2 °C of T_l. Changing temperature at constant h_s inevitably results in a change in D_s^w; conversely, changing T_l at constant D_s^w results in a change in h_s. Three plants, in each of the two sets, were used as replicates. The different treatments were applied to the same leaf from each plant on different days and in random order. This makes comparison between the effects of temperature at constant h_s and at constant D_s^w very sensitive.

All the experiments were carried out at a χ_s^c of 350 μmol mol^{-1}. A complete whole set of experiments was done at quantum flux densities of 200 and 340 μmol m^{-2} s^{-1} on set A and set B plants, respectively. These quantum flux densities gave approximately 70–80 %, of the light-saturated rate of CO_2 assimilation for each set of plants.
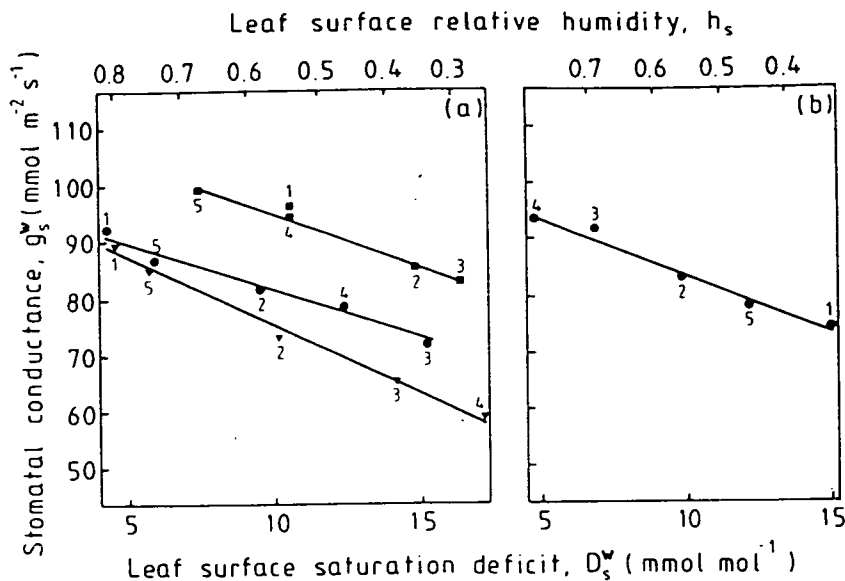
Figure 5.1. Relationship between stomatal conductance (g_s^w) and water saturation deficit at the leaf surface (D_s^w), or relative humidity at the leaf surface (h_s). (a) Data from three *Hedera helix* plants from set A, $I=200$ μmol m^{-2} s^{-1}. R^2 for the linear regressions are 0.97 (■), 0.98 (●), and 0.99 (▼). (b) Data from one plant from set B, $I=340$ μmol m^{-2} s^{-1}. R^2 for the linear regression is 0.98. Measured at $T_l=20$ °C, and $\chi_s^c=350$ μmol mol^{-1}. The numbers beside the symbols show the order in which measurements were taken.

5.3 Results and discussion

5.3.1 Response of g_s^w to humidity at constant temperature

In *Hedera helix* we observed a response of g_s^w to humidity that, under constant T_l and I, was a linear function of both D_s^w, and h_s (Fig. 5.1). For the individual plants, the proportion of the variation in g_s^w that was explained by a linear regression model was 90 % or more. This response showed no hysteresis.

Under constant χ_s^c, Ball (1988, Fig. 2.2.C) measured a linear response to D_s^w at $I=250$ μmol m^{-2} s^{-1}, and a very slightly curved response at $I=525$, and 1375 μmol m^{-2} s^{-1}. A curvilinear response of g_s^w to D_s^w has been previously reported by Bunce (1985) in *Glycine max*, *Abutilon theophrasti*, and *Datura stramonium*. In that set of experiments, carried out under $I=1500$ μmol m^{-2} s^{-1}, the curvature seemed to be linked to high maximum values of g_s^w, and could have been an artifact derived from the calculation procedures used, i.e. a linear regression was first fitted to the relation between total conductance and the leaf-to-air water vapour partial pressure difference, and then g_s^w and D_s^w were computed from this regression. Alternatively
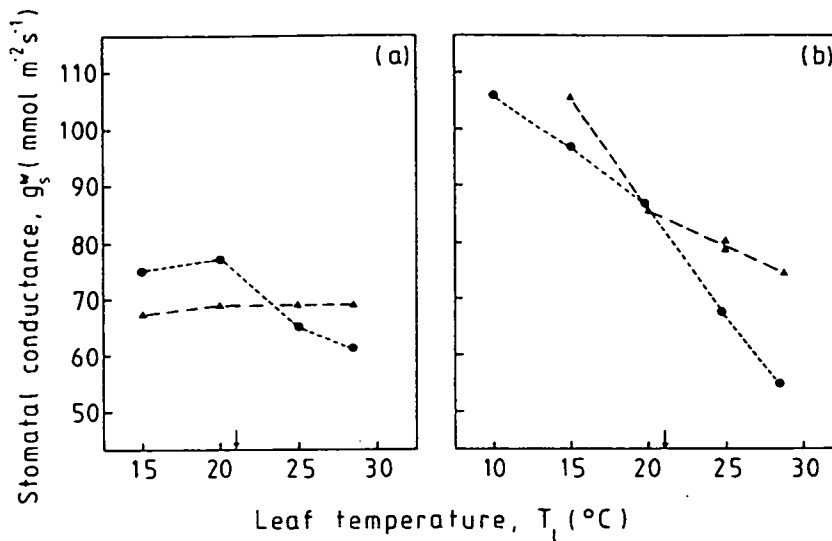
Figure 5.2. Relationship between stomatal conductance (g_s^w) and leaf temperature (T_l) under constant $D_s^w=10$ mmol mol^{-1} (▲), and under constant $h_s=0.60$ (●). (a) Mean of three plants from set A, $I=200$ μmol m^{-2} s^{-1}. (b) Typical plant from set B, $I=340$ μmol m^{-2} s^{-1}. The arrow above the temperature axis shows the point at which humidity is identical for both treatments. Both treatments were applied to the same leaves of the same plants. All measurements were taken at $\chi_s^c=350$ μmol mol^{-1}.

feedback through χ_i^c could have led to the curvature. In Bunce's experiments, CO_2 concentration was not altered to compensate for the effects of the changing g_s^w on χ_s^c or χ_i^c. Reversibility of the response to humidity in whole, attached leaves has been previously reported (Bunce, 1985), but no data were given.

5.3.2 Response of g_s^w to temperature at constant D_s^w or h_s

The response to temperature at constant D_s^w was different to that at constant h_s. In plants from set A there was no response to T_l in the range 15–28 °C under constant D_s^w ($P>0.5$, Fig. 5.2.a), but when h_s was kept constant, g_s^w decreased with increasing T_l —and consequently increasing D_s^w— ($P=0.003$, Fig. 5.2.a). In plants from set B, there was a different and significant effect of T_l under both humidity treatments (Fig. 5.2.b), and the effect of T_l was such that g_s^w was higher at lower temperatures. Under constant D_s^w the effect of an increase in temperature resulted in g_s^w being inversely proportional to h_s (Fig. 5.3.b) (i.e. the opposite to that consistent with the model of Ball *et al.*).

The different response to T_l of the two sets of plants was not totally unexpected as they differed in both growth and measurement conditions. Since stomatal sensitivity

Figure 5.3. Relationship between stomatal conductance (g_s^w) and relative humidity at the leaf surface (h_s), measured under changing leaf temperature (T_l) in the range 10–29 °C. Symbols as in Fig. 5.2. (a) Mean of three plants from set A, $R^2=0.01$, $P>0.5$. (b) Typical plant from set B, $R^2=0.26$, $P=0.13$.

to T_l has been shown to increase with increasing I under constant D_a^w (Osonubi & Davies, 1980), a likely explanation is that the different response was largely the result of the lower I used with set A than with set B.

The optimum temperature for g_s^w varies widely between species and/or growth conditions. Ball (1988, Fig. 2.3.A) observed, in *Glycine max* at constant D_s^w, an approximately linear increase in g_s^w in response to T_l in the range 20–35 °C. In contrast, in *Picea sitchensis* Neilson & Jarvis (1975) observed a T_l response curve having an optimum at 15 °C under constant $D_a^w \approx 5$ mmol mol^{-1}, and in these plants g_s^w was insensitive to χ_i^c and to $D_a^w < 10$ mmol mol^{-1}.

Decreasing g_s^w in response to increasing T_l has been reported in many cases for constant air water vapour content, and consequently decreasing h_s and increasing D_s^w (e.g. Wuenscher & Kozlowski, 1971). Although this is similar to what may happen outdoors during the daily time course of air temperature change, such results shed little light on the nature of the driving variable.

5.3.3 Interaction between humidity and temperature

When the pooled data from both humidity treatments of the temperature-response experiment with plants of set A are plotted against h_s no clear pattern of response
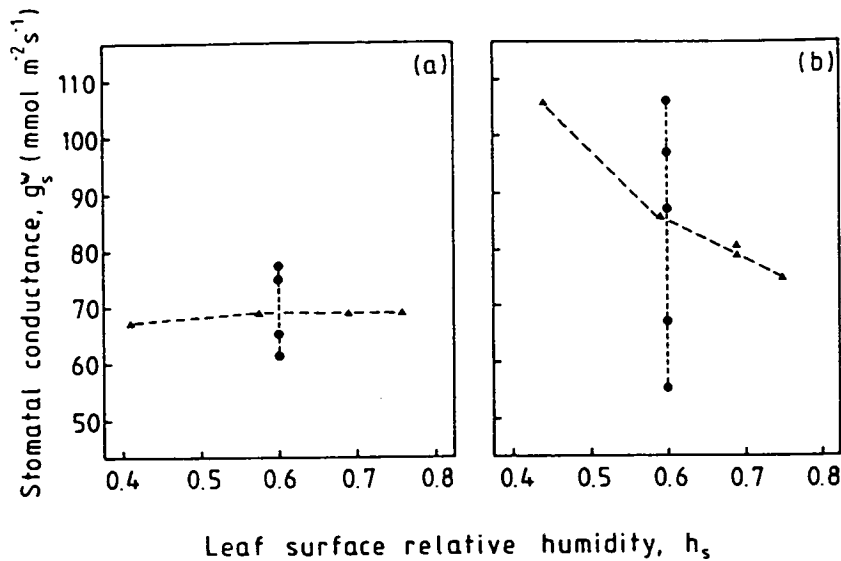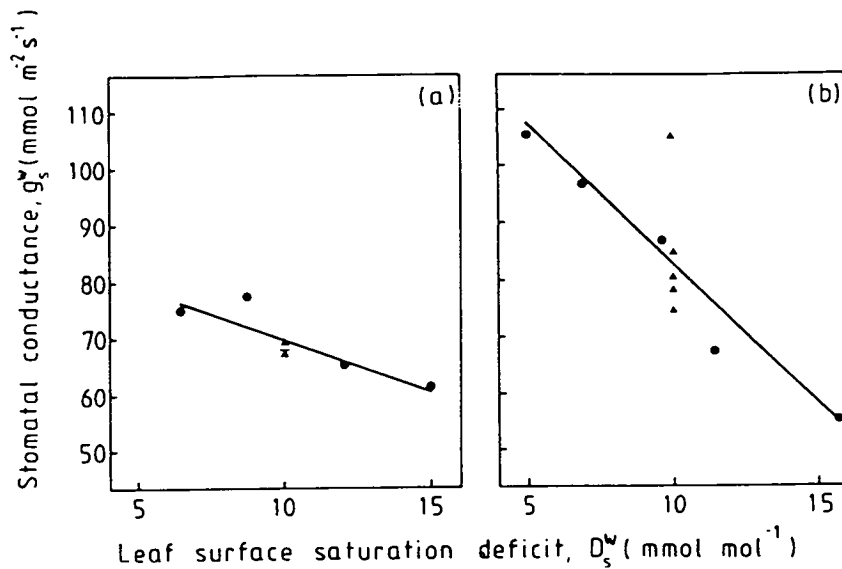
Figure 5.4. Relationship between stomatal conductance (g_s^w) and water vapour deficit at the leaf surface (D_s^w), measured under changing leaf temperature (T_l) in the range 10–29 °C. Symbols as in Fig. 5.2. **(a)** Mean of three plants from set A, $R^2=0.77$, $P=0.004$. **(b)** Typical plant from set B, $R^2=0.75$, $P=0.001$. The triangle with an underscore represents three overlapping data points.

appears ($R^2=0.01$, $P>0.5$), and the data from each treatment show a different pattern of change (Fig. 5.3.a). When these same data are plotted against D_s^w a clear linear decrease in g_s^w in response to increasing D_s^w appears ($R^2=0.77$, $P=0.004$; Fig. 5.4.a): data from both treatments collapse into a single relationship only when expressed as a function of D_s^w. In set B, where there is an effect of both temperature and humidity, the variation in the data cannot be described as a function of only D_s^w or h_s (Figs. 5.3.b & 5.4.b). However, for a typical plant from this set, D_s^w explains 75 % of the variation while h_s explains only 26 %.

Stronger evidence can be obtained by comparing the behaviour of g_s^w under constant T_l with that under constant D_s^w. Changing h_s by altering T_l led to no response of g_s^w (Fig. 5.3.a), or to the opposite response to that observed when changing h_s under constant T_l (Fig. 5.1.b *vs.* Fig. 5.3.b). g_s^w decreased with increasing h_s at constant D_s^w in set B (Fig. 5.3.b). Although there was a response to T_l at constant D_s^w only in set B, the response to humidity did not differ between the two sets of plants in a way that would make both responses compatible with a single mechanism based solely on the sensing of h_s, thus reinforcing our argument. Even Ball (1988, Figs. 2.3.B, 2.3.C & 2.4), observed an effect of T_l on g_s^w at constant h_s, in a setting such that g_s^w increased with

increasing T_l at constant D_s^w, and this effect only disappeared when g_s^w was substituted by g_s^w/A.

5.4   Conclusions

Based on these experiments, the answers, for *Hedera helix*, to the two questions stated in the introduction to this chapter are:

1. Stomata do respond to humidity, and sometimes respond to temperature as well. An inversely proportional response of g_s^w to D_s^w was consistently obtained. The response to T_l at constant D_s^w was sometimes absent, but when present this response was a decrease in g_s^w with increasing T_l.

2. These responses do *not* interact in a way that makes h_s a more appropriate way of expressing humidity than χ_s^w. The apparent relation between g_s^w and h_s at constant D_s^w was different to that at constant T_l, and so h_s was unable to explain the responses of g_s^w to both humidity and temperature.

D_s^w, together with T_l, give a more general and simpler description of the response of g_s^w than h_s. The experiments provide no evidence in favour of a mechanism of humidity sensing based on h_s. There is no means by which the correlation between T_l, and the relationship between D_s^w and h_s can be broken experimentally. However, by using helox, it is possible to test whether the response depends on diffusional flow of water vapour or on sensing water vapour concentration directly. This test, done by Mott & Parkhurst (1991), showed that stomatal response to humidity depends on a diffusional flux, supporting my finding that D_s^w is the preferred expression.

Chapter 6

The boundary layer and stomatal function

6.1 Introduction

In previous chapters I have considered the effect on stomata of the condition of the air at the leaf surface and in the intercellular spaces. However, because between the bulk air and the outermost parts of the leaf there is a boundary layer of air, in this chapter I will analyse stomatal function within a framework that includes the boundary layer. There are two different aspects to the problem: (1) the role of the boundary layer in the mechanism of stomatal response to the condition of the bulk air, and (2) the role of the boundary layer in stomatal responses to χ_a^w, χ_a^c, and wind speed under natural conditions.

Stomatal conductance changes with wind speed when D_a^w and χ_a^c are kept constant (Caldwell, 1970; Grace *et al.*, 1975; van Gardingen & Grace, 1991). However, although the boundary layer has been taken into account in descriptions of the soil-plant-atmosphere water continuum, in the calculation of g_s^w, or in analyses of the control of CO_2 fixation (e.g. Woodrow *et al.*, 1987), its role as a component of the mechanism of stomatal response has remained unexplored, except for the experiments of Bunce (1985) [e.g. the effect of the boundary layer was not included in the feedback analysis made by Farquhar *et al.* (1978)].

In most studies of stomatal responses to humidity and CO_2 the experimentally controlled variables have been those describing bulk air properties. Responses to CO_2 have been studied by controlling χ_a^c and responses to air humidity by altering D_a^w or χ_a^w. In most gas exchange chambers wind speed is kept high so as to reduce the thickness of the boundary layer and make the difference between χ_a^c and χ_s^c, and D_a^w and D_s^w

small, but this is not the case in the real world. Although χ_a^c and D_a^w are variables of ecological interest, it is impossible for stomata to sense them directly. Both direct responses —those occurring within the guard cells— and indirect responses —those depending on events happening in other cells of the leaf— can only depend on the state of system variables inside the boundary layer. For this reason the analysis of stomatal responses to changes in bulk air properties must include the boundary layer as a component of the response mechanism. In nature the state of the air at the leaf surface cannot be considered as an independent variable —it strongly depends on g_s^w for a given state of the bulk air (Jarvis & McNaughton, 1986). The boundary layer is a source of feedback, and so it can alter the apparent behaviour of stomata.

The apparent responses of g_s^w to χ_a^w and χ_a^c depend on the effects of these two variables, g_b^w and g_s^w, on D_s^w and χ_i^c. Control diagrams are useful for visualizing interactions, and I have adapted that given by McNaughton & Jarvis (1991, Fig. 6) by including the effect of changes in g_b^w and assuming constant T_l (Fig. 6.1). A control diagram allows one to trace the propagation of a change in one variable (e.g. $d\chi_a^w$) through the system, and also shows the feedback loops.

Under natural conditions g_b^w can be an important component of g_t^w. The thickness of the boundary layer, and hence the magnitude of g_b^w, varies widely according to leaf size and wind speed. For big leaves the boundary layer can be a few millimeters thick even under moderate wind speed. For ivy leaves of the size of those used in my experiments, thicknesses between 1.0 and 3.3 mm could be expected under natural conditions (assuming wind speeds between 0.1 and 1 m s^{-1}). For one side of the leaf, these represent $g_b^w \approx 290$ mmol m^{-2} s^{-1} and $g_b^w \approx 970$ mmol m^{-2} s^{-1}, respectively[1]. Some species such as *Helianthus annuus* (Körner *et al.*, 1979), and *Tectona grandis* and *Gmelina arborea* (Grace *et al.*, 1982) have high stomatal conductances and their leaves are several times the size of leaves of ivy, thus having thicker boundary layers at the same wind speed. In a rain forest canopy, it was found that g_b^w increased with height, from 240 mmol m^{-2} s^{-1}, for both leaf surfaces in parallel, at the forest floor to 1400 mmol m^{-2} s^{-1} at the top of the canopy (35 m) (Roberts *et al.*, 1990).

Experiments were done to describe the effect of the boundary layer on stomatal response to change in the molar fractions of CO_2 and water vapour in the bulk air. Both actual and simulation experiments were done. The actual experiments included measurements to obtain the data needed to drive the simulations, and measurements of the response of g_s^w to changes in the thickness of the boundary layer. The simulation experiments were done to derive stomatal responses to χ_a^c and D_a^w and their interactions

---

[1] These values arise from calculations based on equations given by Nobel (1983, pages 358, 391–392).
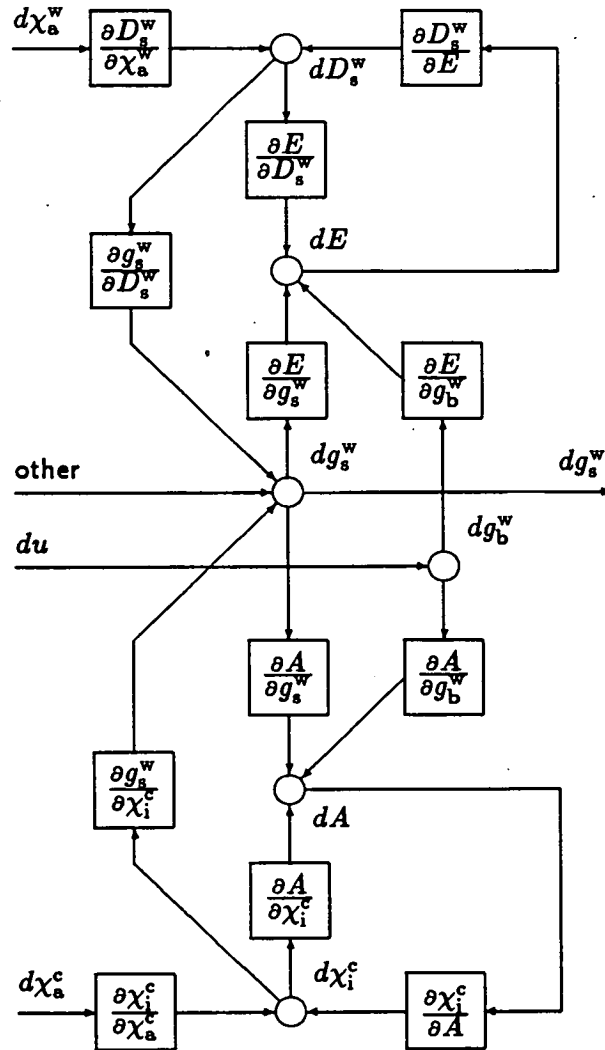
Figure 6.1. Control diagram showing the response of stomatal conductance (g_s^w) to changes in bulk air water vapour molar fraction (χ_a^w), bulk air CO_2 molar fraction (χ_a^c), and wind speed (u), for a hypostomatous leaf. The changes in intercellular CO_2 molar fraction (χ_i^c), leaf surface water vapour deficit (D_s^w), boundary layer conductance (g_s^w), CO_2 flux density (A) and transpiration (E), are also indicated. The top half of the diagram represents E, the bottom half represents A. The circles represent summation points and the boxes represent gain elements, with functions shown as partial derivatives.

with g_b^w.

6.2 Materials and methods

6.2.1 Plant material

Ivy plants were grown in a heated greenhouse. The plants were grown in 16 or 18 cm diameter plastic pots filled with a peat-perlite-vermiculite mix, watered every other day, and fertilized weekly (See Chapter 3 for details).

Two sets of plants were used, in three experiments. The plants were moved more than 75 d before the beginning of the experiments from the greenhouse to a growth room at 20/15 °C day/night, with no humidity control ($h \approx 60$ %), and a photoperiod of 12 h at 500 μmol m^{-2}s^{-1} at leaf level from metal halide lamps (Kolorarc 400W MBIF/BU, Thorn Lighting Ltd., London, U.K.).

6.2.2 Gas exchange measurements

The computer-controlled, open differential gas-exchange system described in Chapter 2 was used. Wind speed was measured with a hot wire anemometer (AVM501, Prosser Scientific Instruments Ltd., Hadleigh, Suffolk, U.K.). g_b^w, for one side of the leaves, was measured at the two wind speeds used in the experiments by means of leaf replicas of Whatman No. 3 filter paper covered on the upper side with aluminium foil and wetted with distilled water.

Steady-state measurements of A and E were made, and no data taken during the first hour after a change in conditions were used. However, the data were checked to see whether a steady state had been reached and this period was extended if necessary. The temperature of leaves and leaf replicas was measured with a thermojunction in contact with their shaded face near the centre of the blade. The leaves to be measured the next day were placed overnight in the gas-exchange chamber in darkness with $\chi_s^c = 350$ μmol mol^{-1}, $D_s^w = 10$ mmol mol^{-1}, $T_l = 20$ °C. Attached non-senescent fully expanded leaves were used in the experiments, the projected area of individual leaves being between 50 and 64 cm^2.

6.2.3 Simulation model

A simple model was developed to compute the apparent steady-state response of stomata to χ_a^w and χ_a^c. Given a known response of g_s^w to D_s^w and χ_i^c, and an A vs. χ_i^c curve, the model computes g_s^w for given g_b^w, χ_a^w and χ_a^c. This model simulates the effect of the boundary layer on the *apparent* response of stomata given a *known* stomatal response

to D_s^w and χ_i^c. It is *not* a model of stomatal responses to CO_2 and humidity, it is instead a model of how these responses are modified by the boundary layer. The MWEB listing of the computer program is given in Appendix A.

The model is represented by a system of two simultaneous non-linear equations in two unknowns:

$$f(D_s^w, \chi_i^c) = 0, \qquad (6.1a)$$

$$ff(D_s^w, \chi_i^c) = 0. \qquad (6.1b)$$

This system of equations embodies the conditions fulfilled by E and A when both flows are in steady-state. As both A and E depend on g_s^w both equations are functions of D_s^w and χ_i^c. The use of D_s^w and χ_i^c in these equations reflects the fact that these are the variables sensed by the guard cells. As A affects χ_i^c, and E affects D_s^w, the two equations have to be solved simultaneously.

Equation 6.1a defines the equilibrium condition for g_s^w with respect to D_s^w, and is:

$$D_a^w \left(1 - \frac{g_t^w}{g_b^w}\right) - D_s^w = 0, \qquad (6.2)$$

or, in words, the value of D_s^w calculated from g_s^w must be the same as that used to compute g_s^w. Equation 6.2 was derived from Equation 2.22, assuming that T_l remains constant.

Equation 6.1b is

$$\chi_a^c - \frac{A}{g_t^c} - \chi_i^c = 0, \qquad (6.3)$$

and defines the steady-state condition for g_s^w with respect to χ_i^c. This equation could have been derived from Equation 2.31, but instead a simpler expression, without a correction for the mass flow of water, was used in the model.

In the equations A is calculated as a function of χ_i^c using spline interpolation from tabulated data, and $g_t^w = (1/g_s^w + 1/g_b^w)^{-1}$ and $g_t^c = (1.60/g_s^w + 1.37/g_b^w)^{-1}$. g_s^w is computed as the product of the conductance observed under standard conditions and scaling factors obtained by spline interpolation from tabulated data:

$$g_s^w = k\, f_0(D_s^w)\, f_1(\chi_i^c), \qquad (6.4)$$

where k is g_s^w at a standard condition, and is a parameter of the model, f_0 and f_1 are spline functions giving the relative effect of D_s^w and χ_i^c on g_s^w. Computing the compound effect of changes in CO_2 and water vapour molar fractions on g_s^w as the

product of f_0 and f_1 assumes that these effects are multiplicative.

The equation given by Nobel (1983)[2] was used to relate mean boundary layer thickness (b) to leaf dimension —i.e. the spatial average of leaf length in the wind direction, not the *equivalent* dimension— (l) and wind speed (u):

$$b = 0.004\sqrt{\frac{l}{u}}. \tag{6.5}$$

This equation gives only an approximation to the mean value of b, because b varies across the leaf surface (see also Section 1.1.3), and because air flow in the field is not laminar. The value of 0.004 for the factor in Equation 6.5 was derived by Nobel from field measurements done by Pearman *et al.* (1972). The conductance of the boundary layer to water vapour is related to its thickness by the molar diffusivity of water vapour in air (D^w), i.e. $g_b^w = D^w/b$.

The system of two simultaneous non-linear equations is solved by an iterative procedure based on a quasi-Newton algorithm using finite differences to approximate the derivatives (Johnston, 1982; Press *et al.*, 1986, were used as a guide). Simulations are driven by four text files containing the data:

1. **Relationship between A and χ_i^c.** Data pairs of χ_i^c, in mol mol^{-1}, and A, in mol m^{-2} s^{-1}, give the points that are used for interpolation.

2. **Relationship between g_s^w and D_s^w.** Data pairs of D_s^w, in mol mol^{-1}, and g_s^w, as a proportion of that in standard conditions, give the points that are used for interpolation.

3. **Relationship between g_s^w and χ_i^c.** Data pairs of χ_i^c, in mol mol^{-1}, and g_s^w, as a proportion of that in standard conditions, give the points that are used for interpolation.

4. **Input file with values for the driving variables.** Each line of this file contains data for the simulation of the steady-state of g_s^w, and A and E, at a particular environmental condition. The driving variables are χ_a^w, χ_a^c, I, T_l, and g_b^w. (I is not used in the current version of the model, and is assumed constant).

The output from the program is another text file, with one line for each line in the input file (4 in the list above). The state variables in the output file are g_s^w, A, E,

---

[2]This equation can be derived from that given by Monteith & Unsworth (1990, Equation 7.1) for a laminar boundary layer.

D_s^w, and χ_i^c. The output also includes the the minimization errors for D_s^w and χ_i^c and a text string that indicates whether the numerical algorithm has succeeded or not in solving the system of equations. g_b^w was converted to u for a given leaf size by means of a simple program written in the programming language AWK.

6.2.4 Experiments

Real world experiments

In one experiment —henceforth experiment I— the response to a change in g_b^w was measured under both constant χ_a^c and χ_a^w (and so changing χ_s^c and D_s^w), and under constant χ_s^c and D_s^w. The value of g_b^w was altered by changing wind speed in the leaf chamber. g_b^w, for one surface of the leaf, was 750 mmol m^{-2} s^{-1} for the 'high' wind speed treatment (0.8 m s^{-1}), and 360 mmol m^{-2} s^{-1} for the 'low' wind speed (0.2 m s^{-1}) treatment. The lowest g_b^w was 2.5 times the highest value of g_s^w observed, and the small errors in its measurement should not have caused significant errors in the estimation of g_s^w. The same sequence of treatments was applied to each of three plants from set B.

In a second experiment —experiment II— response curves of g_s^w and A to D_s^w and χ_i^c were measured. The response to D_s^w was measured at constant $\chi_i^c \approx 200$ μmol mol^{-1}, and that to χ_i^c at constant $D_s^w = 7$ mmol mol^{-1}. The response to D_s^w in the range 5–16 mmol mol^{-1} was measured, D_s^w being changed in random order because there is no hysteresis in the humidity response of ivy stomata under these conditions (See Chapter 5). For measuring the response to CO$_2$, χ_i^c was first decreased to approximately 120 μmol mol^{-1} and then increased in 5–7 steps to 300–350 μmol mol^{-1}. Three plants from set A were used.

In a third experiment —experiment III— the interaction between the responses of g_s^w and A to χ_i^c and D_s^w was studied in a 2 × 2 factorial arrangement ($\chi_i^c = 200$ and 290 μmol mol^{-1}, $D_s^w = 6$ and 12 mmol mol^{-1}). The four treatments were applied to each plant in a fixed sequence: (1) low D_s^w and low χ_i^c, (2) high D_s^w and low χ_i^c, (3) low D_s^w and high χ_i^c, and (4) high D_s^w and high χ_i^c. This sequence was selected to obtain a decrease, or no change, in g_s^w with successive treatments, and in this way preventing hysteresis from affecting the results. This is valid only because there is no effect of the time of day on g_s^w (See Section 3.4). Three plants from set B were used.

Simulation experiments

Simulations were done driving the model with the g_s^w and A response curves to χ_i^c measured at constant D_s^w, and the g_s^w response curve to D_s^w measured at constant

χ_i^c (from experiment II above). The apparent responses of g_s^w to changes in χ_a^w and χ_a^c were calculated for $g_b^w = 100-1000$ mmol m^{-2} s^{-1}. The response to wind speed was also computed. To assess how much of this response is dependent on changes in χ_s^w and how much on changes in χ_s^c, simulations were also done with hypothetical stomata insensitive to D_s^w.

6.3 Results and discussion

6.3.1 Responses to D_s^w and χ_i^c

Experiment I

Changing wind speed caused a change in g_s^w (Fig. 6.2), as previously observed in other species (Grace *et al.*, 1975; Bunce, 1985). Decreasing g_b^w under constant χ_a^c and D_a^w caused an increase in g_s^w, but restoring χ_s^c and D_s^w to their initial values caused g_s^w to decrease as much as it had increased. Subsequently, increasing g_b^w to its original value keeping χ_a^c and D_a^w constant at their new values caused a decrease in g_s^w that once more reverted when χ_s^c and D_s^w were restored to their initial state. This sequence of treatments was repeated in three plants with almost identical results, a typical time course is shown in Fig. 6.2 and the means in Table 6.1. In treatments 1 and 3, which had different wind speeds but the same χ_s^c and D_s^w, g_s^w and A were not significantly different. The differences in g_s^w and A between treatments 1 and 2 shows the effects of a decrease in wind speed, and between 3 and 4 the effects of an increase in wind speed, in both cases under constant χ_a^c and D_a^w but with changing χ_s^c and D_s^w.

In an experiment where CO_2 concentration was not controlled, Bunce (1985) attributed all the effect of wind speed to its effect on D_s^w. The data presented here show that in ivy there are two effects, one through water vapour and another through CO_2 (Table 6.1). Whether there is an effect through CO_2 or not depends on stomatal sensitivity to CO_2. In ivy there was also a small effect of wind speed on A, caused by its effect on χ_s^c (Table 6.1). A similar effect was also previously observed in other species by Bunce (1988a).

Experiment II

In this experiment, responses of g_s^w and A to CO_2 and water vapour were measured one at a time, keeping the other variable constant at the place where it is sensed by stomata. g_s^w decreased linearly with increasing χ_i^c under constant D_s^w (Fig. 6.4), and g_s^w decreased linearly with increasing D_s^w under constant χ_i^c (Fig. 6.3). To the best of my knowledge, there are no previous reports of a g_s^w response to D_s^w measured under
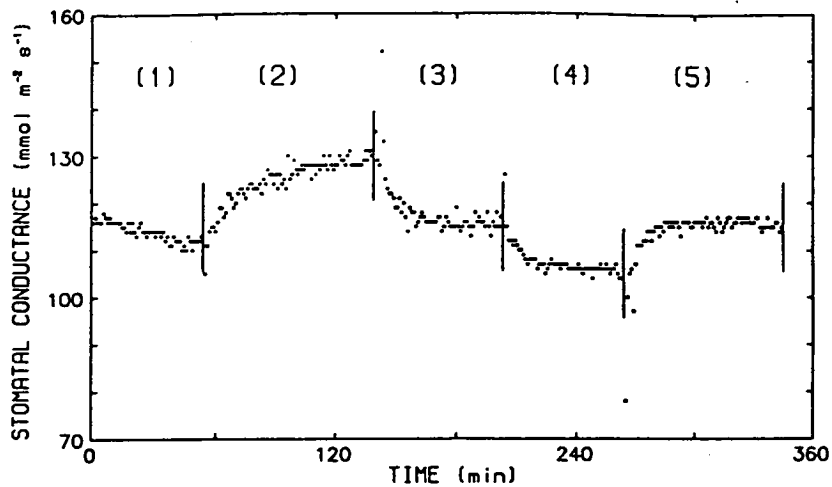
Figure 6.2. Effect of boundary layer conductance (g_b^w) on stomatal conductance (g_s^w) in a typical leaf. g_b^w was altered by changing the wind speed. Five different treatments were applied in sequence: (1) $g_b^w = 750$ mmol m^{-2} s^{-1}, $\chi_i^c = 200$ μmol mol^{-1}, $D_s^w = 7$ mmol mol^{-1}, $\chi_a^c = 345$ μmol mol^{-1}, $D_a^w = 8.1$ mmol mol^{-1}; (2) $g_b^w = 360$ mmol m^{-2} s^{-1}, bulk air mol fractions as in (1); (3) $g_b^w = 360$ mmol m^{-2} s^{-1}, $\chi_i^c = 200$ μmol mol^{-1}, $D_s^w = 7$ mmol mol^{-1}; (4) $g_b^w = 750$ mmol m^{-2} s^{-1} and bulk air mol fraction as in (3); (5) restored to $g_b^w = 750$ mmol m^{-2} s^{-1}, $\chi_i^c = 200$ μmol mol^{-1}, $D_s^w = 7$ mmol mol^{-1}. ($T_l = 20$ °C, and $I = 500$ μmol m^{-2} s^{-1}). The vertical bars indicate the times when conditions were changed.

Table 6.1. Effect of boundary layer conductance (g_b^w) on stomatal conductance (g_s^w), CO_2 flux density (A), and leaf surface CO_2 molar fraction (χ_s^c). g_b^w was altered by changing the wind speed. The sequence of treatments is indicated in Fig. 6.2. Means, and standard errors (in brackets) are given. Tukey's *hsd* test for multiple comparisons was used. Significance was calculated using the error mean square from an ANOVA for a randomized complete blocks design, each one of the three plants used being a block. Different letters indicate $P < 0.06$, according to this test.

Treatment	g_s^w	A	χ_s^c
	(mmol m^{-2} s^{-1})	(μmol m^{-2} s^{-1})	(μmol mol^{-1})
1	116(3.1) b	8.5(0.31) a	327(3.5) b
2	129(3.8) a	8.0(0.19) a	314(4.7) a
3	116(2.0) b	8.3(0.32) a	326(3.2) b
4	105(3.6) c	8.6(0.35) a	341(3.3) c
5	113(1.2) b	8.3(0.39) a	329(3.2) b
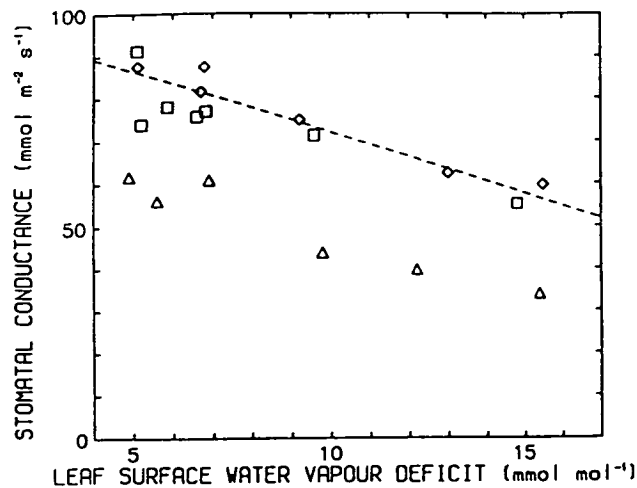
Figure 6.3. Relationship between stomatal conductance (g_s^w) and leaf surface water vapour deficit (D_s^w) measured at constant leaf temperature and intercellular CO_2 mol fraction $(T_1=20\ °C$, $\chi_i^c \approx 200\ \mu mol\ mol^{-1}$, and $I= 490\ \mu mol\ m^{-2}\ s^{-1})$. The different symbols indicate data from different plants, the dashed line is the relationship used in the model.

constant χ_i^c, or of a g_s^w response to χ_i^c measured under constant D_s^w. The response to D_s^w was similar to that measured under constant χ_a^c and high g_b^w (Fig. 5.1). A slightly curved response of g_s^w to D_a^w has been observed under constant χ_a^c in *Picea sitchensis*, but a linear response in *Pinus sylvestris* (Sandford, 1984, Figs. 7.1 & 5.1). Under constant D_a^w, the response of g_s^w to χ_i^c in other species have been found to be variable and usually not linear, and to depend on I and D_a^w (Jarvis & Morison, 1981; Morison & Gifford, 1983; Morison, 1987).

A increased with χ_i^c (Fig. 6.5), and the A *vs.* χ_i^c curve was similar to that reported for low light grown ivy plants (Bauer & Thöni, 1988, Fig. 5). The CO_2 compensation concentration calculated by extrapolation was 42 $\mu mol\ mol^{-1}$ (S.E.=8.9 $\mu mol\ mol^{-1}$). This is very close to the value of 38 $\mu mol\ mol^{-1}$ that has been measured in *Hedera helix* at 20 °C and under saturating I (Bauer & Bauer, 1980).

No effect of D_s^w on A was observed under constant χ_i^c, for $D_s^w \leq 15$ mmol mol^{-1} (Fig. 6.6). However, in some plants there was a slight decrease in A at $D_s^w > 15$ mmol mol^{-1}, but this was not a consistent response (data not shown). It is usually assumed that A is not affected by D_s^w under constant χ_i^c, but there have been reports of a decrease of A in response to increase in D_a^w and E independent of stomatal response (e.g. Sharkey, 1984; Bunce, 1988b). Our data do not rule out such an effect in ivy at high values of
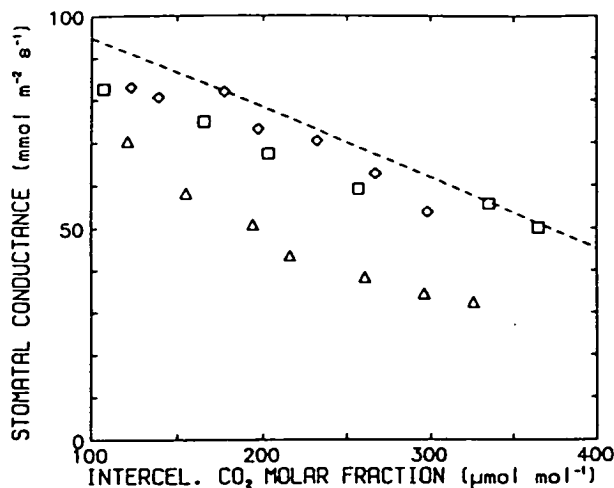
Figure 6.4. Relationship between stomatal conductance (g_s^w) and intercellular CO_2 mol fraction (χ_i^c) measured at constant leaf temperature and leaf surface water vapour deficit $(T_l = 20\ °C,\ D_s^w = 7\ \text{mmol mol}^{-1},\ \text{and}\ I = 490\ \mu\text{mol m}^{-2}\,\text{s}^{-1})$. The different symbols indicate data from different plants, the dashed line is the relationship used in the model.

D_s^w and E.

The ratio χ_i^c / χ_s^c decreased with increasing D_s^w (Fig. 6.7), and with increasing χ_i^c (Fig. 6.8). However, the slopes were not significantly different from zero at $P=0.05$ ($P=0.12$ for D_s^w, and $P=0.07$ for χ_i^c).

Experiment III

In the factorial experiment there were effects of both D_s^w and χ_i^c on g_s^w in agreement with experiment II, but in the factorial experiment g_s^w was higher than in the previous experiment. The ANOVA of the untransformed g_s^w data yielded a significant interaction term ($P=0.03$), indicating that the effects of χ_i^c and D_s^w are not additive. Using logarithms to transform these same data before computing the ANOVA, yielded a non-significant interaction (Table 6.2). That the effects of χ_i^c and D_s^w were additive in the log-transformed data indicates that the raw effects of χ_i^c and D_s^w on g_s^w were multiplicative, as assumed in the model. This kind of interaction has been assumed in models for other species (Jarvis, 1976; Avissar *et al.*, 1985). As expected the effect of χ_i^c on A was highly significant, but no effect of D_s^w on A or interaction between D_s^w and χ_i^c was observed (Table 6.2).

The ratio χ_i^c / χ_s^c was affected by D_s^w and χ_i^c (Table 6.2), decreasing with increase
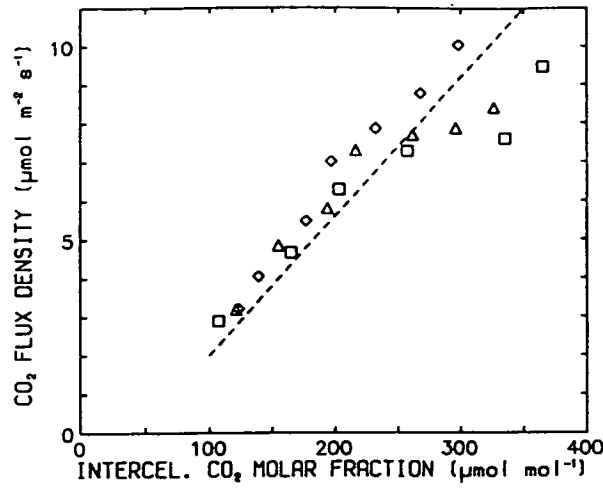
Figure 6.5. Relationship between CO_2 flux density (A) and intercellular CO_2 mol fraction (χ_i^c) measured at constant leaf temperature and leaf surface water vapour deficit $(T_l = 20\ °C$, $D_s^w = 7$ mmol mol^{-1}, and $I = 490\ \mu$mol m^{-2} s^{-1}). The different symbols indicate data from different plants, the dashed line is the relationship used in the model.
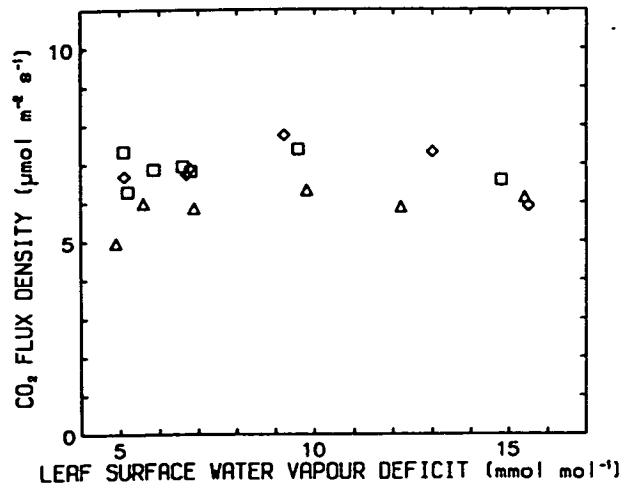
Figure 6.6. Relationship between CO_2 flux density (A) and leaf surface water vapour deficit (D_s^w) measured at constant leaf temperature and intercellular CO_2 mol fraction $(T_l = 20\ °C$, $\chi_i^c \approx 200\ \mu$mol mol^{-1}, and $I = 490\ \mu$mol m^{-2} s^{-1}). The different symbols indicate data from different plants.
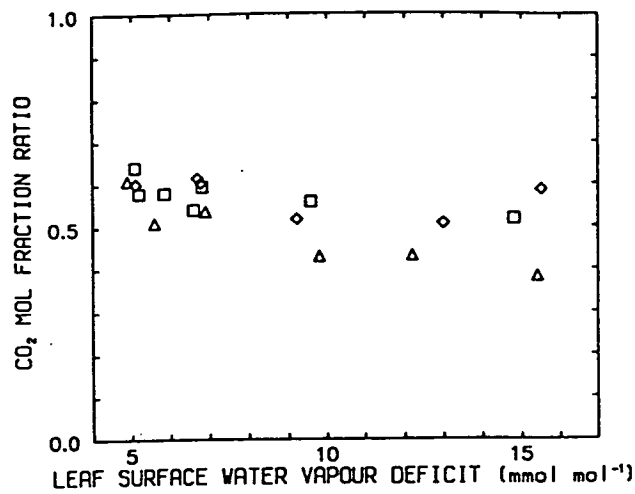
Figure 6.7. Relationship between the χ_i^c/χ_s^c ratio and leaf surface water vapour deficit (D_s^w) measured at constant leaf temperature and intercellular CO_2 mol fraction ($T_l=$ 20 °C, $\chi_i^c \approx 200$ μmol mol^{-1}, and $I=490$ μmol m^{-2} s^{-1}). The different symbols indicate data from different plants.

Figure 6.8. Relationship between the χ_i^c/χ_s^c ratio and intercellular CO_2 mol fraction (χ_i^c) measured at constant leaf temperature and leaf surface water vapour deficit ($T_l=$ 20 °C, $D_s^w=7$ mmol mol^{-1}, and $I=490$ μmol m^{-2} s^{-1}). The different symbols indicate data from different plants.

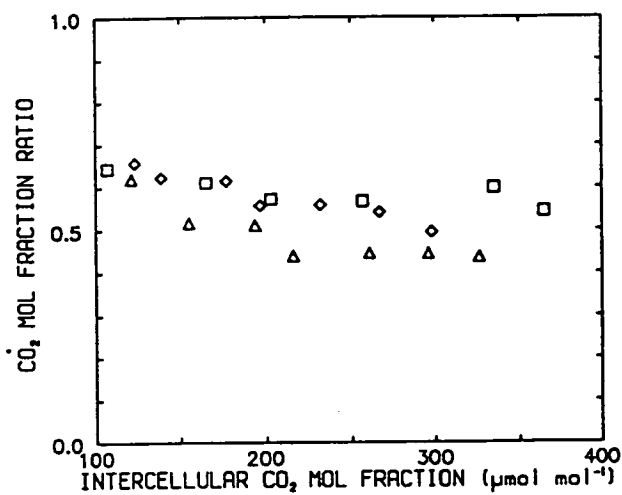**Table 6.2.** Effects of leaf surface water vapour deficit (D_s^w) and intercellular CO_2 concentration (χ_i^c) on stomatal conductance (g_s^w), CO_2 flux density (A), and the χ_i^c/χ_s^c ratio. $T_l=20$ °C, $I=500$ μmol m^{-2} s^{-1}. **Part A:** means and standard errors of the means (in brackets). **Part B:** summary table of analysis of variance. A complete randomized blocks design was used, the plants being the blocks. M.S.: mean square, P: probability.

Part A: means and standard errors				
χ_i^c	D_s^w	g_s^w	A	χ_i^c/χ_s^c
(μmol mol^{-1})	(mmol mol^{-1})	(mmol m^{-2} s^{-1})	(μmol m^{-2} s^{-1})	(mol mol^{-1})
200	6	127(17.5)	8.5(0.30)	0.64(0.023)
200	12	73(12.6)	8.5(0.39)	0.51(0.048)
290	6	66(18.4)	12.1(0.59)	0.48(0.079)
290	12	44(9.0)	12.4(0.90)	0.38(0.055)

Part B: analysis of variance							
Source of variation	d.f.	log(g_s^w) M.S.	P	A M.S.	P	χ_i^c/χ_s^c M.S.	P
χ_i^c	1	1.126	<0.001	41.11	<0.001	0.063	0.002
D_s^w	1	0.650	0.001	0.09	0.662	0.041	0.005
interac.	1	0.025	0.233	0.08	0.680	0.001	0.531
plants	2	0.408	0.001	2.95	0.027	0.030	0.006
error	6	0.014	—	0.42	—	0.002	—

in both D_s^w and χ_i^c. The measurements at different χ_i^c were made by changing χ_s^c, and so are equivalent to those reported in the literature, except that I kept D_s^w constant. However, in contrast to previous reports that χ_i^c/χ_s^c (or χ_i^c/χ_a^c) is not affected by change in χ_s^c (e.g. Louwerse, 1980), in ivy there was a significant, although small, effect. In experiment II this effect was also observed, although not significant. There was no interaction between the effects of χ_i^c and D_s^w on χ_i^c/χ_s^c (Table 6.2).

In other species it has been observed that the effects of changes in χ_i^c and D_a^w on g_s^w are proportional to the current value of g_s^w: dg_s^w/dD_a^w and $dg_s^w/d\chi_i^c$ were linearly correlated with g_s^w in four grass species (Morison & Gifford, 1983). It is difficult to assess whether this is also true for ivy from the response curves to χ_i^c and D_s^w (Figs. 6.4 & 5.1), but the fact that the effects of χ_i^c and D_s^w on $log(g_s^w)$ do not interact, i.e. are additive, seems to indicate that the effects of χ_i^c and D_s^w on g_s^w are proportional to g_s^w (Table 6.2).

The data in Table 6.1 show that the effect of wind speed on g_s^w is fully explained
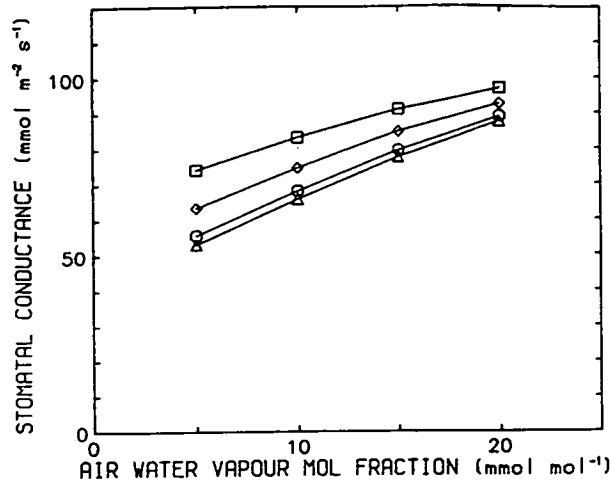
Figure 6.9. Simulated relationship between stomatal conductance (g_s^w) and bulk air water vapour molar fraction (χ_a^w) for ($\square$) $g_b^w = 100$, ($\diamond$) $g_b^w = 200$, ($\circ$) $g_b^w = 500$, and ($\triangle$) $g_b^w = 1000$ mmol m^{-2} s^{-1}, under constant leaf temperature and bulk air CO_2 mol fraction ($T_l = 20$ °C, $\chi_a^c = 350$ μmol mol^{-1}, and $I = 500$ μmol m^{-2} s^{-1}). Simulation based on response data in Figs. 6.3, 6.4, & 6.5.

by its effect on the CO_2 and water vapour molar fractions at the leaf surface, and the data in Table 6.2 show that the effects of CO_2 and humidity affect g_s^w multiplicatively, thus bearing out the two main assumptions of the model.

6.3.2   Simulated responses of g_s^w and A to bulk air state variables

Water vapour molar fraction

The model was used to calculate the responses of g_s^w and A to χ_a^w. Using as input the relationships indicated with dashed lines in Figs. 6.3, 6.4 & 6.5, the model yields the results in Figs. 6.9, 6.10, 6.11 & 6.12. As expected, g_s^w increased with χ_a^w, the slope being steeper at higher values of g_b^w (Fig. 6.9). The response to g_b^w was larger at lower ambient humidity, and the stomata partially compensated for the decrease in g_b^w—i.e. g_s^w was higher at lower values of g_b^w.

Because of the change in g_s^w, χ_i^c changed in response to both χ_a^w and g_b^w (Fig. 6.10), and so A also changed (Fig. 6.11). The magnitude of the effect of χ_a^w on A depended on the value of g_b^w, this being a reflection of the effect of χ_a^w on χ_i^c. The simulated response of χ_i^c to χ_a^w, lower χ_i^c values at lower χ_a^w, is similar to that observed in real experiments (Sandford, 1984, Fig. 7.8). The slope of this response was sensitive to g_b^w,
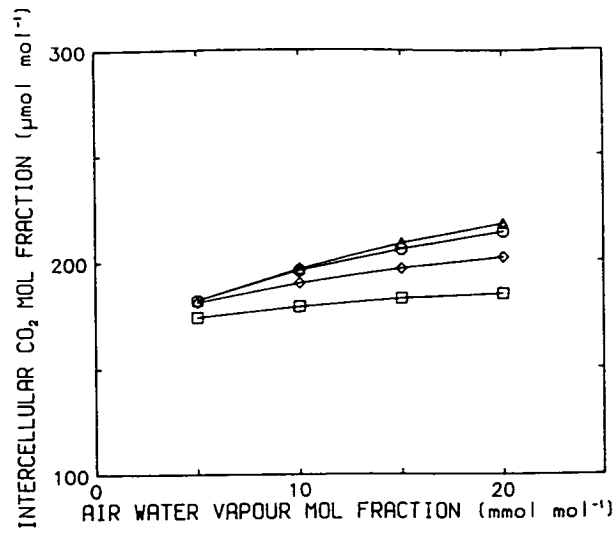
Figure 6.10. Simulated relationship between intercellular CO_2 mol fraction (χ_i^c) and bulk air water vapour molar fraction (χ_a^w) for (□) $g_b^w = 100$, (◇) $g_b^w = 200$, (○) $g_b^w = 500$, and (△) $g_b^w = 1000$ mmol m^{-2} s^{-1}, under constant leaf temperature and bulk air CO_2 mol fraction ($T_l = 20\,^\circ$C, $\chi_a^c = 350$ μmol mol^{-1}, and $I = 500$ μmol m^{-2} s^{-1}). Simulation based on response data in Figs. 6.3, 6.4, & 6.5.
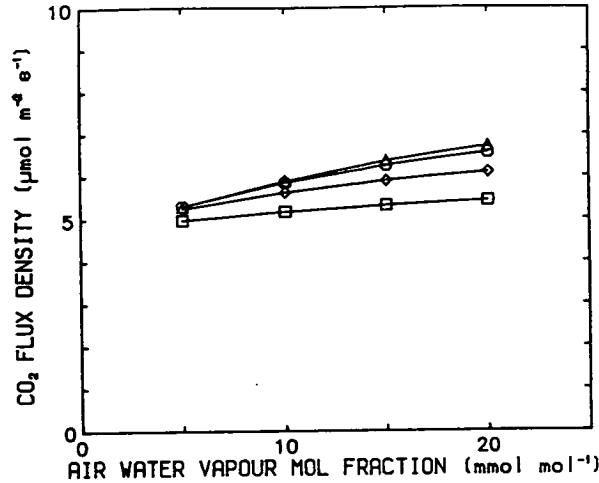
Figure 6.11. Simulated relationship between CO_2 flux density (A) and bulk air water vapour molar fraction (χ_a^w) for (□) $g_b^w = 100$, (◇) $g_b^w = 200$, (○) $g_b^w = 500$, and (△) $g_b^w = 1000$ mmol m^{-2} s^{-1}, under constant leaf temperature and bulk air CO_2 mol fraction ($T_l = 20\,^\circ$C, $\chi_a^c = 350$ μmol mol^{-1}, and $I = 500$ μmol m^{-2} s^{-1}). Simulation based on response data in Figs. 6.3, 6.4, & 6.5.
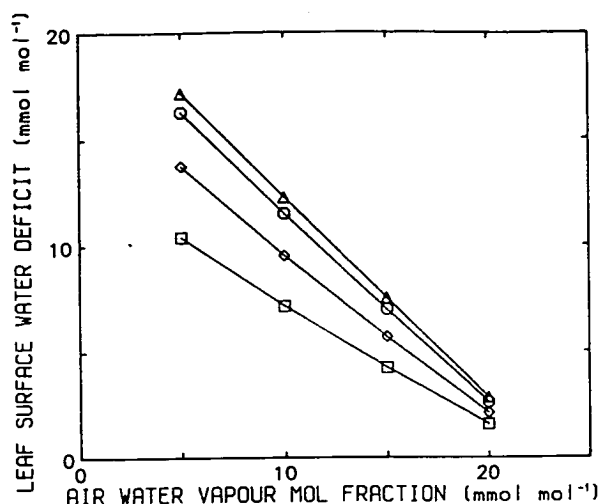
Figure 6.12. Simulated relationship between leaf surface water vapour deficit (D_s^w) and bulk air water vapour molar fraction (χ_a^w) for ($\square$) $g_b^w = 100$, ($\Diamond$) $g_b^w = 200$, ($\circ$) $g_b^w = 500$, and ($\triangle$) $g_b^w = 1000$ mmol m^{-2} s^{-1}, under constant leaf temperature and bulk air CO_2 mol fraction ($T_l = 20$ °C, $\chi_a^c = 350$ μmol mol^{-1}, and $I = 500$ μmol m^{-2} s^{-1}). Simulation based on response data in Figs. 6.3, 6.4, & 6.5.

being steeper at higher values of g_b^w. The simulated response of A to g_b^w was small, as it also was in the 'wind speed' experiment (Fig. 6.11 *vs.* Table 6.1).

The response of g_s^w is both a reflection and a cause of the changes in χ_i^c and D_s^w (Figs. 6.10 & 6.12). As expected, D_s^w increased with decreasing χ_a^w, but the relationship between D_s^w and χ_a^w was different at different values of g_b^w. As a consequence of this, both the slope and the intercept of the response of g_s^w to χ_a^w changed with g_b^w. At high values of g_b^w the response was steeper, and g_s^w was lower than at low values of g_b^w.

Part of the effect of χ_a^w on g_s^w was through CO_2. This seems paradoxical, but is an unavoidable effect on g_s^w of the decrease in χ_i^c that occurs in response to a decrease in χ_a^w. This indirect effect of χ_a^w on g_s^w can be seen in the control diagram in Fig. 6.1 by following the path that starts at $d\chi_a^w$, and goes through $\partial D_s^w/\partial \chi_a^w$, dD_s^w, $\partial g_s^w/\partial D_s^w$, dg_s^w, $\partial A/\partial g_s^w$, dA, $\partial \chi_i^c/\partial A$, $d\chi_i^c$, $\partial g_s^w/\partial \chi_i^c$, and ends at dg_s^w. Because a decrease in χ_i^c normally leads to higher g_s^w ($\partial g_s^w/\partial \chi_i^c < 0$), this effect is a source of negative feedback on g_s^w.

The boundary layer is also a source of positive feedback. If χ_a^w remains unchanged, an increase in g_s^w causes a decrease in D_s^w, and this decrease in D_s^w would lead to further increase in g_s^w. Negative feedback through CO_2 stabilizes the response to D_s^w because an increase in χ_a^w leads to an increase in both g_s^w and χ_i^c. In the model χ_i^c is

Figure 6.13. Simulated relationship between stomatal conductance (g_s^w) and bulk air CO_2 molar fraction (χ_a^c) for ($\square$) $g_b^w = 100$, ($\diamond$) $g_b^w = 200$, ($\circ$) $g_b^w = 500$, and ($\triangle$) $g_b^w = 1000$ mmol m^{-2} s^{-1}, under constant leaf temperature and water vapour molar fraction in the bulk air ($T_l = 20$ °C, $\chi_a^w = 15$ mmol mol^{-1}, and $I = 500$ μmol m^{-2} s^{-1}). Simulation based on stomatal response data in Figs. 6.3, 6.4, & 6.5.

the only source of negative feedback, but in the real world other sources of feedback could be present.

If the response of stomata to D_s^w is a direct effect —i.e. feedforward—, and not an indirect effect of leaf water status, then a source of negative feedback is required for stability. This is so because, as explained above, the boundary layer is a source of *positive* feedback on g_s^w. In the absence of negative feedback, the response of g_s^w to D_s^w would have only two stable states: fully open, and fully closed stomata. In a 'noisy' environment the state of an individual stoma would be unpredictable.

Carbon dioxide molar fraction

The model was also used to calculate the responses of g_s^w and A to χ_a^c. Using as input the relationships indicated by dashed lines in Figs. 6.3, 6.4, & 6.5, the model yields the results in Figs. 6.13, 6.14, 6.15 & 6.16. g_s^w decreased with χ_a^c, the slope being similar at the different values of g_b^w (Fig. 6.13). χ_i^c followed the change in χ_a^c, and had a large effect on A (Figs. 6.14 & 6.15).

In contrast to the response of g_s^w to D_s^w, the response of χ_i^c is inherently stable because there is negative feedback between g_s^w and χ_i^c. The variable sensed by stomata is χ_i^c, and its value is affected by g_t^w (g_b^w and g_s^w in series). However, positive feedback
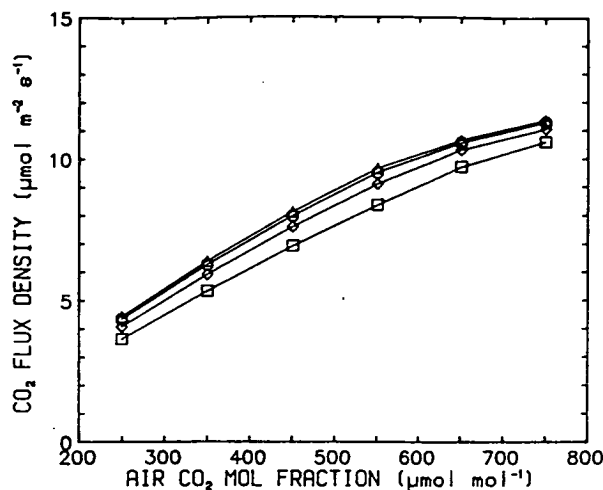
Figure 6.14. Simulated relationship between CO_2 flux density (A) and bulk air CO_2 molar fraction (χ_a^c) for (□) $g_b^w = 100$, (◇) $g_b^w = 200$, (○) $g_b^w = 500$, and (△) $g_b^w = 1000$ mmol m^{-2} s^{-1}, under constant leaf temperature and water vapour molar fraction in the bulk air ($T_l = 20$ °C, $\chi_a^w = 15$ mmol mol^{-1}, and $I = 500$ μmol m^{-2} s^{-1}). Simulation based on stomatal response data in Figs. 6.4, 6.4, & 6.5.
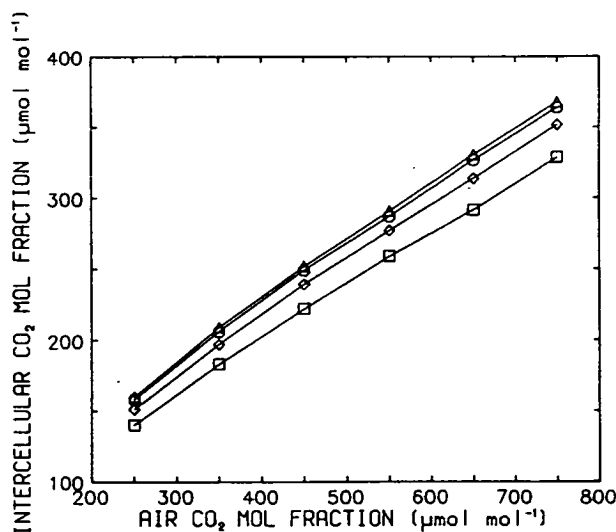
Figure 6.15. Simulated relationship between intercellular CO_2 mol fraction (χ_i^c) and bulk air CO_2 molar fraction (χ_a^c) for (□) $g_b^w = 100$, (◇) $g_b^w = 200$, (○) $g_b^w = 500$, and (△) $g_b^w = 1000$ mmol m^{-2} s^{-1}, under constant leaf temperature and water vapour molar fraction in the bulk air ($T_l = 20$ °C, $\chi_a^w = 15$ mmol mol^{-1}, and $I = 500$ μmol m^{-2} s^{-1}). Simulation based on response data in Figs. 6.4, 6.4, & 6.5.
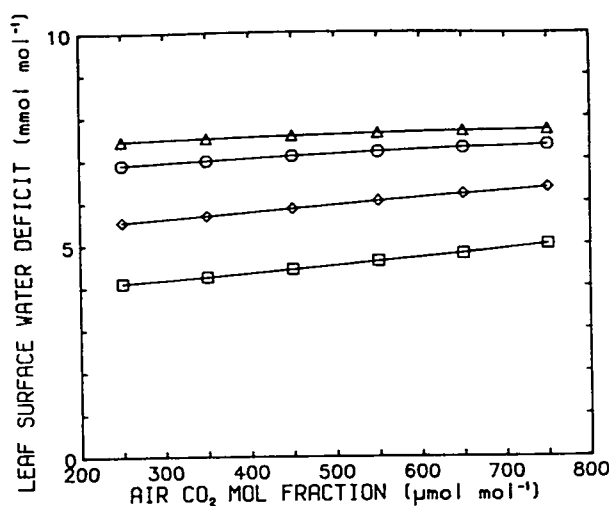
Figure 6.16. Simulated relationship between leaf surface water vapour deficit (D_s^w) and bulk air CO_2 molar fraction (χ_a^c) for ($\square$) $g_b^w = 100$, ($\Diamond$) $g_b^w = 200$, ($\circ$) $g_b^w = 500$, and ($\triangle$) $g_b^w = 1000$ mmol m^{-2} s^{-1}, under constant leaf temperature and water vapour molar fraction in the bulk air ($T_l = 20$ °C, $\chi_a^w = 15$ mmol mol^{-1}, and $I = 500$ μmol m^{-2} s^{-1}). Simulation based on response data in Figs. 6.4, 6.4, & 6.5.

through D_s^w partly cancels the negative feedback attributable to χ_i^c. This feedback through D_s^w is a consequence of the change in D_s^w in response to χ_a^c (Fig. 6.16). This source of feedback can be seen in the control diagram (Fig. 6.1) by following the path that starts at $d\chi_a^c$, and goes through dg_s^w, dE, and dD_s^w, ending at dg_s^w. The simulated effect of g_b^w on the response of g_s^w to CO_2 is not the same as that on the response of g_s^w to humidity. The apparent sensitivity of g_s^w to χ_a^w is higher at larger g_b^w. In contrast, the apparent sensitivity of g_s^w to χ_a^c is not much affected by g_b^w: only the intercept changes (Figs. 6.9 & 6.13).

The response to CO_2 is affected by the gain of the humidity response loop $(\partial g_s^w / \partial D_s^w)$, and by the gain of the CO_2 response loop $(\partial g_s^w / \partial \chi_i^c)$. If the total gain of this loop is > 0 the boundary layer behaves as an amplifier. By running the model with data adjusted to make the stomata insensitive to D_s^w $(\partial g_s^w / \partial D_s^w = 0$; in practice $f_0(D_s^w) = 1$, for any value of D_s^w, in Equation 6.4), the apparent sensitivity of g_s^w to changes in χ_a^c is reduced at low values of g_b^w (Fig. 6.17). The normal response to D_s^w amplifies the response to χ_a^c under constant D_a^w, the gain depending on g_b^w.

At a given χ_a^c, g_s^w is smallest at $D_s^w = D_a^w$ i.e. $g_b^w = \infty$. The magnitude of the effect on g_s^w of a change in g_b^w depends on the relation between g_b^w and g_s^w, i.e. when $g_b^w / g_s^w \approx 10$ this effect is very small. However, under low wind speed, when this ratio is smaller,
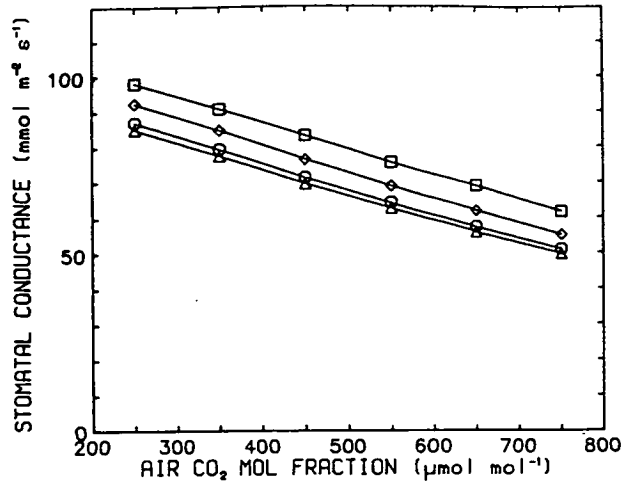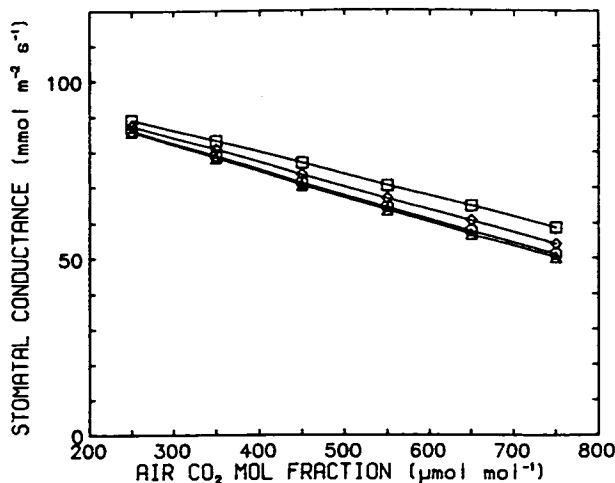
Figure 6.17. Simulated relationship between stomatal conductance (g_s^w) and bulk air CO_2 molar fraction (χ_a^c) for ($\square$) $g_b^w = 100$, ($\Diamond$) $g_b^w = 200$, ($\circ$) $g_b^w = 500$, and ($\triangle$) $g_b^w = 1000$ mmol m^{-2} s^{-1}, under constant leaf temperature and water vapour molar fraction in the bulk air ($T_l = 20$ °C, $\chi_a^w = 15$ mmol mol^{-1}, and $I = 500$ μmol m^{-2} s^{-1}). The stomata were assumed to be insensitive to humidity. Simulation based on response data in Figs. 6.4, & 6.5.

the effect of the boundary layer on g_s^w is larger.

Wind speed

The profile of water vapour mol fraction across the boundary layer has been measured for single leaves, and it depends on E and wind speed (Kitano & Eguchi, 1987a; Kitano & Eguchi, 1987b). Based on data for *Picea sitchensis* it has been proposed that reversible responses of stomata to wind depend on a response to humidity at the leaf surface (Grace *et al.*, 1975). This hypothesis seemed to be confirmed by the results of Bunce (1985). However, although a change in humidity at the leaf surface is the most obvious effect of the boundary layer, as suggested by Meidner & Mansfield (1968, page 100), CO_2 must also be involved in the stomatal response to wind speed in those species and conditions in which stomata are sensitive to CO_2. The model takes into account the effects of both D_s^w and χ_i^c on g_s^w.

Wind speed alters g_b^w, so it affects the apparent response of stomata to χ_a^w and χ_a^c (Figs. 6.9 & 6.13). The results generated by the model for different values of g_b^w, given above, can be plotted against wind speed for a leaf of a given dimension, obtaining in this way a response curve of g_s^w to wind speed (solid line in Fig. 6.18). The relationship

between wind speed and the thickness of the boundary layer is not linear. Most of the effect of wind on g_s^w occurs at low wind speeds (<0.5 m s^{-1}).

Working with a model makes it easy to answer the question: how important is the part of the effect of wind speed on g_s^w that is mediated by the response of g_s^w to CO_2? By running the model with stomata insensitive to D_s^w the effect through χ_i^c can be isolated from that through humidity. In ivy, at $\chi_a^w=15$ mmol mol^{-1} and $T_l=20$ °C, the effect mediated by χ_i^c is roughly one third of the total effect of wind speed (broken line in Fig. 6.18).

The thickness of the boundary layer depends on the dimension of the leaf. At a given χ_a^w and χ_a^c, a large and a small leaf with identical responses of g_s^w to D_s^w and χ_i^c would show different values of g_s^w at the same wind speed. This has methodological implications for the measurement of A, E, and g_s^w in the field. Data measured with a diffusion porometer by briefly enclosing a leaf is not comparable to data measured in a gas-exchange system. In the field, the wind speed prevailing at the time of the porometric measurement, as well as leaf size, affects the observed g_s^w. Field experiments with gas-exchange systems that track environmental conditions (e.g. Koch *et al.*, 1971), give results that are biased whenever the wind speed inside the cuvette is different to that outside. Some of the species in which very high g_s^w have been observed have large leaves (Körner *et al.*, 1979; Grace *et al.*, 1982), and it would be interesting to know whether this very high g_s^w results from differences in stomatal sensitivity to χ_i^c and D_s^w or whether it is caused by the thicker boundary layer of large leaves.

6.3.3 Caveat

The experiments discussed above show the effects of the boundary layer on stomatal responses in leaves artificially kept at a constant temperature. This is a simplification that helps us understand the responses to CO_2 and humidity, but is unrealistic because it does not take into account the effect of E and g_b^w on the temperature of the leaf. Evaporative cooling is a source of negative feedback on D_s^w, and so indirectly on g_s^w, and of either positive or negative feedback on g_s^w through T_l, depending on the sign of the response of stomata to T_l. Keeping leaf temperature constant makes these feedback loops ineffective. In nature the feedback through T_l could help to stabilize g_s^w, preventing oscillation, as demonstrated by Farquhar and Cowan (1974), but as g_s^w in *Hedera helix* was stable under constant T_l this simplification does not invalidate our argument. When E is high, feedback can also occur through the bulk water status of the leaf.
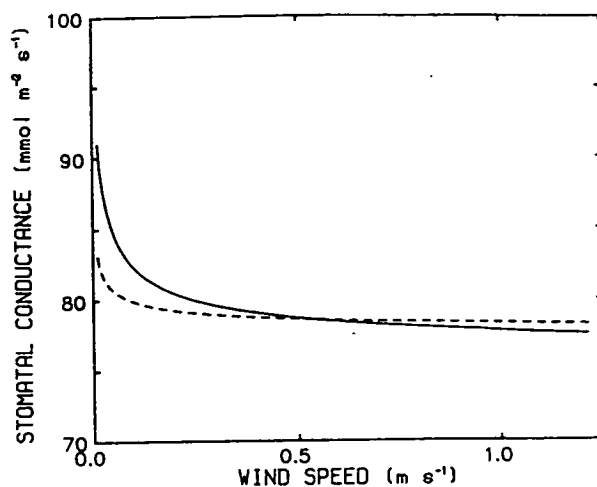
Figure 6.18. Simulated relationship between stomatal conductance (g_s^w) and wind speed (u) under constant leaf temperature, bulk air water vapour mol fraction and bulk air CO_2 mol fraction $(T_l = 20\ °C, \chi_a^c = 350\ \mu mol\ mol^{-1}, \chi_a^w = 15\ mmol\ mol^{-1}$ and $I = 500\ \mu mol\ m^{-2}\ s^{-1})$. A leaf mean dimension of 7 cm was assumed in the calculations. The solid line is the simulated response for a normal ivy leaf, the broken line is the simulated response for a leaf with stomata insensitive to D_s^w. Simulation based on response data in Figs. 6.3, 6.4, & 6.5.

6.4 Conclusions

As stomata of ivy are sensitive to both CO_2 and humidity, the effect of the boundary layer conductance and wind speed on g_s^w, is mediated by both CO_2 and water vapour mol fractions at the leaf surface. The effect of the boundary layer on χ_i^c and D_s^w also modifies the apparent responses of stomata to χ_a^c and χ_a^w. The apparent response to χ_a^c depends on the stomatal sensitivity to both CO_2 and humidity, as the apparent response to χ_a^w also does. A decrease in g_b^w causes a small increase in g_s^w that reduces its impact on g_t^w. A feedforward response to humidity would need compensatory negative feedback through another variable for stability.

Chapter 7

Models of stomatal responses to the environment

7.1 Introduction

In this chapter I will discuss the problems that arise when the difference between empirical and mechanistic models is not taken into consideration when interpreting their behaviour. First I will discuss these problems in general, and afterwards in relation to a model of stomatal behaviour developed recently (Ball *et al.*, 1987; Ball, 1988). In the discussion below, I will follow Hall & Day (1977) and Ören (1984) in the use of terms referring to models and modelling[1].

Models must be tested for their agreement with both agreed theory and experimental data. A theoretical analysis of a model includes the identification of all the assumptions involved and a check of the consistency of its logic structure. The *validation* of a model is a test of its agreement with the object modelled.

---

[1] Definitions, following Hall & Day (1977) and Ören (1984),

System. A *system* is any object whose behaviour is of interest.

Model. A *model* is any abstraction or simplification of a system.

State variable. *State variables* are quantitative representations of the entities of the system that change (e.g. with time, in dynamic models).

Driving variable. Inputs from outside the system of interest are called *forcing functions, or driving variables*.

Simulation. A *simulation* is an experiment done with a model.

Structure. The *structure* of a model is given by the functional relation, without specification of values for the parameters.

Behaviour. The *behaviour* of a model is defined by the value of the state variables.

The empirical validation of a model's behaviour does *not* constitute a validation of its structure or assumptions, and least of all, of the way in which the results of the simulation are being interpreted. There are different kinds of validation: (1) validation of model *behaviour*, (2) validation of model *structure*, and (3) validation of the *interpretation* of the results.

As discussed in Section 1.2.1, empirical models are also called descriptive because they simply describe the relationship between two or more variables while mechanistic models include indications of causality (Hall & Day, 1977). The behaviour of an empirical model can be valid or invalid, depending on whether it agrees with experimental data or not, but the structure of an empirical model is assumed *a priori* to be invalid —i.e. the functional relation is of no interest, as in curve fitting. The aim for mechanistic models is to mimic the structure of a real system —i.e. the functional structure of the model is expected to be a reflection of that of the real system. However, valid behaviour does not guarantee a valid structure. In a mechanistic model it is assumed that its structure can be validated, but its validation needs much more support than the simple agreement of observed and predicted final behaviour. The validation of the structure requires the validation of the internal behaviour of the model —i.e. causal relationships must be experimentally demonstrated. For the interpretation of the results of a simulation to be valid it is also necessary to prove the validity of all the assumptions, explicit and implicit, involved in the interpretation.

The interpretation of the results of simulations often includes the inference of causal relationships. The distinction between causal relationship and correlation seems in practice to get blurred when complex models are involved. The process for establishing causal relationships cannot be reversed. The nature and existence of the causal links must be demonstrated *a priori* to the construction of a mechanistic model. Empirical models cannot be used to prove causal relationships. It is easy to recognize that a correlation between an arbitrary set of variables does not necessarily imply causation. However when these same variables are transformed by means of a complex model, correlations are in some cases erroneously used to infer causation.

7.2 Analysis of Ball's empirical model

7.2.1 The model

A simple, quantitative, empirical model of stomatal conductance has been recently developed (Ball *et al.*, 1987; Ball, 1988). The model was based on data from a series of gas-exchange experiments in which the responses of g_s^w to many variables and their

interactions were studied. This model provided a concise description of Ball's data set, and has been successfully fitted to data from other species (Leuning, 1990).

Ball (1988, page 11) says: 'The empirical approach which we have used in this work does not presuppose knowledge of the mechanistic bases of the responses described by the model. Nevertheless, the analysis may provide insights into the mechanistic basis of guard cell function.' I agree with this possibility, with the caveat that it requires many *a priori* assumptions, but I completely disagree with his interpretation of the results.

Ball (1988, page 21) also says that '...normalizing stomatal conductance with respect to A is a means of separating the influence associated with photosynthesis from the presumably separate responses of stomata to CO_2 and humidity.' and 'The mechanistic basis of the linear conductance/assimilation relationship is not clear and we reiterate that this empirical analysis is not predicated upon any particular relationship.' Nevertheless, as I show below, when Ball used the model to conclude that g_s^w responds to h_s, he implicitly interpreted this 'association' between g_s^w and A as causation, and this is what I want to challenge.

7.2.2 Is Ball's interpretation of the model valid?

The model in its simplest form[2] is:

$$g_s^w = kA\frac{h_s}{\chi_s^c} \tag{7.1}$$

and the good fit of some data sets to this model was used as a basis for stating that '...stomata respond to relative humidity' (Ball *et al.*, 1987). However by rearranging the equation above we obtain:

$$A = k^{-1}g_s^w \frac{\chi_s^c}{h_s} \tag{7.2}$$

so, this model could as well be used to conclude that *assimilation rate responds to* $1/h_s$. This counter-example demonstrates that implicit assumptions are more important to the outcome of this reasoning process than the actual data. Why is this so? The reason is that we are unconsciously assuming, when making these mechanistic interpretations of the model, that all the variables to the right of the equals sign can be treated as driving variables —i.e. we are assuming that these variables are *exogenous* to the system modelled. We are assuming *a priori* that A controls g_s^w, or vice versa. The former is what the authors who developed the model have assumed and this reflected

---

[2]for some species $g_s^w = k_0 + k_1 A\frac{h_s}{\chi_s}$ was used

not only in their interpretation of the model but also in the way in which they have plotted the data.

It has been observed that a feedback loop links g_s^w and A (Farquhar *et al.*, 1978), which means that A and g_s^w are interdependent (Fig. 6.1). It has also been shown that both A and g_s^w can respond independently of each other to environmental variables (Jarvis & Morison, 1981), including light (Meidner, 1968; Karlsson *et al.*, 1983; Aphalo & Sánchez, 1986) and humidity (Bunce, 1988b) (See also discussions in Chapters 4 & 6). From this evidence it follows that neither of the two assumptions is correct — neither A controls g_s^w, nor g_s^w controls A. Neither A nor g_s^w can be considered to be driving variables in the real world. They are both state variables, and it is impossible to experimentally control them without altering *any* environmental variable.

Two main objections can be made to the original interpretation of the model. Firstly, it does not take into account that equation 7.1 is only partially determined because there are two unknowns in it: A and g_s^w. This means that there are an infinite number of pairs of values of A and g_s^w that satisfy this equation. Secondly, a functional relationship has been taken as equivalent to a causal relationship. In this I follow Bunge (1959, pages 92–95) who raises several objections to a functional view of causation, some of which are as follows: '(a) Functions express *constant relations* ... But functions are insufficient to state anything concerning the cause that *produces* the state or the phenomenon in question ... (b) Functional relations are *reversible* whenever the functions in question are single valued ... whereas genuine causal connections are essentially *asymmetrical* ... The failure to account for the genetic connections is a shortcoming of the functional relation. But not all connections in the world are genetic; in many, perhaps in most, cases we are confronted with interdependence, as it is shown by the pervasiveness of the function concept in the sciences.'

7.2.3 An alternative interpretation

What it is possible to say is that there is a relationship between A and g_s^w, and that they are not independent. This is not a simple one way relationship, A and g_s^w affect each other through χ_i^c, and the relationship also depends on their responses to other variables. The parallel responses of g_s^w and A to I and other variables contribute, under natural conditions, to the correlation between A and g_s^w, but, as discussed in Chapter 4, this correlation can be experimentally broken.

By eliminating A and g_s^w from the model we obtain an expression showing what it is that remains constant when A and g_s^w change concurrently in response to I, D_s^w,

and T_l. Assimilation rate is

$$A \approx g_s^c (\chi_s^c - \chi_i^c) \tag{7.3}$$

and

$$g_s^c = 0.63 g_s^w. \tag{7.4}$$

By substituting equations 7.3 and 7.4 in 7.1, and then rearranging we get

$$g_s^w = 0.63 k g_s^w \left(1 - \frac{\chi_i^c}{\chi_s^c} \right) h_s, \tag{7.5}$$

eliminating g_s^w and rearranging we get:

$$\chi_i^c = \chi_s^c \left(1 - \frac{1.60}{k h_s} \right) \tag{7.6}$$

which is the solution for χ_i^c given by Ball (1988, Equation A2.3). This relationship remains true for all the data that fit the model, whatever the measurement conditions. It is invariant for changes in T_l, I, and D_s^w. χ_i^c/χ_s^c is a function only of h_s —i.e. *simultaneous* changes of A and g_s^w in response to other variables do not affect this relationship.

To return to Equation 7.2, the dependence of A on $1/h_s$, is somewhat puzzling. However, once we realize that g_s^w is not an independent variable but an increasing function of h_s, it is easy to visualize '$1/h_s$' as a 'correction' for the steeper increase of g_s^w than of A as h_s increases. The increase in A, when g_s^w increases in response to h_s, is less than proportional because (1) the increase in χ_i^c is less than proportional to the increase in g_s^w because as χ_i^c increases, A also increases, affecting $Cs - Ci$, and (2) because the relationship between A and χ_i^c is not linear. In other words, '$1/h_s$' corrects A for the effect of the curvature of the A vs. χ_i^c relationship, and for the dependence of $\chi_s^c - \chi_i^c$ on A. Of course, this is also valid as an explanation for the apparent response of g_s^w to h_s in equation 7.1. But because of our preconceptions it is not as easy to accept it for equation 7.1 as it is for equation 7.2. Ball's model gives no evidence in favour, or against, a hypothetical response of stomata to h_s. Such evidence must come from experiments such as those discussed in Chapter 5, which indicate that stomata respond to D_s^w —not h_s.

The confusion surrounding the interpretation of this model stems from the fact that it does not predict the state of a single state variable, but rather a relationship between the state of two variables —A and g_s^w. To use it for predicting the state of one of these two variables we need a value for the other variable under *the same state of the driving variables*. With this model if we have an *independent* estimate or measurement of A

we can predict g_s^w, or if we have g_s^w we can predict A. It is as much a model of CO_2 assimilation as it is a model of stomatal conductance. It could be stated as

$$\frac{g_s^w}{A} = k\frac{h_s}{\chi_s^c}. \tag{7.7}$$

In the original statement of the model A is a driving variable, and this is not a problem for its use as a predictive tool. However, when making a mechanistic interpretation it is necessary to take into account which variables are operationally independent in the real world, and which are not.

7.2.4 Is the behaviour of the model valid?

Having identified the assumptions and logic behind the model, we may still test it by contrasting its operational behaviour with experimental data. It has been observed that g_s^w and A are usually linearly correlated under constant χ_a^c or χ_s^c and D_s^w (Wong et al., 1979; Louwerse, 1980). This was also the case in ivy (Fig. 4.4 & Table 4.1). If in Ball's model we replace χ_s^c and h_s with constants we obtain $g_s^w = k'A$, which agrees with what has been observed in the real world. However, although this correlation is consistent, most authors have been cautious not to take it as evidence of a causal link (e.g. Wong et al., 1985c). As discussed in Chapter 4, there is a link between A and g_s^w caused by feedback through χ_i^c and also parallel responses of g_s^w and A to I (see also Chapter 6).

When χ_a^c is altered χ_i^c changes in such a way that the ratio χ_i^c/χ_a^c remains roughly constant (Louwerse, 1980; Morison & Gifford, 1983). These authors found that in some species the linear regression of χ_i^c on χ_a^c did not go exactly through the origin, implying that the ratio is not truly constant. This is also the case in ivy (See Fig. 6.8 and discussion in Chapter 6). As the model, in its simplest from, assumes a fixed ratio, it only approximates reality, but as deviations from a constant ratio are not too big, its behaviour can be considered satisfactory in this respect.

When D_s^w or T_l change, χ_i^c generally changes. As discussed in Chapter 5, stomatal responses to water vapour mol fraction and temperature are not consistent with a single response through h_s. However, as we have seen, Ball's model implies that χ_i^c changes linearly with h_s under constant χ_s^c. In four grasses χ_i^c/χ_a^c changed almost linearly with D_a^w (Morison & Gifford, 1983). In ivy χ_i^c/χ_s^c changed very little in response to D_s^w, being none the less higher at low D_s^w (Fig. 6.7). The response of χ_i^c/χ_s^c to h_s was different under constant T_l from that under constant D_s^w, and the biggest effect was that of T_l under constant h_s (Fig. 7.1). In Ball's model temperature and humidity are represented by a single input variable, h_s, so this model is very unrealistic in its
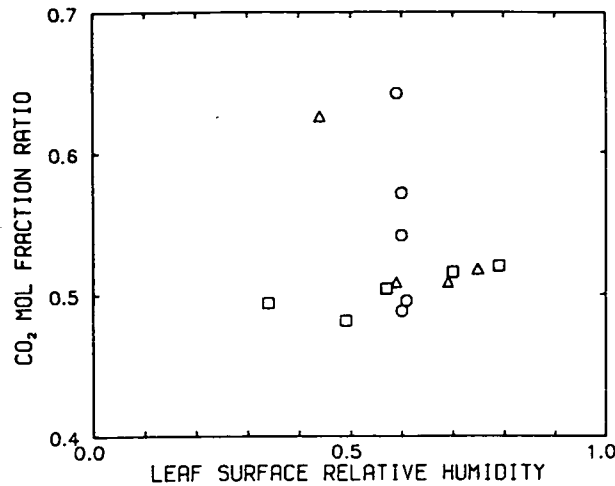
Figure 7.1. Ratio between intercellular and leaf surface CO_2 mol fractions *vs.* leaf surface relative humidity. Measured ($\square$) under constant temperature (T_l=20 °C), or changing temperature and ($\triangle$) constant leaf surface water vapour deficit (D_s^w=10 mmol mol^{-1}), or ($\circ$) constant leaf surface relative humidity (h_s=0.60); I=340 μmol m^{-2} s^{-1}. Data from one typical ivy plant from the experiment described in Chapter 5 obtained at the same time as data in Figs. 5.1b & 5.4b.

treatment of the response to these variables.

At a single temperature h_s and D_s^w are linearly related, so problems appear only when a range of values of T_l is considered. This causes the model eventually to break down, as in the case of T_l and humidity data for ivy —for these data a linear regression of A on g_s^w gives a better fit than Ball's model (Fig. 7.2). As these data were measured at constant χ_s^c, the only difference between the linear regression and Ball's model is in whether h_s is taken into account or not. Lloyd (1991) also found that for his data alternative models gave a better fit than Ball's. He found that models that used D_s^w instead of h_s gave better fits and more consistent results at different values of I and T_l.

7.2.5 Related models

Ball (1988), for data from some species, observed an intercept different from zero, the model then becoming

$$g_s^w = k_0 + k_1 A \frac{h_s}{\chi_s^c}. \tag{7.8}$$
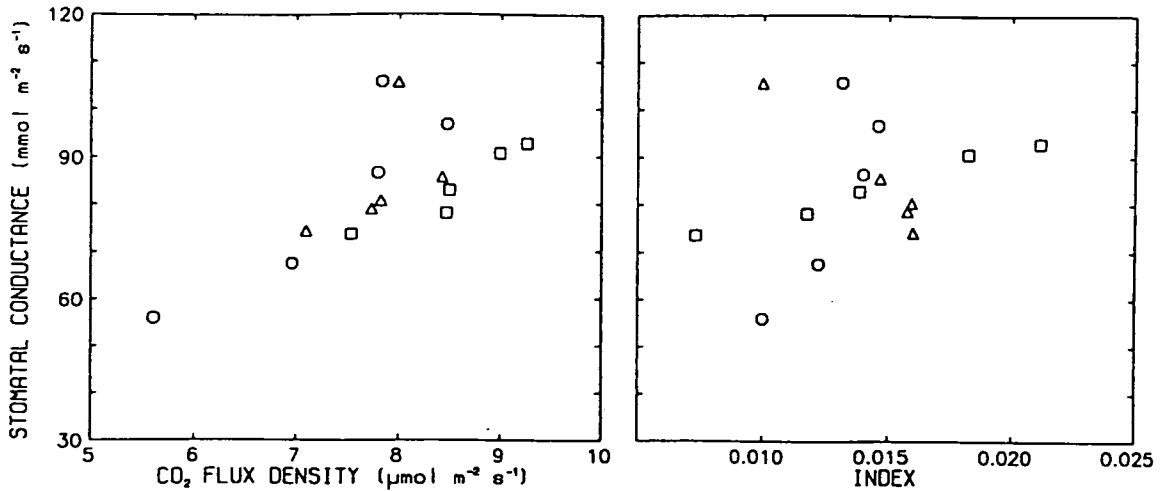
Figure 7.2. Scatter diagrams of stomatal conductance (g_s^w) and CO_2 flux density (A) (left) and of g_s^w and Ball's index ($A h_s/\chi_s^c$) (right) at a range of temperature and humidity. Data measured under constant temperature (T_l=20 °C) ($\Box$), or changing temperature and constant leaf surface water vapour deficit (D_s^w=10 mmol mol^{-1}) ($\triangle$), or constant leaf surface relative humidity (h_s=0.60) (o); I=340 μmol m^{-2} s^{-1}. Data from one typical plant from the experiment described in Chapter 5 obtained at the same time as data in Figs. 5.1b, 5.4b & 7.1.

Leuning (1990) found a small improvement in the correlation with data from *Eucalyptus grandis* by replacing χ_s^c with $\chi_s^c - \Gamma$ where Γ is the CO_2 compensation point, his model being

$$g_s^w = k_0 + k_1 A \frac{h_s}{\chi_s^c - \Gamma}. \tag{7.9}$$

Lloyd (1991) tested several models, including Equations 7.8 and 7.9, and found that the best fit of g_s^w response data to humidity and temperature for *Macadamia integrifolia* was to the model

$$g_s^w = \frac{1 - k_1(1 - |T_l/T_{opt}|)}{k_2\sqrt{D_s^w}}, \tag{7.10}$$

were T_{opt} is the optimal T_l for g_s^w. This model does not include A, or χ_s^c, and so is closer to models like that of Jarvis (1976), than to Ball's model. That Lloyd found the best fit to this model is probably a consequence of his data sets not including responses to I and χ_s^c. In these data sets, measured in the laboratory, two values of I were used, but the models were fitted separately to data for each value of I. Another of the

models tested by this author,

$$g_s^w = k_0 + k_1 \frac{A}{D_s^w \chi_i^c}, \tag{7.11}$$

also gave a better fit than Equation 7.9 to the data for *Macadamia integrifolia*. This model differs from Ball's model in that h_s has been replaced by $1/D_s^w$, and χ_s^c has been replaced by χ_i^c. This model includes D_s^w, but not T_l, being inadequate because, as discussed in Chapter 5, g_s^w frequently responds to T_l. But, the main problem is that this model also includes the factor A/χ_i^c, that under constant χ_i^c, is a function of g_s^w. If we have χ_s^c, χ_i^c, and A, then we can calculate $g_s \approx A/(\chi_s^c - \chi_i^c)$, and we do not need a model.

7.3   A new model

Based on the insight gained from this analysis, I have developed a new, but related, model that is a more flexible option than the original one. It is more flexible because I took into account both my data for ivy and Ball's data during its development. Only the treatment of temperature and humidity responses have been changed from Ball's model. The new model includes as driving variables both T_l and D_s^w, instead of only h_s. The equation

$$g_s^w = \frac{A}{\chi_s^c}[k + f_1(D_s^w) + f_2(T_l) + f_3(D_s^w, T_l)] \tag{7.12}$$

defines a family of models in which the slope of the A vs. g_s^w relationship is a function of both D_s^w and T_l. χ_i^c for this model is given by

$$\chi_i^c = \chi_s^c \left[1 - \frac{1.60}{k + f_1(D_s^w) + f_2(T_l) + f_3(D_s^w, T_l)}\right]. \tag{7.13}$$

I suggest the following expressions for f_i:

$$f_1 = k_1 D_s^w, \tag{7.14}$$

$$f_2 = k_2 T_l, \tag{7.15}$$

and

$$f_3 = k_3 D_s^w T_l. \tag{7.16}$$

This new model was tested by fitting it to data from ivy, and comparing the residual sum of squares to that of the fit to other models (Table 7.1). As what was changed was the description of humidity and temperature responses, the data used was from the

Table 7.1. Comparison between models of stomatal response. Residual sums of squares from least squares fits to data for *Hedera helix* from the experiments described in Chapter 5. Data were the mean of three plants for set A (T_l=15–28 °C, D_s^w=6–15 mmol mol^{-1}, h_s=0.4–0.75, I=200 μmol m^{-2}s^{-1}, χ_s^c=350 μmol mol^{-1}), and that from a typical plant for set B (T_l=10–28, D_s^w=5–15, h_s=0.4–0.75, I=340 μmol m^{-2}s^{-1}, χ_s^c=350 μmol mol^{-1}). Values for the coefficients given in Table B.1, page 132.

Model	Eq.	$SS_{residual}$ set A (n=8)	$SS_{residual}$ set B (n=15)
1. $g_s^w = k$	—	184	2568
2. $g_s^w = kA$	—	51	1359
3. $g_s^w = k\frac{Ah_s}{\chi_s^c}$	7.1	782	6168
4. $g_s^w = \frac{A}{\chi_s^c}(k_0 + k_1D_s^w + k_2T_l)$	—	30	690
5. $g_s^w = \frac{A}{\chi_s^c}(k_0 + k_1D_s^w + k_2T_l + k_3D_s^wT_l)$	7.12	25	564
6. $g_s^w = k_0 + k_1D_s^w$	—	43	851
7. $g_s^w = k_0 + k_1D_s^w + k_2T_l$	—	42	272
8. $g_s^w = \frac{1-k_1(1-|T_l/T_{opt}|)}{k_2\sqrt{D_s^w}}$	7.10	90	1373

experiments in which these responses were measured. From the linear regression of g_s^w on A for these data, and also from the response to light, it is clear that the intercept is very close to zero (Figs. 4.4 & 7.2), so models that include an intercept were not considered.

For the data from ivy, Ball's model gave the worst fit, even worse than the fit to a constant —i.e. the mean value of g_s^w (model 3 *vs.* model 1 in Table 7.1). The linear regression, through the origin, of g_s^w on A (model 2 in Table 7.1) explained 72 % of the variation around the mean in set A and 47 % in set B. The new model was tested with and without an interaction term (Equation 7.16). Without an interaction term (model 4 in Table 7.1) it gave a good fit, that was only slightly improved by the addition of an interaction term (model 5 in Table 7.1). The interaction term could be important in other data sets. For data sets in which the response to T_l has an optimum, a more complicated function could be necessary to describe this response.

Models that do not include A as a driving variable were also tested. These models (6–8 in Table 7.1) are unable to describe responses to variables for which A is a surrogate, but give good fits to the D_s^w and T_l response data for ivy. Even very simple models (6 & 7 in Table 7.1) give much better fits than Ball's model —the residual sum of squares for these models was the smallest, or nearly so. The model that gave

the best fit with Lloyd's data for *Macadamia integrifolia* (model 8 in Table 7.1), gives larger sums of squares than the simple models. As discussed in Chapter 5 regressions of g_s^w on h_s give very unsatisfactory fits to the responses of g_s^w to D_s^w and T_l for ivy.

7.4 Conclusions

Ball's model is not a model of g_s^w but a model of the relationship between A and g_s^w. Its original interpretation was flawed, but a different interpretation highlights many of the properties of the coordinated changes of A and g_s^w. In this respect it is a useful empirical, operational tool for some predictive purposes but, as any empirical model, it is of no use for defining causal relationships.

Ball's model, although not mechanistic, is fairly realistic in its treatment of responses to I and other variables that do not affect the A *vs.* g_s^w relationship. It is also realistic in its treatment of the effect of χ_s^c on the apparent relationship between A and g_s^w. Its behaviour in response to I and χ_s^c is realistic only under 'normal' conditions, but is not satisfactory under some experimental conditions, such as monochromatic light. The behaviour of Ball's model is not realistic with respect to the effect of water vapour and temperature on g_s^w/A, but works properly under restricted conditions such as when g_s^w increases with temperature.

As a prediction tool its usefulness is limited to this restricted set of conditions, and hindered by the need of A as an input variable. When combined with a model of A it can be used in the prediction of g_s^w (Leuning, 1990; Collatz *et al.*, 1991). When the model is used in this way, A becomes a surrogate for variables that affect both A and g_s^w, but not the relationship between them. One of the most important of these variables is I, but replacing A with $f(I)$ would be of no use because Ball's model, and the model I developed, are both models of the relationship between A and g_s^w. A completely new model, that takes into account the effects on g_s^w of I, χ_i^c, D_s^w, and T_l would have to be developed.

Including in Ball's model a more realistic treatment of responses to T_l and D_s^w should make its use by extrapolation much safer, and its use with other species such as ivy possible. The new model proposed is a step in this direction.

"Stomatal conductance" models that use the correlation with A look, at first sight, very attractive because of their simplicity (few parameters). However, this simplicity comes at a high price: a complicated model is needed to simulate A if they are to be driven by environmental variables alone. Models that do not rely on A as a surrogate for environmental variables, need more parameters, at least one for each variable considered.

Chapter 8

Discussion

8.1 The contribution of this thesis

In the preface I defined the objective of this thesis by four questions. In the sections that follow I shall answer these questions, and also comment on the methods used.

8.1.1 What is the relationship between stomatal action and the rate of photosynthesis?

As discussed in Chapter 4, the mechanism behind the correlation between A and g_s^w is complex. This mechanism includes parallel, but independent, responses of photosynthesis and stomata to I, and an indirect response of stomata to A through CO_2. The consequence of this correlation under normal environmental conditions is that χ_i^c remains nearly constant. This value of χ_i^c is dependent on some variables such as D_s^w and χ_a^c, but it is almost independent of others such as I.

Although it was clear from previous work that stomata respond directly to light, it was not clear whether the only additional response was through CO_2, or whether there was some other metabolite involved in this response. The experiments dicussed in Chapter 4 clearly show that there is no need to postulate the existence of a messenger other than CO_2 to explain the response of stomata to light.

The relationship between stomatal action and the rate of photosynthesis is not simply a cause-effect relationship between A and g_s^w. Neither g_s^w controls A, nor A controls g_s^w, but instead, this relationship depends on coordinated, but in part independent, responses of g_s^w and A to the environment. This coordination is effected by information being passed between processes that take place in the mesophyll and in the guard cells at the time g_s^w and A are responding to the environment, and also by information acquired by the genetic code of the plant during evolution. The question of why the

111

responses of g_s^w and A are coordinated in a way that usually keeps χ_i^c constant, has to be answered by means of optimization hypotheses that go beyond the scope of this thesis.

8.1.2 What is the nature of the interaction between stomatal responses to humidity and temperature?

From experiments described in the literature it was impossible to know which was the best way of expressing humidity when studying stomatal responses. The experiments described in Chapter 5 together with those recently done by Mott & Parkhurst (1991) make an important contribution towards solving this problem, by showing that relative humidity is inadequate, and that D_s^w should be preferred.

The experiments described in Chapter 5 clearly show that responses of g_s^w to T_l and D_s^w are independent and that they cannot be explained by a single response to h_s. As the response to T_l usually displays an optimum, the apparent response to h_s changes with T_l. From my data it is clear that it is more appropriate to use D_s^w than h_s when describing stomatal responses to humidity. The good fit of some data sets to h_s is a fortuitous consequence of using a range of T_l within which g_s^w increases with increasing temperature, and of scaling g_s^w as g_s^w/A.

8.1.3 What is the role of the boundary layer in the control of stomatal opening?

Depending on leaf dimension and wind speed g_b^w can significantly alter the apparent response of g_s^w to χ_a^c and χ_a^w. Because of the feedback loops involved, the responses of g_s^w to χ_a^c and χ_a^w each include responses to both χ_i^c and D_s^w. The boundary layer alters the state of the variables sensed by the guard cells —i.e. χ_i^c and D_s^w— and so it is a source of feedback

A feedforward, i.e. direct, response of guard cells to D_s^w requires negative feedback through another variable for stability because positive feedback would otherwise lead to either completely open or completely closed stomata.

The experiments and simulations in Chapter 6 show that, as long as stomata are sensitive to both χ_i^c and D_s^w, responses of g_s^w to wind speed have two components, one resulting from changes in χ_a^c —and χ_i^c— and another from changes in D_s^w.

The effect of wind speed —and hence g_b^w— on stomata has received little attention from plant ecophysiologists. No previous analysis has been made of the involvement of both CO_2 and humidity in the responses of stomata to wind, or of the effect of g_b on the apparent responses of stomata to changes in χ_a^c and χ_a^w. The results given in Chapter 6

indicate that, for given responses of g_s^w to χ_i^c and D_s^w, the apparent responses of g_s^w to D_a^w and χ_a^c depend on the size of the leaf and wind speed, showing that this effect of the boundary layer should be considered when comparing data measured under different conditions, or with different methods. When scaling up from responses of stomata to the response of g_s^w for a whole leaf, the effect of the boundary layer must be considered, and the value of g_s^w resulting from scaling up will depend on leaf dimension and wind speed.

8.1.4 Is our current knowledge, and are the resulting models, good enough for predicting short-term responses of stomata to changes in the environment?

No valid mechanistic model of stomatal responses is available. As discussed in Chapters 1 and 7, a distinction must be made between models that include A as a driving variable and those that rely only on environmental variables. From the discussion in Chapter 4, it follows that any mechanistic model of g_s^w should include I and χ_i^c as driving variables. In empirical models A has been used as a surrogate for these and other variables. This is safe as long as the correlation between A and g_s^w holds.

Several different empirical models have been found to give the best fit to different data sets. Ball's model is apparently too simple, and treats the responses of g_s^w/A to T_l and D_s^w inadequately. However it is a good starting point for developing more complex and flexible models with wider validity. For this purpose, it is necessary to understand the logic behind this type of model to be able to give a sound interpretation to them. Further development is necessary before we may have a model to use in canopy or regional scale models.

The discussion in Chapter 7 is a contribution to the understanding of why Ball's model fits some data sets, and why it fails in other cases. This chapter also makes a contribution towards the interpretation of Ball's model. I propose a modification to this model that is empirical, but based on current knowledge about stomatal responses to D_s^w and T_l, and their correlation with changes in A. This model is not tailored to one data set, but it takes into account other information with the aim of obtaining a model of more general usefulness.

Our current knowledge is not good enough for developing models of responses of stomata to short term changes in the environment that are generally valid. Several different models are available, but they succeed in describing the responses of g_s^w to the environment only for certain species or conditions, and as most of them are empirical, there is little in common in their mathematical structures.

8.1.5 Methods

Equipment

I rewrote the gas-exchange system software incorporating algorithms to calculate and control in real time the molar fractions of CO_2 and water vapour at the leaf surface, which makes this gas-exchange system one of the few with this capability. I hope this software is going to be useful to other people using this system in the future, and also to people writing programs for other gas-exchange systems.

Modelling technique

Modelling was used as a tool to explore the consequences of the effect of a physical part of the system —the boundary layer— on the response of stomata. The model was kept as simple as possible, and the computer program written using a style that has been called 'literate programming' (Bentley & Knuth, 1986) with the aim of making it as readable as possible. As far as I know, this technique has not been used before for simulation models, but could be very useful by making program listings understandable to non-programmers and in this way subject to the same peer review criteria as experimentation.

Experimental design

No attempt was made to measure response surfaces to two or more variables as a way of studying interactions. This was an experimental design decision based on the practical difficulties of such an approach. Experiments involving measurement of g_s^w are complicated by hysteresis of some responses, such as the responses to CO_2 and light. This has two consequences: firstly, a random order of application of treatments leads to large experimental errors, and secondly, when many points are needed to build a response surface it is not possible to use a systematic approach without biasing the results —or at least limiting their validity to the particular sequence used.

To keep such apparent experimental errors small and to reduce the probability of bias in the results it is preferable to apply all the treatments, to each experimental unit (leaf or plant), in the shortest possible time. To reduce both error and bias, the number of treatments per experiment was kept low, and the hypotheses were tested by comparison of response curves rather than means. In some measure, the experiments in this thesis show how simple experiments can be designed to address complex questions, and how adequate statistical design can help to increase the sensitivity of the experiments without increasing the number of measurements.

8.2 Implications for the future of stomatal conductance modelling

8.2.1 Current knowledge and models

Knowledge about stomatal responses to single variables is more substantial than that about the interactions between them. In the literature there are some descriptions of interactions in different species (e.g. Lösch & Tenhunen, 1981; Ball, 1988), mostly from response surface experiments. A way of obtaining this information more efficiently would be to use simple factorial experiments (e.g. two variables at two or three levels) combined with the measurement of dose response curves for individual variables —i.e. the approach taken in Chapter 6.

Field measurements do not lead to a mechanistic explanation, because different environmental variables are correlated, and although this approach can be useful for deriving empirical functions to predict the response of g_s^w in the field, it has many limitations if we want to identify which variables are driving stomatal action, and how (Jarvis, 1976). Field measurements are also useful for understanding how responses at the leaf or stomatal level are influenced by correlations between environmental variables, and by processes occurring at the canopy level (e.g. Grantz & Meinzer, 1991).

Mechanistic models of leaf g_s^w should simulate responses of stomata to the variables defined at the place where they are sensed, and take interactions between variables into account. The large number of variables to which stomata respond make the number of possible interactions also large, and significant interactions need to be identified and measured before attempting to simulate stomatal responses in a complex environment [e.g. in *Commelina communis* the sensitivity of g_s^w to χ_i^c depends on I (Jarvis & Morison, 1981)]. Many possible interactions remain unknown or poorly specified because even though they may have been measured, the state of variables not studied has not been kept constant at the place where these variables are sensed by the guard cells, e.g. constant χ_a^c instead of constant χ_i^c (cf. the experiments described in Chapter 6).

The models that have been developed reflect the state of our knowledge of stomatal function. Few models of g_s^w are mechanistic (e.g. Penning de Vries, 1972), most are empirical, some are driven only by environmental variables (e.g. Jarvis, 1976), but others take advantage of the correlation between A and g_s^w (e.g. Ball, 1988).

The correlation between A and g_s^w is useful practically because it allows the use of A as a surrogate for a range of environmental and plant variables. This is not an ideal approach, but is one that is within reach from our current knowledge of stomatal behaviour. However, it is very important to realize that, even though A can be used as

a driving variable in the calculation of g_s^w, A does not control g_s^w in reality —i.e. there is no simple causal link between A and g_s^w, A and g_s^w are interdependent. The need to simultaneously calculate A and g_s^w is a problem of models based on the correlation between A and g_s^w, but it is a problem that mechanistic models also have —i.e. χ_i^c would be needed as a driving variable in any mechanistic model of g_s^w, and because of this, such a model would also require the simultaneous calculation of g_s^w and A.

Mechanistic submodels of the responses of leaf g_s^w to environmental variables are needed to build models at larger spatial and longer time scales, such as the scales of whole plants, canopies and stands. A mechanistic model of whole leaf g_s^w could be based on an empirical model of stomatal responses, without including the complexity of the mechanism of solute transport and accumulation in guard cells (e.g. ion channels, ion pumps, membrane potentials, and second messengers).

But the response of g_s^w should be scaled-up taking into account the effect of the boundary layer, instead of simply multiplying the leaf area by a value of g_s^w calculated from χ_a^w and χ_a^c. By changing the object studied, we also change the reference point —i.e. the position where molar fractions are not affected by the surface fluxes being measured or modelled. What we call boundary layer depends on this reference point, so depending on the spatial scale at which we work, we have a leaf boundary layer, a canopy boundary layer, or a planetary boundary layer. We can think of these boundary layers as being nested one inside the other.

8.2.2   Towards a mechanistic model of canopy conductance

Mechanistic, or at least partly mechanistic, models of leaf g_s^w that take into account the direct responses of stomata to CO_2, light, temperature, water vapour deficit and the place where these variables are sensed, and also the responses to hormones, will be more robust than the empirical models currently in use. In many species responses of adaxial and abaxial stomata will have to be modelled separately. With the exception of the effects mediated through chemical signals, these direct responses have been taken into account in the empirical model proposed in Chapter 7.

At the scale of the whole leaf, the effects on the variables sensed by the stomata of boundary layer thickness, shading by the mesophyll, CO_2 flux density, and leaf energy balance should be taken into account. The effect of changes in the leaf water status occurring directly and through chemical signals also needs to be considered. Some of these effects —boundary layer, CO_2 flux density and leaf energy balance— have been taken into account in the model proposed by Collatz *et al.* (1991).

When scaling up to a whole plant, the difference in CO_2 molar fraction and water vapour molar fraction in different layers of the air volume occupied by the plant, leaf display and shading between leaves, soil water deficit and photoassimilate supply-demand balance need to be considered.

When scaling up from a single plant to a forest or field crop the effect of the canopy boundary layer and the concurrent response of the different plants making up the canopy will need to be included.

McNaughton & Jarvis (1991) have provided an analysis of the scaling up of water fluxes, and analogous equations could be developed for CO_2 from their diagrams. The model MAESTRO provides a description of light interception that could be used for computing the light regime in different layers of a canopy (Wang & Jarvis, 1990). The main limitation to the development of a mechanistic model of canopy conductance seems to be the unavailability of a mechanistic model of stomatal conductance. A model that explicitly does the scaling up from stomata to canopy will be computationally intensive, and probably impractical for predictive use, but will help to the understanding of the scaling up mechanism. Such a model could be used to find out when and why simpler models (e.g. 'big leaf' canopy models) break down (see the comparison of different canopy models in Finnigan & Raupach, 1987).

8.3   Possible practical applications of the results

8.3.1   Forecasting the effects of global change

Submodels to calculate canopy conductance (G_s^w) are an important part of models that are used for predicting the behaviour of vegetation in response to global change and the influence of vegetation on the atmosphere, both under current and future conditions. There are two approaches to modelling G_s^w: (1) scaling from leaves to canopies, or (2) deriving G_s^w from flux measurements (Baldocchi *et al.*, 1991). The first approach involves scaling up and requires a knowledge of responses of g_s^w to environmental variables, and of how g_s^w is integrated in a canopy. The second approach depends on assumptions about the homogeneity and extension of the canopy, and about soil evaporation. Usually the estimates of G_s^w obtained using this second approach differ from those obtained from integration of measurements or simulations at leaf level (Finnigan & Raupach, 1987; Baldocchi *et al.*, 1991).

The results presented in this thesis are useful with respect to the first of these two approaches to the calculation of G_s^w by providing information about which variables are involved, how they interact, and how the thickness of the boundary layer affects

stomatal action. The model proposed in Chapter 7 is simple enough to be useful in this context, and more flexible than that proposed by Ball *et al.* (1987).

8.3.2 Agriculture and forestry

In many parts of the world, a limited water resource is the most important constraint on agriculture and forest production. The ability to predict plant water use and CO_2 fixation under different environmental and management conditions is important for devising management strategies that will generate ecologically sustainable and economically viable production systems.

The prediction of water use and CO_2 fixation by plant canopies requires prediction of conductances, including stomatal conductance. A better knowledge of the mechanistic basis of stomatal function will help us understand the physiological basis of these processes and in this way make modelling and decision making more robust.

The results presented are also important for plant breeding because the ability to predict the performance of ideotypes of stomatal behaviour could be used to set the objectives of a selection programme based on an ecophysiological knowledge of plant function. In this context we need to select for plant characteristics that are important for the performance of the whole crop stand. Thus the use of physiological criteria in plant breeding requires both a knowledge of plant functioning and of how plants interact with each other and with the environment. To be able to predict the effect of plant characteristics on the performance of the crop or forest stand we need also to develop principles for scaling up.

8.4 The future

Many aspects of the response of g_s^w and G_s^w to the environment remain unknown. There is no consistent data set, measured on a single species, of the responses of g_s^w to all the variables to which stomata are sensitive, measured taking into consideration the place where the variables are sensed. Until this kind of information is available for several species, including crops, weeds, trees, sun- and shade-loving plants, generalizations will be very difficult —we will not be able to recognize species specific idiosyncrasies from generally occurring features.

Attempts at developing dynamic models of g_s^w have been empirical (Aphalo, 1988), or they have considered only the response to I (e.g. Kirschbaum *et al.*, 1988). The dynamics of stomatal responses to I can be important in the lower strata of canopies, but probably does not have a big effect on G_s^w.

Heterogeneity of stomatal aperture in different parts of a leaf affects calculations of

χ_i^c and D_s^w (see Section 2.2.1). van Kraalingen (1990) has done simulations with a model to asses the consequences of patchiness in stomatal aperture on the results derived from gas-exchange experiments. This heterogeneity of stomatal action across the leaf surface can cause measurement artifacts, and needs further investigation, especially with respect to its dynamics.

We are just beginning to be able to scale-up steady-state responses from the leaf scale up to the whole plant and canopy scales, but the models at the smaller scale are still crude and limit our progress. Although it is true that when scaling up we usually need less detail about the processes occurring and a smaller scale than when we are dealing directly with systems at this smaller scale, it is also true that we need to understand much of this detail, before being able to decide how much of this detail is needed.

When scaling-up, the heterogeneity of the canopy is usually dealt with by dividing the canopy into layers that are assumed to be homogeneous. More sophisticated methods of integration should be developed. Spatial and temporal integration is just one aspect of scaling-up, but should not be neglected because advances in integration methods could make models less computationally intensive.

When I started this project I received the comment 'Why are you studying stomata? We already know all that can be learnt about them.' After three years of research by me and by others, it is clear that this person was wrong. Stomatal physiology remains as fascinating and challenging as ever. We can expect quick advance in the next few years because the techniques for measurement are available, and because the development of the field is of increasing importance in a globally changing environment.

Appendix A

The BOUNDARY model

The listing of the computer program which implements the model described in Chapter 6 is included in this appendix. It was written in Modula-2 using the MWEB system. It makes use of modules from the M2Simul library of tools for simulation model program writing.

The MWEB system is an implementation of the WEB system of 'literate' programming for the language Modula-2. It consists in two preprocessors that are used to generate a Modula-2 file and a TeX file. The first is compiled and executed, the second is used to generate the formated output given here. This output is generated automatically from the MWEB source file and although nicely formated is the 'listing' of the program.

1. Introduction. This program calculates the effect of the boundary layer on the apparent sensitivity of stomata to environmental variables. It was written by Pedro J. Aphalo in June and July, 1990.

It was written in Modula-2 (Wirth, 1985) using MWEB (Sewell, 1989) and TeX (Knuth, 1986). It makes imports from modules of the M2Simul library previously developed by the author (Aphalo, 1989).

define *banner* $\equiv$ `˙This␣is␣BOUNDARY,␣Version␣0.0˙`

2. The model simulates the effect of the boundary layer, based on a description of the response of the plant. This model does not simulate the response of stomata per se but rather the physical effect of the boundary layer conductance on the concentrations seen by the stomata and its effect on the apparent response when, as in natural conditions, these concentrations are not independent variables.

As we are not interested in the description of stomatal responses we do not want to assume any particular functional form for their response. For this reason we are going to use interpolated values from tabulated data.

The problem can be set up as a system of two simultaneous equations:

$$D_s = f(D_s, C_i)$$
$$C_i = g(D_s, C_i)$$

where only state variables are shown. This system is equivalent to:

$$0 = f(D_s, C_i) - D_s$$
$$0 = g(D_s, C_i) - C_i$$

or

$$0 = f_{error}(D_s, C_i)$$
$$0 = g_{error}(D_s, C_i)$$

Both f_{error} and g_{error} are functions of g_s and environment variables. D_s and C_i are the only state variables of our model. An iterative procedure must be used to solve this system under each environmental condition of interest. g_s and the rates of CO_2 assimilation and of transpiration can be computed from the values of state and environment variables.

3. Structure of the program. The program reads environmental data from an input file, and saves the results to an output file. Following a top down design we lay down the general structure, whose components will be filled in later.

module *boundary*;
  ⟨Import list 4⟩
  type ⟨Types of the program 5⟩
  var ⟨Global variables of the program 6⟩
  ⟨Procedure definitions of the program 8⟩
  begin
    display_line(*banner*);
    ⟨Get file names 42⟩;
    ⟨Open files 37⟩;
    ⟨Setup the functions 14⟩;
    ⟨Setup the equations 7⟩;
    ⟨Compute behavior 25⟩;
    ⟨Close files 39⟩;
  end *boundary*.

4. The system of equations. Taking advantage of Modula-2's procedure data type we are going to build a vector of function procedures to store the system of equations, and a vector of *reals* to store its state. As we are going to use the module ⟨Equations⟩ to solve this system, the vectors have to be compatible with those used there.

  define *solve_eqs* ≡ ⟨Solve⟩   (* procedure *)
  define *behaviour* ≡ ⟨BehaviorType⟩   (* type *)
  define *dummy_bhv* ≡ ⟨point⟩
  define *dummy_real* ≡ 0.0
  define *equation* ≡ ⟨ModelFunc⟩   (* type *)
  define *eq_vector* ≡ ⟨ModelFuncArray⟩   (* type *)
  define *state_vector* ≡ ⟨ModelArray⟩   (* type *)
  define *Ds* ≡ 0   (* Index for D_s in *state_vector* *)
  define *Ci* ≡ 1   (* Index for C_i in *state_vector* *)
⟨Import list 4⟩ ≡
  from ⟨Equations⟩ import *behaviour*, *equation*, *state_vector*, *eq_vector*, *solve_eqs*;
See also sections 9, 12, 34, 35, and 41.
This code is used in section 3.

5. ⟨Types of the program 5⟩ ≡
  environment_variables = (*Wa*, *Ca*, *I*, *Tl*, *gb*);   (* forcing variables *)
  env_vector = **array** *environment_variables* **of** *real*;
This code is used in section 3.

6. ⟨Global variables of the program 6⟩ ≡
guessed_state, *steady_state*: *state_vector*;
env_state: *env_vector*;
equations: *eq_vector*;
See also sections 13, 18, 29, and 36.
This code is used in section 3.

7. ⟨Setup the equations 7⟩ ≡
    equations[*Ds*] ← *Ds_error_proc*;
    equations[*Ci*] ← *Ci_error_proc*;
This code is used in section 3.

8. We use Teten's equation (Murray, 1967) to calculate the saturated vapour pressure, and by dividing it by the total pressure we get a mol fraction. The temperature is in °C, and the atmospheric pressure in Pa is assumed constant. We also assume *temperature* > 0 °C.

⟨Procedure definitions of the program 8⟩ ≡
procedure *W_sat*(*temperature* : *real*): *real*;
    const *P_atm* = $1.013 \cdot 10^{+5}$;   (* Pa *)
    var *P_water*: *real*;
    begin
        P_water ← $6.1078 \cdot 10^{+2}$ * *exp*(17.269 * *temperature*/(237.3 + *temperature*));
        return *P_water*/*P_atm*;   (* $PaPa^{-1} \equiv mol\,mol^{-1}$ *)
    end *W_sat*;
See also sections 15, 16, 20, 21, 22, 23, and 24.
This code is used in section 3.

9. Modula-2 has no exponentiation operator, so we have to import a procedure from a library module .

    define *exp* ≡ ⌐ᵤexp⌐

⟨Import list 4⟩ +≡
    from ⌐ᵤMathLib0ᵤ⌐ import *exp*;

10. We define W_l and D_a as macros.

    define *Wl* ≡ *W_sat*(*env_state*[*Tl*])
    define *Da* ≡ (*Wl* − *env_state*[*Wa*])

11. We also define macros for computing the total conductances to water vapour and CO_2. The constant '1.60' is the ratio between the difussivities of water vapour and CO_2 in air. For g_b a smaller value is used because the process is not fully diffusive.

    define *gt*(#) ≡ (1.0/(1.0/*env_state*[*gb*] + 1.0/*gs_proc*(#)))
    define *gt_CO2*(#) ≡ (1.0/(1.37/*env_state*[*gb*] + 1.60/*gs_proc*(#)))

12. Stomatal response is calculated as the product of a conductance value for standard conditions and functions that describe the effect of individual variables as a proportion of this value. For these stomatal response functions we use interpolation from tables of data read from disk files. We use procedures and types imported from the module ⌈Splines⌋ from the M2Simul library. The structure of these data files is described in the M2Simul library. These files should contain g_s values in the range 0 to 1, as functions of I in μmol m^{-2} s^{-1}, and D, and C$_i$ in mol mol^{-1}.

define *spline_handle* ≡ ⌈␣Spline⌋

define *init_gs_qfd*(#) ≡ ⌈␣CreateSpline⌋ (#, *gs_qfd_spl*, *gs_qfd_ok*);

define *init_gs_Ds*(#) ≡ ⌈␣CreateSpline⌋ (#, *gs_Ds_spl*, *gs_Ds_ok*);

define *init_gs_Ci*(#) ≡ ⌈␣CreateSpline⌋ (#, *gs_Ci_spl*, *gs_Ci_ok*);

define *gs_qfd*(#) ≡ ⌈␣FunVal⌋ (*gs_qfd_spl*, #)

define *gs_Ds*(#) ≡ ⌈␣FunVal⌋ (*gs_Ds_spl*, #)

define *gs_Ci*(#) ≡ ⌈␣FunVal⌋ (*gs_Ci_spl*, #)

define *gs_max* ≡ 80.0 · 10^{-3} (* mol m^{-2} s^1 *)

⟨ Import list 4 ⟩ +≡

from ⌈␣Splines␣⌋ import ⌈␣Spline⌋ , ⌈␣CreateSpline⌋ , ⌈␣FunVal⌋ ;

13. ⟨ Global variables of the program 6 ⟩ +≡
gs_qfd_spl, *gs_Ds_spl*, *gs_Ci_spl*: *spline_handle*;
gs_qfd_ok, *gs_Ds_ok*, *gs_Ci_ok*: *boolean*;

14. ⟨ Setup the functions 14 ⟩ ≡
init_gs_qfd(*gs_qfd_file*);
init_gs_Ds(*gs_Ds_file*);
init_gs_Ci(*gs_Ci_file*);

See also section 19.

This code is used in section 3.

15. ⟨ Procedure definitions of the program 8 ⟩ +≡
procedure *gs_proc*(*sys_state* : *state_vector*): *real*;
begin
return *gs_max* * *gs_qfd*(*env_state*[*I*]) * *gs_Ds*(*sys_state*[*Ds*]) * *gs_Ci*(*sys_state*[*Ci*]);
end *gs_proc*;

16. ⟨ Procedure definitions of the program 8 ⟩ +≡
procedure *Ds_proc*(*sys_state* : *state_vector*): *real*;
begin
return *Da* * (1.0 − *gt*(*sys_state*)/*env_state*[*gb*]);
end *Ds_proc*;

17. We are also going to use interpolation from tabulated data for describing the rate of CO_2 assimilation as a function of C$_i$. Assimilation data must be in mol m^{-2} s^{-1} as a function of C$_i$ in mol mol^{-1}.

define *init_A_Ci*(#) ≡ ⌈␣CreateSpline⌋ (#, *A_Ci_spl*, *A_Ci_ok*);

define *A_Ci*(#) ≡ ⌈␣FunVal⌋ (*A_Ci_spl*, #)

18. ⟨ Global variables of the program 6 ⟩ +≡
A_Ci_spl: spline_handle;
A_Ci_ok: boolean;

19. ⟨ Setup the functions 14 ⟩ +≡
  init_A_Ci(A_Ci_file);

20. ⟨ Procedure definitions of the program 8 ⟩ +≡
procedure *A_proc(sys_state : state_vector): real;*
  begin
    return *A_Ci(sys_state[Ci]);*
  end *A_proc;*

21. ⟨ Procedure definitions of the program 8 ⟩ +≡
procedure *E_proc(sys_state : state_vector): real;*
  begin
    return *Da ∗ gt(sys_state);*
  end *E_proc;*

22. We are going to use a rough approximation to compute C_i. We are not going to correct it for the effects of the mass flow of water vapour.
⟨ Procedure definitions of the program 8 ⟩ +≡
procedure *Ci_proc(sys_state : state_vector): real;*
  begin
    return *env_state[Ca] − A_proc(sys_state)/gt_CO2(sys_state);*
  end *Ci_proc;*

23. Now we are going to define function procedures for each of the equations in the model. The equations are defined as 'error' functions: they return the difference between the current value of D_s or C_i and that corresponding to the value of g_s expected at these concentrations. These differences must be zero when the system is in steady state.
⟨ Procedure definitions of the program 8 ⟩ +≡
procedure *Ds_error_proc(time : real; sys_data : state_vector; behav : behaviour): real;*
  begin
    return *Ds_proc(sys_data) − sys_data[Ds];*
  end *Ds_error_proc;*

24. ⟨ Procedure definitions of the program 8 ⟩ +≡
procedure *Ci_error_proc(time : real; sys_data : state_vector; behav : behaviour): real;*
  begin
    return *Ci_proc(sys_data) − sys_data[Ci];*
  end *Ci_error_proc;*

25. Running the simulation. For each environmental condition we must repeat several steps. The details of each of these steps are going to be filled in in the following sections.

⟨ Compute behavior 25 ⟩ ≡
 while ¬*end_of_data* do
  ⟨ Load environment data 26 ⟩
  if *done* then
   ⟨ Compute a guess 27 ⟩
   ⟨ Compute one data point 28 ⟩
   ⟨ Save state data 30 ⟩
   ⟨ Show vital signs 32 ⟩
  end ;
 end ;

This code is used in section 3.

26. We read the environment data from a free format file. Each line is expected to contain five *real* values, one for each of the following variables: W_a (mol mol^{-1}), C_a (mol mol^{-1}), I (μmol m^{-2} s^{-1}), T_l (°C), and g_b (mol m^{-2} s^{-1}).

⟨ Load environment data 26 ⟩ ≡
 read_real(*in_file*, *env_state*[Wa]);
 read_real(*in_file*, *env_state*[Ca]);
 read_real(*in_file*, *env_state*[I]);
 read_real(*in_file*, *env_state*[Tl]);
 read_real(*in_file*, *env_state*[gb]);

This code is used in section 25.

27. To solve the equations, we first need a guess for D_s and C_i. We take the bold approach of using $D_s = 0.75\,D_a$ and $C_i = 200.0\,\mu$mol mol^{-1} as the starting point for the minimisation. If environmental data were sorted by g_b it could be better to use as a guess the values of D_s and C_i calculated for the previous data point.

 define *num_eq* ≡ 2
 define *max_iterations* ≡ 100

⟨ Compute a guess 27 ⟩ ≡
 guessed_state[Ds] ← 0.75 ∗ Da;
 guessed_state[Ci] ← 200.0 · 10^{-6};

This code is used in section 25.

28. ⟨ Compute one data point 28 ⟩ ≡
 iterations ← *max_iterations*;
 solve_eqs(*equations*, *num_eq*, *guessed_state*, *iterations*, *steady_state*);
 actual_iterations ← *iterations*;
 Ds_error ← *Ds_error_proc*(*dummy_real*, *steady_state*, *dummy_bhv*);
 Ci_error ← *Ci_error_proc*(*dummy_real*, *steady_state*, *dummy_bhv*);

This code is used in section 25.

29. ⟨ Global variables of the program 6 ⟩ +≡
iterations, *actual_iterations*: *cardinal*;
Ds_error, *Ci_error*: *real*;

30. We save the state variables D_s and C_i, and their 'errors'. We also save g_s, A and E calculated for this condition. The output consists in seven *real* values per line: g_s (mol m^{-2} s^{-1}), A (mol m^{-2} s^{-1}), E (mol m^{-2} s^{-1}), D_s (mol mol^{-1}), C_i (mol mol^{-1}), D_s error (mol mol^{-1}), and C_i error (mol mol^{-1}).

⟨ Save state data 30 ⟩ ≡
    write_real(*out_file* , *gs_proc*(*steady_state*));
    write_real(*out_file* , *A_proc*(*steady_state*));
    write_real(*out_file* , *E_proc*(*steady_state*));
    write_real(*out_file* , *steady_state*[*Ds*]);
    write_real(*out_file* , *steady_state*[*Ci*]);
    write_real(*out_file* , *Ds_error*);
    write_real(*out_file* , *Ci_error*);
See also section 31.
This code is used in section 25.

31. We save the outcome of all computations, even if they are suspect, but mark them in the file as such. We add a text string at the end of each line that indicates whether the solution computed was `GOOD` or `BAD`. `GOOD` means that the iterative algorithm has converged.

⟨ Save state data 30 ⟩ +≡
    if (*actual_iterations* < *max_iterations*) **then**
        write_str(*out_file* , `˽GOOD`); *new_line*(*out_file*);
    else
        write_str(*out_file* , `˽BAD`); *new_line*(*out_file*);
    end ;

32. ⟨ Show vital signs 32 ⟩ ≡
    display_dot;
This code is used in section 25.

33. System dependent part. What follows is highly dependent on the compiler and library used. This is the part of the program that would need to be changed to be able to compile it in a different computer or with a different compiler. The program could also be modified to use the standard input and output when no filenames are supplied in the command line.
    We used Logitech's Modula-2 compiler for MS-DOS, Version 3.0.

34. CRT screen output.
    define *display_line*(#) ≡ ⟦˽InOut.WriteString⟧ (#); ⟦˽InOut.WriteLn⟧
    define *display_dot* ≡ ⟦˽InOut.Write(`.`)⟧
⟨ Import list 4 ⟩ +≡
    import ⟦˽InOut⟧;

35. File input and ouput.

define *lookup* ≡ ⎢␣Lookup⎢

define *close* ≡ ⎢␣Close⎢

define *not_done*(#) ≡ (#.⎢res⎢ ≠ ⎢done⎢)

define *end_of_data* ≡ (*in_file*.⎢eof⎢)

define *done* ≡ ⎢␣Done␣⎢

define *write_str* ≡ ⎢␣WriteString⎢

define *write_real* ≡ ⎢␣WriteReal⎢

define *new_line* ≡ ⎢␣WriteLn⎢

define *read_real* ≡ ⎢␣ReadReal⎢

define *text_file* ≡ ⎢␣File⎢

⟨ Import list 4 ⟩ +≡

    from ⎢␣FileSystem␣⎢ import *lookup*, ⎢␣Response⎢ , *text_file*, *close*;

    from ⎢␣FileInOut␣⎢ import *write_str*, *write_real*, *read_real*, *done*, *new_line*;

36. ⟨ Global variables of the program 6 ⟩ +≡
in_file, *out_file*: *text_file*;
in_filename, *out_filename*: **array** [0 .. 65] **of** *char*;

37. ⟨ Open files 37 ⟩ ≡
  lookup(*in_file*, *in_filename*, *false*);
  if *not_done*(*in_file*) **then**
    fatal_error(`unable␣to␣open␣input␣file`);
  end ;

See also section 38.

This code is used in section 3.

38. ⟨ Open files 37 ⟩ +≡
  lookup(*out_file*, *out_filename*, *true*);
  if *not_done*(*out_file*) **then**
    fatal_error(`unable␣to␣open␣output␣file`);
  end ;

39. ⟨ Close files 39 ⟩ ≡
  close(*in_file*);
  close(*out_file*);

This code is used in section 3.

40. File names for tabulated data files to be used to get stomatal and assimilation responses by spline interpolation.

    define *gs_qfd_file* ≡ `gs_qfd.dat`

    define *gs_Ds_file* ≡ `gs_ds.dat`

    define *gs_Ci_file* ≡ `gs_ci.dat`

    define *A_Ci_file* ≡ `a_ci.dat`

41.   Reading file names from the command line.

define *arg_count* ≡ ⎿␣ArgCount⏌

define *arg* ≡ ⎿␣Arg⏌

⟨ Import list 4 ⟩ +≡
    from ⎿␣CommandLine␣⏌ **import** *arg_count, arg*;

42.   ⟨ Get file names 42 ⟩ ≡
    if *arg_count*( ) = 2 **then**
        arg(1, *in_filename*);
        arg(2, *out_filename*);
    else
        fatal_error(˙usage:␣boundary␣infile␣outfile˙);
    end ;

This code is used in section 3.

43.   Error handling;

define *fatal_error*(#) ≡ *display_line*(˙Fatal␣error!˙); *display_line*(#); ⎿␣HALT␣⏌

44.   References.

Aphalo, P. J. 1989. *M2Simul Library, User's Manual.* Unpublished.

Knuth, D.E. 1984. *The TEXbook.* Addison Wesley, Reading.

Murray, F.W. 1967. On the computation of saturation vapour pressure. *Journal of Applied Meteorology,* **6**, 203–204.

Sewell, W. 1989. *Weaving a program: literate programming in WEB.* Van Nostrand Reinhold, New York.

Wirth, N. 1985. *Programming in Modula-2, (3ed).* Springer-Verlag, Berlin.

45.   Index.

⟨ Close files 39 ⟩   Used in section 3.
⟨ Compute a guess 27 ⟩   Used in section 25.
⟨ Compute behavior 25 ⟩   Used in section 3.
⟨ Compute one data point 28 ⟩   Used in section 25.
⟨ Get file names 42 ⟩   Used in section 3.
⟨ Global variables of the program 6, 13, 18, 29, 36 ⟩   Used in section 3.
⟨ Import list 4, 9, 12, 34, 35, 41 ⟩   Used in section 3.
⟨ Load environment data 26 ⟩   Used in section 25.
⟨ Open files 37, 38 ⟩   Used in section 3.
⟨ Procedure definitions of the program 8, 15, 16, 20, 21, 22, 23, 24 ⟩   Used in section 3.
⟨ Save state data 30, 31 ⟩   Used in section 25.
⟨ Setup the equations 7 ⟩   Used in section 3.
⟨ Setup the functions 14, 19 ⟩   Used in section 3.
⟨ Show vital signs 32 ⟩   Used in section 25.
⟨ Types of the program 5 ⟩   Used in section 3.

Appendix B

Comparison of models

Table B.1. Comparison between models of stomatal response. Values of the coefficients from least squares regressions of different models to data for *Hedera helix* from the experiments described in Chapter 5. See Table 7.1 for equations and residual sums of squares. Data were the mean of three plants for set A (T_l=15–28 °C, D_s^w=6–15 mmol mol^{-1}, h_s=0.4–0.75, I=200 μmol m^{-2} s^{-1}, χ_s^c=350 μmol mol^{-1}), and that from a typical plant for set B (T_l=10–28, D_s^w=5–15, h_s=0.4–0.75, I=340 μmol m^{-2} s^{-1}, χ_s^c=350 μmol mol^{-1}). For model 8, T_{opt} is under the heading k_0.

Model	Set	k_0	k_1	k_2	k_3
1.	A	69.00	—	—	—
1.	B	83.72	—	—	—
2.	A	12.79	—	—	—
2.	B	10.59	—	—	—
3.	A	7338	—	—	—
3.	B	5748	—	—	—
4.	A	4643	-66.6	23.5	—
4.	B	5078	-3.73	-69.2	—
5.	A	5728	-184.5	-23.9	5.01
5.	B	6633	-186.3	-148.8	8.98
6.	A	88.05	-1.84	—	—
6.	B	118.2	-3.49	—	—
7.	A	87.33	-2.01	0.11	—
7.	B	136.0	-2.04	-1.56	—
8.	A	1.065	0.011	0.006	—
8.	B	0.204	-0.001	0.004	—

References

APHALO, P. J. 1988. *Valor adaptativo de la modulación de la actividad de los fotosistemas que controlan la apertura de los estomas. Su evaluación mediante un modelo de simulación.* M.Sc. thesis, Facultad de Agronomía, Universidad de Buenos Aires, Buenos Aires, Argentina.

APHALO, P. J. 1989. *M2Simul Library, User's Manual.* Unpublished.

APHALO, P. J., & SÁNCHEZ, R. A. 1986. Stomatal responses to light and drought stress in variegated leaves of *Hedera helix*. *Plant Physiology*, **81**, 768–773.

APHALO, P. J., GIBSON, D., & DI BENEDETTO, A. H. 1991. Responses of growth, photosynthesis, and leaf conductance to white light irradiance and end-of-day red and far-red pulses in *Fuchsia magellanica* Lam. *New Phytologist*, **117**, 461–471.

AVISSAR, R., AVISSAR, P., MAHRER, Y., & BRAVDO, B. A. 1985. A model to simulate response of plant stomata to environmental conditions. *Agricultural and Forest Meteorology*, **34**, 21–29.

BALDOCCHI, D. D., LUXMOORE, R. J., & HATFIELD, J. L. 1991. Discerning the forest from the trees: an essay on scaling canopy stomatal conductance. *Agricultural and Forest Meteorology*, **54**, 197–226.

BALL, J. T. 1987. Calculations related to gas exchange. *Pages 445–476 of:* Zeiger *et al.* (1987).

BALL, J. T. 1988. *An Analysis of Stomatal Conductance.* Ph.D. thesis, Stanford University, U.S.A.

BALL, J. T., WOODROW, I. E., & BERRY, J. A. 1987. A model predicting stomatal conductance and its contribution to the control of photosynthesis under different environmental conditions. *Pages 221–224 of:* Biggins (1987).

133

BAUER, H., & BAUER, U. 1980. Photosynthesis in leaves of the juvenile and adult phase of ivy (*Hedera helix*). *Physiologia Plantarum*, **49**, 366–372.

BAUER, H., & THÖNI, W. 1988. Photosynthetic light acclimation in fully developed leaves of the juvenile and adult phases of *Hedera helix*. *Physiologia Plantarum*, **73**, 31–37.

BENTLEY, J., & KNUTH, D. 1986. Programing pearls. Literate programing. *Communications of the ACM*, **29**, 364–369.

BIGGINS, J. (ed). 1987. *Progress in Photosynthesis Research*. Vol. 4. Dordrecht: Martinus Nijhoff Publishers.

BROGÅRDH, T., & JOHNSSON, A. 1975. Regulation of transpiration in *Avena*. Responses to white light steps. *Physiologia Plantarum*, **35**, 115–125.

BUDDE, R. J. A., & RANDALL, D. D. 1990. Light as a signal influencing the phosphorylation status of plant proteins. *Plant Physiology*, **94**, 1501–1504.

BUNCE, J. A. 1985. Effect of boundary layer conductance on the response of stomata to humidity. *Plant, Cell and Environment*, **8**, 55–57.

BUNCE, J. A. 1988a. Effects of boundary layer conductance on substomatal pressures of carbon dioxide. *Plant, Cell and Environment*, **11**, 205–208.

BUNCE, J. A. 1988b. Nonstomatal inhibition of photosynthesis by water stress. Reduction in photosynthesis at high transpiration rate without stomatal closure in field-grown tomato. *Photosynthesis Research*, **18**, 357–362.

BUNGE, M. 1959. *Causality. The Place of the Causal Principle in Modern Science.* Cambridge: Harvard University Press.

CALDWELL, M. M. 1970. The effect of wind on stomatal aperture, photosynthesis, and transpiration of *Rhododendron ferrugineum* L. and *Pinus cembra* L. *Centralblatt für das Gesamte Forstwesen*, **87**, 193–201.

COLLATZ, G. J., BALL, J. T., GRIVET, C., & BERRY, J. A. 1991. Physiological and environmental regulation of stomatal conductance, photosynthesis and transpiration: a model that includes a laminar boundary layer. *Agricultural and Forest Meteorology*, **54**, 107–136.

COMMISSION INTERNATIONALE DE L'ÉCLARAIGE. 1982. *Colorimetry*. Second edn. Publication CIE No. 15.2 (TC-1.3).

COWAN, I. R. 1977. Stomatal behaviour and environment. *Advances in Botanical Research*, 4, 117–228.

COWAN, I. R. 1988. Stomatal physiology and gas exchange in the field. *Pages 160–182 of:* STEFFEN, W. L., & DENMEAD, O. T. (eds), *Flow and Transport in the Natural Environment: Advances and Applications.* Berlin: Springer-Verlag.

COWAN, I. R., & FARQUHAR, G. D. 1977. Stomatal function in relation to leaf metabolism and environment. *Pages 471–501 of:* JENNINGS, D. H. (ed), *Integration of Activity in Higher Plants.* Cambridge: Cambridge University Press.

COWAN, I. R., RAVEN, J. A., HARTUNG, W., & FARQUHAR, G. D. 1982. A possible role for abscisic acid in coupling stomatal conductance and photosynthetic carbon metabolism in leaves. *Australian Journal of Plant Physiology*, 9, 489–498.

DAHSE, I., WILLMER, C. M., & MEIDNER, H. 1990. Tentoxin suppresses stomatal opening by inhibiting photophosphorylation. *Journal of Experimental Botany*, 41, 1109–1113.

DAVIES, W. J., MANSFIELD, T. A., & HETHERINGTON, A. M. 1990. Sensing of soil water status and the regulation of plant growth and development. *Plant, Cell and Environment*, 13, 709–719.

DUBBE, D. R., FARQUHAR, G. D., & RASCHKE, K. 1978. Effect of abscisic acid on the gain of the feedback loop involving carbon dioxide and stomata. *Plant Physiology*, 62, 413–417.

EDWARDS, A., & BOWLING, D. J. F. 1985. Evidence for a CO_2 inhibited proton extrusion pump in the stomatal cells of *Tradescantia virginiana*. *Journal of Experimental Botany*, 36, 91–98.

EMERSON, J. D., & STRENIO, J. 1983. Boxplots and batch comparison. *Chap. 3, pages 58–96 of:* HOAGLIN, D. C., MOSTELLER, F., & TUKEY, J. W. (eds), *Understanding Robust and Exploratory Data Analysis.* New York: Wiley.

FARQUHAR, G. D., & COWAN, I. R. 1974. Oscillations in stomatal conductance. *Plant Physiology*, 54, 769–772.

FARQUHAR, G. D., DUBBE, D. R., & RASCHKE, K. 1978. Gain of the feedback loop involving carbon dioxide and stomata: Theory and measurement. *Plant Physiology*, 62, 406–412.

FARQUHAR, G. D., SCHULZE, E.-D., & KÜPPERS, M. 1980. Responses to humidity by stomata of *Nicotiana glauca* L. and *Corylus avellana* L. are consistent with the optimization of carbon dioxide uptake with respect to water loss. *Australian Journal of Plant Physiology*, **7**, 315–327.

FINNIGAN, J. J., & RAUPACH, M. R. 1987. Transfer processes in plant canopies in relation to stomatal characteristics. *Pages 385–429 of:* Zeiger *et al.* (1987).

FISCHER, R. A. 1968. Stomatal opening: role of potassium uptake by guard cells. *Science*, **160**, 784–785.

FITES, J. A., & TESKEY, R. O. 1988. CO_2 and water vapour exchange of *Pinus taeda* in relation to stomatal behavior: test of an optimization hypothesis. *Canadian Journal of Forest Research*, **18**, 150–157.

FUJINO, M. 1967. Role of adenosinetriphosphate and adenosinetriphosphatase in stomatal movement. *Science Bulletin of the Faculty of Education, Nagasaki University*, **18**, 1–47.

GALLAND, P. 1989. Photosensory adaptation in plants. *Botanica Acta*, **102**, 11–20.

GRACE, J. 1977. *Plant Response to Wind.* London: Academic Press.

GRACE, J. 1991. Physical and ecological evaluation of heterogeneity. *Functional Ecology*, **5**, 192–201.

GRACE, J., & WILSON, J. 1976. The boundary layer over a *Populus* leaf. *Journal of Experimental Botany*, **27**, 231–241.

GRACE, J., MALCOLM, D. C., & BRADBURY, I. K. 1975. The effect of wind and humidity on leaf diffusive resistance in Sitka spruce seedlings. *Journal of Applied Ecology*, **12**, 931–940.

GRACE, J., OKALI, D. U. U., & FASEHUN, F. E. 1982. Stomatal conductance of two tropical trees during the wet season in Nigeria. *Journal of Applied Ecology*, **19**, 659–670.

GRANTZ, D. A. 1990. Plant response to atmospheric humidity. *Plant, Cell and Environment*, **13**, 667–679.

GRANTZ, D. A., & MEINZER, F. C. 1991. Regulation of transpiration in field-grown sugarcane: evaluation of the stomatal response to humidity with the Bowen ratio technique. *Agricultural and Forest Meteorology*, **53**, 169–183.

GRIME, J. P., HODGSON, J. G., & HUNT, R. 1988. *Comparative Plant Ecology: a Functional Approach to Common British Species.* London: Unwin Hyman.

HALL, A. E., SCHULZE, E.-D., & LANGE, O. L. 1976. Current perspectives of steady-state stomatal responses to environment. *Pages 169–188 of:* LANGE, O. L., KAPPEN, L., & SCHULZE, E.-D. (eds), *Water and Plant Life.* Berlin: Springer-Verlag.

HALL, C. A. S., & DAY, J. W. 1977. Systems and models: terms and basic principles. *Pages 6–36 of:* HALL, C. A. S., & DAY, J. W. (eds), *Ecosystem Modeling in Theory and Practice: An Introduction with Case Histories.* New York: John Wiley & sons.

HEATH, O. V. S. 1950. Studies in stomatal behaviour. V. The role of carbon dioxide in the light response of stomata. Part I. Investigation of the cause of abnormally wide stomatal opening within porometer cups. *Journal of Experimental Botany,* 1, 29–62.

HEATH, O. V. S., & MILTHORPE, F. L. 1950. Studies in stomatal behaviour. V. The role of carbon dioxide in the light response of stomata. Part II. Preliminary experiments on the interrelations of light intensity, carbon dioxide concentration, and rate of air flow in controlling the movement of wheat stomata. *Journal of Experimental Botany,* 1, 227–243.

HOLMES, M. G. 1989. Photoregulation of water use efficiency in the natural environment. *Page not numbered of:* GÖRING, H. (ed), *Stomata '89.* Colloquia Pflanzenphysiologie, no. 13. Berlin: Humboldt University. Abstract only.

HOLMES, M. G., & KLEIN, W. H. 1985. Evidence for phytochrome involvement in light-mediated stomatal movement in *Phaseolus vulgaris* L. *Planta,* 166, 348–353.

JARVIS, P. G. 1976. The interpretation of the variation in leaf water potential and stomatal conductance found in canopies in the field. *Philosophical Transactions of the Royal Society of London, Series B,* 273, 593–610.

JARVIS, P. G., & MANSFIELD, T. A. (eds). 1981. *Stomatal Physiology.* Cambridge: Cambridge University Press.

JARVIS, P. G., & MCNAUGHTON, K. G. 1986. Stomatal control of transpiration: scaling up from leaf to region. *Advances in Ecological Research,* 15, 1–49.

JARVIS, P. G., & MORISON, J. I. L. 1981. The control of transpiration and photosynthesis by the stomata. *Pages 247–279 of:* Jarvis & Mansfield (1981).

JOHNSSON, M., ISSAIAS, S., BROGÅRDH, T., & JOHNSSON, A. 1976. Rapid, blue-light-induced transpiration response restricted to plants with grass-like stomata. *Physiologia Plantarum,* **36,** 229–232.

JOHNSTON, R. L. 1982. *Numerical methods.* New York: Wiley.

JONES, H. G. 1990. Control of growth and stomatal behaviour at the whole plant level: Effects of soil drying. *Pages 81–93 of:* DAVIES, W. J., & JEFFCOAT, B. (eds), *Importance of Root to Shoot Communication in the Responses to Environmental Stress.* Bristol: British Society for Plant Growth Regulation.

KARLSSON, P. E., & ASSMANN, S. M. 1990. Rapid and specific modulation of stomatal conductance by blue light in ivy (*Hedera helix*). *Plant Physiology,* **94,** 440–447.

KARLSSON, P. E., HÖGLUND, H. O., & KLOCKARE, R. 1983. Blue light induces stomatal transpiration in wheat seedlings with chlorophyll deficiency caused by SAN 9789. *Physiologia Plantarum,* **57,** 417–421.

KIRSCHBAUM, M. U. F., GROSS, L. J., & PEARCY, R. W. 1988. Observed and modelled stomatal responses to dynamic light environments in the shade plant *Alocasia macrorrhiza. Plant, Cell and Environment,* **11,** 111–121.

KITANO, M., & EGUCHI, H. 1987a. Air humidity whithin the boundary layer of a transpiring leaf. II. Profile of water vapor density within the boundary layer. *Biotronics,* **16,** 47–55.

KITANO, M., & EGUCHI, H. 1987b. Air humidity within the boundary layer of a transpiring leaf. I. Relationship between transpiration and water vapor density at leaf surface. *Biotronics,* **16,** 39–45.

KNAPP, A. K., VOGELMANN, T. C., McCLEAN, T. M., & SMITH, W. K. 1988. Light and chlorophyll gradients within *Cucurbita* cotyledons. *Plant, Cell and Environment,* **11,** 257–263.

KNUTH, D. E. 1984. *The TEXbook.* Reading: Addison Wesley.

KOCH, W., LANGE, O. L., & SCHULZE, E.-D. 1971. Ecophysiological investigations on wild and cultivated plants in the Negev Desert. I. Methods: A mobile laboratory for measuring carbon dioxide and water vapour exchange. *Oecologia,* **8,** 296–309.

KONDO, N. 1989. Biochemical changes in guard cells on stomatal closure induced by abscisic acid. *Pages 219–226 of:* Tazawa *et al.* (1989).

KÖRNER, CH., SCHEEL, J. A., & BAUER, H. 1979. Maximum leaf diffusive conductance in vascular plants. *Photosynthetica*, **13**, 45–82.

KUIPER, P. J. C. 1964. Dependence upon wavelength of stomatal movement in epidermal tissue of *Senecio odoris*. *Plant Physiology*, **39**, 952–955.

LAISK, A., OJA, V., & KULL, K. 1980. Statistical distribution of stomatal apertures of *Vicia faba* and *Hordeum vulgare* and the *spannungsphase* of stomatal opening. *Journal of Experimental Botany*, **31**, 49–58.

LANGE, O. L., LÖSCH, R., SCHULZE, E.-D., & KAPPEN, L. 1971. Responses of stomata to changes in humidity. *Planta*, **100**, 76–86.

LEUNING, R. 1990. Modelling stomatal behaviour and photosynthesis of *Eucalyptus grandis*. *Australian Journal of Plant Physiology*, **17**, 159–175.

LEVERENZ, J. W., & JARVIS, P. G. 1979. Photosynthesis in Sitka spruce. VIII. The effects of light flux density and direction on the rate of net photosynthesis and the stomatal conductance of needles. *Journal of Applied Ecology*, **16**, 919–932.

LLOYD, J. 1991. Modelling stomatal responses to environment in *Macadamia integrifolia*. *Australian Journal of Plant Physiology*. Submitted.

LÖSCH, R., & TENHUNEN, J. D. 1981. Stomatal responses to humidity — phenomenon and mechanism. *Pages 137–161 of:* Jarvis & Mansfield (1981).

LOUWERSE, W. 1980. Effects of CO_2 concentration and irradiance on the stomatal behaviour of maize, barley and sunflower. *Plant, Cell and Environment*, **3**, 391–398.

LUDLOW, M. M., & WILSON, G. L. 1971. Photosynthesis of tropical pasture plants. I. Illuminance, carbon dioxide concentration, leaf temperature, and leaf-air vapour pressure difference. *Australian Journal of Biological Sciences*, **24**, 449–470.

MACROBBIE, E. A. C. 1988. Control of ion fluxes in stomatal guard cells. *Botanica Acta*, **101**, 140–148.

MANSFIELD, T. A. 1983. Movements of stomata. *Science Progress*, **68**, 519–542.

MANSFIELD, T. A. 1986. The physiology of stomata: new insights into old problems. *Pages 155-224 of:* STEWARD, F. C. (ed), *Water and Solutes in Plants.* Plant Physiology, vol. 9. Orlando: Academic Press.

MANSFIELD, T. A., HETHERINGTON, A. M., & ATKINSON, C. J. 1990. Some current aspects of stomatal physiology. *Annual Review of Plant Physiology,* **41**, 55–75.

MARMÈ, D. 1988. The role of calcium in the regulation of plant cellular metabolism. *Pages 201-208 of:* GERDAY, CH., GILLES, R., & BOLIS, L. (eds), *Calcium and Calcium Binding Proteins: Molecular and Functional Aspects.* Berlin: Springer-Verlag.

McAINSH, M. R., BROWNLEE, C., & HETHERINGTON, A. M. 1990. Abscisic acid-induced elevation of guard cell cytosolic Ca^{2+} precedes stomatal closure. *Nature,* **343**, 186–188.

McNAUGHTON, K. G., & JARVIS, P. G. 1991. Effects of spatial scale on stomatal control of transpiration. *Agricultural and Forest Meteorology,* **54**, 279–301.

MEIDNER, H. 1968. The comparative effects of blue and red light on the stomata of *Allium cepa* L. and *Xanthium pennsylvanicum. Journal of Experimental Botany,* **19**, 146–151.

MEIDNER, H. 1987. Three hundred years of research into stomata. *Pages 7-27 of:* Zeiger *et al.* (1987).

MEIDNER, H., & HEATH, O. V. S. 1959. Stomatal responses to temperature and carbon dioxide concentration in *Allium cepa* L. and their relevance to midday closure. *Journal of Experimental Botany,* **10**, 206–219.

MEIDNER, H., & MANSFIELD, T. A. 1968. *Physiology of Stomata.* London: McGraw-Hill.

MONTEITH, J. L., & UNSWORTH, M. H. 1990. *Principles of Environmental Physics.* Second edn. London: Edward Arnold.

MORISON, J. I. L. 1987. Intercellular CO_2 concentration and stomatal response to CO_2. *Pages 229-251 of:* Zeiger *et al.* (1987).

MORISON, J. I. L. 1990. Plant and ecosystem responses to increasing atmospheric CO_2. *Trends in Ecology and Evolution,* **5**, 69–70.

MORISON, J. I. L., & GIFFORD, R. M. 1983. Stomatal sensitivity to carbon dioxide and humidity. A comparison of two C_3 and two C_4 grass species. *Plant Physiology*, **71**, 789–796.

MORISON, J. I. L., & JARVIS, P. G. 1983a. Direct and indirect effects of light on stomata. I. In Scots pine and Sitka spruce. *Plant, Cell and Environment*, **6**, 95–101.

MORISON, J. I. L., & JARVIS, P. G. 1983b. Direct and indirect effects of light on stomata. II. In *Commelina communis* L. *Plant, Cell and Environment*, **6**, 103–109.

MOTT, K. 1988. Do stomata respond to CO_2 concentrations other than intercellular? *Plant Physiology*, **86**, 200–203.

MOTT, K. A. 1990. Sensing of atmospheric CO_2 by plants. *Plant, Cell and Environment*, **13**, 731–737.

MOTT, K. A., & PARKHURST, D. F. 1991. Stomatal responses to humidity in air and Helox. *Plant, Cell and Environment*. In press.

MURRAY, F. W. 1967. On the computation of saturation vapour pressure. *Journal of Applied Meteorology*, **6**, 203–204.

NEILSON, R. E., & JARVIS, P. G. 1975. Photosynthesis in Sitka spruce [*Picea sitchensis* (Bong.) Carr.]. IV. Response of stomata to temperature. *Journal of Applied Ecology*, **12**, 879–891.

NELSON, S. D., & MAYO, J. M. 1975. The occurrence of functional non-chlorophyllous guard cells in *Paphiopedilum spp. Canadian Journal of Botany*, **53**, 1–7.

NOBEL, P. S. 1983. *Biophysical Plant Physiology and Ecology*. San Francisco: W. H. Freeman.

NONAMI, H., SCHULZE, E.-D., & ZIEGLER, H. 1990. Mechanisms of stomatal movement in response to air humidity, irradiance and xylem water potential. *Planta*, **183**, 57–64.

ÖREN, T. I. 1984. Model-based activities: a paradigm shift. *Pages 3–40 of:* ÖREN, T. I., ZEIGLER, B. P., & ELZAS, M. S. (eds), *Simulation and Model-Based Methodologies: An Integrative View*. NATO ASI Series, Series F: Computer and Systems Sciences, vol. 10. Berlin: Springer-Verlag.

OSONUBI, O., & DAVIES, W. J. 1980. The influence of water stress on the photosynthetic performance and stomatal behaviour of tree seedlings subjected to variation in temperature and irradiance. *Oecologia*, **45**, 3–10.

PALLAGHY, C. K. 1971. Stomatal movement and potassium transport in epidermal strips of *Zea mays*: the effect of CO_2. *Plant Physiology*, **101**, 287–295.

PEARMAN, G. I., WEAVER, H. L., & B., TANNER C. 1972. Boundary layer heat transfer coefficients under field conditions. *Agricultural Meteorology*, **10**, 83–92.

PEMADASA, M. A. 1981. Photocontrol of stomatal movements. *Biological Reviews*, **56**, 551–588.

PENNING DE VRIES, F. W. T. 1972. A model simulating transpiration of leaves with special attention to stomatal functioning. *Journal of Applied Ecology*, **9**, 57–77.

PENNY, M. G., & BOWLING, D. J. F. 1974. A study of potassium gradients in the epidermis of intact leaves of *Commelina communis* L. in relation to stomatal opening. *Planta*, **119**, 17–25.

PENNY, M. G., KELDAY, L. S., & BOWLING, D. J. F. 1976. Active chloride transport in the leaf epidermis of *Commelina communis* in relation to stomatal activity. *Planta*, **130**, 291–294.

PRESS, W. H., FLANNERY, B. P., TEUKOLSKY, S. A., & VETTERLING, W. T. 1986. *Numerical Recipies*. Cambridge: Cambridge University Press.

RAGHAVENDRA, A. S. 1990. Blue light effects on stomata are mediated by the guard cell plasma membrane redox system distinct from the proton translocating ATPase. *Plant, Cell and Environment*, **13**, 105–110.

RAMOS, C., & HALL, A. E. 1982. Relationships between leaf conductance, intercellular CO_2 partial pressure and CO_2 uptake rate in two C_3 and two C_4 plant species. *Photosynthetica*, **16**, 343–355.

RASCHKE, K., & FELLOWS, M. 1971. Stomatal movements in *Zea mays*: shuttle of potassium and chloride between guard cells and subsidiary cells. *Planta*, **101**, 296–316.

RASCHKE, K., HANEBUTH, W. F., & FARQUHAR, G. D. 1978. Relationship between stomatal conductance and light intensity in leaves of *Zea mays* L., derived from experiments using the mesophyll as shade. *Planta*, **139**, 73–77.

RASCHKE, K., HEDRICH, R., RECKMANN, U., & SCHROEDER, J. I. 1988. Exploring biophysical and biochemical components of the osmotic motor that drives stomatal movement. *Botanica Acta*, **101**, 283–294.

ROBERTS, J., CABRAL, O. M. R., & DE AGUIAR, L. F. 1990. Stomatal and boundary-layer conductances in an amazonian terra firme rain forest. *Journal of Applied Ecology*, **27**, 336–353.

ROSE, P. Q. 1980. *Ivies*. Poole: Blandford Press.

SANDFORD, A. P. 1984. *The responses of the stomata of conifers to humidity and water potential*. Ph.D. thesis, University of Edinburgh.

SANDFORD, A. P. 1987. *The manual for the computer controlled gas-exchange system*. Department of Forestry and Natural Resources, University of Edinburgh, Edinburgh. Unpublished.

SCARTH, G. W. 1932. Mechanism of the action of light and other factors on stomatal movement. *Plant Physiology*, **7**, 481–504.

SCHROEDER, J. I., & HAGIWARA, S. 1989. Cytosolic calcium regulates ion channels in the plasma membrane of *Vicia faba*. *Nature*, **338**, 427–430.

SCHWARTZ, A., & ZEIGER, E. 1984. Metabolic energy for stomatal opening. Roles of photophosphorylation and oxidative phosphorylation. *Planta*, **161**, 129–136.

SEWELL, W. 1989. *Weaving a program: literate programing in WEB*. New York: Van Nostrand Reinhold.

SHACKEL, K. A., & BRINCKMANN, E. 1985. *In situ* measurement of epidermal cell turgor, leaf water potential, and gas exchange in *Tradescantia virginiana* L. *Plant Physiology*, **78**, 66–70.

SHARKEY, T. D. 1984. Transpiration-induced changes in the photosynthetic capacity of leaves. *Planta*, **160**, 143–150.

SHARKEY, T. D., & OGAWA, T. 1987. Stomatal responses to light. *Pages 195–208 of:* Zeiger *et al.* (1987).

SHARKEY, T. D., & RASCHKE, K. 1981a. Effect of light quality on stomatal opening in leaves of *Xanthium strumarium* L. *Plant Physiology*, **68**, 1170–1174.

SHARKEY, T. D., & RASCHKE, K. 1981b. Separation and measurement of direct and indirect effects of light on stomata. *Plant Physiology*, **68**, 33–40.

SHERIFF, D. W. 1984. Epidermal transpiration and stomatal responses to humidity: some hypotheses explored. *Plant, Cell and Environment*, 7, 669–677.

SHIMAZAKI, K.-I. 1989. Energetic role of chloroplasts and mitochondria in stomatal movement. *Pages 227–230 of:* Tazawa et al. (1989).

SKAAR, H., & JOHNSSON, A. 1980. Light induced transpiration in a chlorophyll deficient mutant of *Hordeum vulgare. Physiologia Plantarum*, 49, 210–214.

SMITH, S., WEYERS, J. D. B., & BERRY, W. G. 1989. Variation in stomatal characteristics over the lower surface of *Commelina communis* leaves. *Plant, Cell and Environment*, 12, 653–659.

SNAITH, P. J., & MANSFIELD, T. A. 1982. Control of the CO_2 responses of stomata by indol-3ylacetic acid and abscisic acid. *Journal of Experimental Botany*, 33, 360–365.

SQUIRE, G. R., & MANSFIELD, T. A. 1972. A simple method of isolating stomata on detached epidermis by low pH treatment: observations of the importance of the subsidiary cells. *New Phytologist*, 71, 1033–1043.

STRYER, L. 1988. *Biochemistry*. Third edn. New York: W. H. Freeman.

SUSSMAN, M. R., & SUROWY, T. K. 1987. Physiology and molecular biology of membrane ATPases. *Oxford Surveys of Plant Molecular and Cell Biology*, 4, 47–70.

TAZAWA, M., KATSUMI, M., MASUDA, Y., & OKAMOTO, H. (eds). 1989. *Plant Water Relations and Growth under Stress*. Tokyo: Myu K.K.

THORPE, M. R. 1978. Correction of infra-red gas analyser readings for changes in reference tube CO_2 concentration. *Plant, Cell and Environment*, 1, 59–60.

THORPE, M. R., WARRIT, B., & LANDSBERG, J. J. 1980. Responses of apple leaf stomata: a model for single leaves and a whole tree. *Plant, Cell and Environment*, 3, 23–27.

TURNER, N. C. 1970. Response of adaxial and abaxial stomata to light. *New Phytologist*, 69, 647–653.

TUTIN, T. G., HEYWOOD, V. H., BURGES, N. A., MOORE, D. M., VALENTINE, D. H., WALTERS, S. M., & WEBB, D. A. (eds). 1968. *Flora Europaea*. Vol. 2. Cambridge: Cambridge University Press.

VAN GARDINGEN, P., & GRACE, J. 1991. Plants and wind. *Advances in Botanical Research.* In press.

VAN GARDINGEN, P. R., JEFREE, C. E., & GRACE, J. 1989. Variation in stomatal aperture in leaves of *Avena fatua* L. observed by low-temperature scanning electron microscopy. *Plant, Cell and Environment,* **12,** 887–898.

VAN KRAALINGEN, D. W. G. 1990. Implications of non-uniform stomatal closure on the gas exchange calculations. *Plant, Cell and Environment,* **13,** 1001–1004.

VIRGIN, H. I. 1957. Stomatal transpiration of some variegated plants and of chlorophyll deficient mutants of barley. *Physiologia Plantarum,* **10,** 170–186.

VOGEL, S. 1978. Organisms that capture currents. *Scientific American,* **239,** 108–117.

VOGELMAN, T. C., KNAPP, A. K., McCLEAN, T. M., & SMITH, W. K. 1988. Measurement of light within thin plant tissues with fiber optics microprobes. *Physiologia Plantarum,* **72,** 623–630.

VON CAEMMERER, S., & FARQUHAR, G. D. 1981. Some relationships between the biochemistry of photosynthesis and the gas exchange of leaves. *Planta,* **153,** 376–387.

WANG, Y. P., & JARVIS, P. G. 1990. Description and validation of an array model — MAESTRO. *Agricultural and Forest Meteorology,* **51,** 257–280.

WARDLE, K., & SHORT, K. C. 1981. Responses of stomata in epidermal strips of *Vicia faba* to carbon dioxide and growth hormones when incubated on potassium chloride and potassium iminodiacetate. *Journal of Experimental Botany,* **32,** 303–309.

WEYERS, J., & MEIDNER, H. 1990. *Methods in Stomatal Research.* Harlow: Longman.

WEYERS, J. D. B., PATERSON, N. W., FITZSIMONS, P. J., & DUDLEY, J. M. 1982. Metabolic inhibitors block ABA-induced stomatal closure. *Journal of Experimental Botany,* **33,** 1270–1278.

WILLIAMS, W. E. 1983. Optimal water-use efficiency in a California shrub. *Plant, Cell and Environment,* **6,** 145–151.

WILSON, C. L., PUSEY, P. L., & OTTO, B. 1981. Plant epidermal sections and imprints using cyanoacrylate adhesives. *Canadian Journal of Plant Science,* **61,** 781–783.

WIRTH, N. 1985. *Programming in Modula-2.* Third edn. Berlin: Springer-Verlag.

WONG, S. C., COWAN, I. R., & FARQUHAR, G. D. 1979. Stomatal conductance correlates with photosynthetic capacity. *Nature,* **282**, 424–426.

WONG, S. C., COWAN, I. R., & FARQUHAR, G. D. 1985a. Leaf conductance in relation to rate of CO_2 assimilation. I. Influence of nitrogen nutrition, phosphorous nutrition, photon flux density, and ambient partial pressure of CO_2 during ontogeny. *Plant Physiology,* **78**, 821–825.

WONG, S. C., COWAN, I. R., & FARQUHAR, G. D. 1985b. Leaf conductance in relation to rate of CO_2 assimilation. II. Effects of short-term exposures to different photon flux densities. *Plant Physiology,* **78**, 826–829.

WONG, S. C., COWAN, I. R., & FARQUHAR, G. D. 1985c. Leaf conductance in relation to rate of CO_2 assimilation. III. Influences of water stress and photoinhibition. *Plant Physiology,* **78**, 830–834.

WOODROW, I. E., BALL, J. T., & BERRY, J. A. 1987. A general expression for the control of the rate of photosynthetic CO_2 fixation by stomata, the boundary layer and radiation exchange. *Pages 225–228 of:* Biggins (1987).

WOOLLEY, J. T. 1971. Reflectance and transmittance of light by leaves. *Plant Physiology,* **47**, 656–662.

WUENSCHER, J. E., & KOZLOWSKI, T. T. 1971. The response of transpiration resistance to leaf temperature as a desiccation resistance mechanism in tree seedlings. *Physiologia Plantarum,* **24**, 254–259.

ZEIGER, E. 1983. The biology of stomatal guard cells. *Annual Review of Plant Physiology,* **34**, 441–475.

ZEIGER, E. 1986. The photobiology of stomatal movements. *Pages 391–413 of:* KENDRICK, R. E., & KRONENBERG, G. H. M. (eds), *Photomorphogenesis in Plants.* Dordrecht: Martinus Nijhoff Publishers.

ZEIGER, E. 1990. Light perception in guard cells. *Plant, Cell and Environment,* **13**, 739–747.

ZEIGER, E., & HEPLER, P. K. 1977. Light and stomatal function: blue light stimulates swelling of guard cell protoplasts. *Science,* **196**, 887–889.

ZEIGER, E., BLOOM, A. J., & HEPLER, P. K. 1977. Ion transport in stomatal guard cells: A chemiosmotic hypothesis. *What's New in Plant Physiology*, **9**, 29–31.

ZEIGER, E., FIELD, C., & MOONEY, H. A. 1981. Stomatal opening at dawn: possible roles of the blue light response in nature. *Pages 391–407 of:* SMITH, H. (ed), *Plants and the Daylight Spectrum.* London: Academic Press.

ZEIGER, E., FARQUHAR, G.D., & COWAN, I.R. (eds). 1987. *Stomatal Function.* Stanford: Stanford University Press.

ZHANG, J., & DAVIES, W. J. 1991. Antitranspirant activity in xylem sap of maize plants. *Journal of Experimental Botany*, **42**, 317–321.

ZIEGLER, H. 1987. The evolution of stomata. *Pages 29–57 of:* Zeiger *et al.* (1987).